

PDF hosted at the Radboud Repository of the Radboud University Nijmegen

The following full text is a publisher's version.

For additional information about this publication click this link.

<http://hdl.handle.net/2066/113216>

Please be advised that this information was generated on 2018-07-08 and may be subject to change.

**ELEKTRONENSONDE RÖNTGENMICROANALYSE
VAN BIOLOGISCHE PREPARATEN
VERBETERING VAN EEN AANTAL KWANTIFICERINGSPROCEDURES**

ABRAHAM BOEKESTEIN

**ELEKTRONENSONDE RÖNTGENMICROANALYSE
VAN BIOLOGISCHE PREPARATEN
VERBETERING VAN EEN AANTAL KWANTIFICERINGSPROCEDURES**

Promotores : Prof. Dr. A.M. Stadhouders

Prof. Dr. M.M.A. Sassen

Co-referent: Dr. A.L.H. Stols

**ELEKTRONENSONDE RÖNTGENMICROANALYSE
VAN BIOLOGISCHE PREPARATEN
VERBETERING VAN EEN AANTAL KWANTIFICERINGSPROCEDURES**

Proefschrift

ter verkrijging van de graad van doctor in de wiskunde en
natuurwetenschappen aan de Katholieke Universiteit te Nijmegen,
op gezag van de Rector Magnificus

Prof. Dr. J.H.G.I.Giesbers

volgens het besluit van het College van Dekanen in het openbaar
te verdedigen op woensdag 19 december 1984 des
namiddags te 2.00 uur precies

door

ABRAHAM BOEKESTEIN

geboren te Naaldwijk



krips repro meppel

Dankwoord

Aan allen die hebben bijgedragen aan de totstandkoming van dit proefschrift wil ik graag hartelijk dank zeggen. Van de sectie Signaal en Data Analyse van de afdeling Medische Informatie Verwerking wil ik met name Geert Elemans, Paul Sutthoff en Frans Smolders bedanken voor de nuttige assistentie bij het opzetten van het computerprogramma BIOFLEX. Martin Van 't Hoff van de afdeling Mathematisch Statistische Analyse wil ik bedanken voor het uitvoeren van een aantal statistische analyses op de resultaten van de ZAF-correctie. Chris van Eekelen en Gemma Kuijpers wil ik graag bedanken voor de nauwgezetheid en de betrokkenheid bij het uitvoeren van het onderzoek met microdruppels en bloedplaatjes. De Technische en Fysische Dienst voor de Landbouw (Directeur drs. A.M.K. Van Beek) wil ik gaarne bedanken voor de betoonde flexibiliteit en praktische ondersteuning bij de afronding van dit proefschrift. Hierbij wil ik met name noemen Willem van der Maat, Frans van Korlaar en Peter Wennekes die de lijntekeningen hebben vervaardigd en Herman Elerie en Günther Klickermann voor het nodige fotowerk. Birgitta Hachmang-Rissenbeek bedank ik voor het met zorg typen van verschillende delen van het manuscript.

De onderzoeken vermeld in dit proefschrift zijn voor het grootste deel verricht in het Instituut voor Submicroscopische Morfologie van de Katholieke Universiteit te Nijmegen onder de supervisie van Prof. Dr. A.M. Stadhouders en Dr. A.L.H. Stols. Dit onderzoek maakte deel uit van het onderzoekprogramma: 'Kwantitatieve microscopie, celbiologie en epidemiologie van (pre-)maligne afwijkingen'.

Aan Marisa

Inhoud

Lijst van symbolen en afkortingen	9
Hoofdstuk 1. Algemene inleiding: Fysische principes en kwantificering in de röntgenmicroanalyse	11
Kwantitatieve röntgenmicroanalyse van dikke biologische preparaten	23
Hoofdstuk 2. Quantitation in X-ray microanalysis of biological bulk specimens	25
Hoofdstuk 3. A comparison of ZAF-correction methods in quantitative X-ray microanalysis of light-element specimens	39
Hoofdstuk 4. Quantitative biological X-ray microanalysis of bulk specimens: an analysis of inaccuracies involved in ZAF-correction	43
Hoofdstuk 5. Surface roughness and the use of a peak to background ratio in the X-ray microanalysis of bio-organic bulk specimens	55
Kwantitatieve röntgenmicroanalyse van dunne biologische preparaten	63
Hoofdstuk 6. Bereiding van microdruppels	65
Hoofdstuk 7. X-ray microanalysis of picoliter microdroplets: Improvement of the method for quantitative X-ray microanalysis of samples of biological fluids	75
Hoofdstuk 8. Kwantitatieve röntgenmicroanalyse van microdruppel preparaten	85
Hoofdstuk 9. Elemental analysis of individual rat blood platelets by electron probe X-ray microanalysis using a direct quantification method	101
Summary	113
Samenvatting	115
Curriculum vitae	117

Lijst van symbolen en afkortingen

α	detector elevatie	
β	detector azimuth	
γ	afnamehoek van de röntgenstraling	
δ	relatieve fout	
θ	hoek van inval op het Bragg kristal	
λ	golflengte	
ρ	dichtheid	($\frac{m}{m^3}$)
$\phi(\rho z)$	verdeling van de door de bundelelektronen opgewekte ionisaties als functie van de massadikte	
ψ	kantelhoek van het preparaat	
ω	fluorescentie rendement	

Computerprogramma's

BGSUB	achtergrondaf trek programma, onderdeel van EDIT
BICEP	kwantificeringsprogramma voor dunne biologische preparaten
BIOFLEX	kwantificeringsprogramma voor dikke biologische preparaten
BLANK	achtergrondaf trek programma van EDAX dat gebruik maakt van een standaard voor de achtergrond
EDIT	verzameling programma's voor het EDAX 707B systeem (1974)
FRAME	kwantificeringsprogramma voor dikke preparaten van het National Bureau of Standards (USA)
FRAME-P	kwantificeringsprogramma voor 'particles'
INT	programma van EDAX om piekintensiteiten te berekenen
MAGIC IV	kwantificeringsprogramma voor dikke preparaten
MIC	kwantificeringsprogramma voor dikke biologische preparaten
MODEL	kwantificeringsprogramma voor biologische preparaten
PZAF	kwantificeringsprogramma voor 'particles'
STRIP	programma van EDAX voor het 'strippen' van pieken uit een ED spectrum
ZAF	ZAF-programma van het TRACOR TN2000 systeem (1978), (versie 10D)

Apparatuur

Camebax MBX70	'electronprobe X-ray microanalyzer', CAMECA
EDAX 707B	energie-dispersief röntgenmicroanalyse systeem, EDAX (1974)
EDAX 9100/65	energie-dispersief röntgenmicroanalyse systeem, EDAX (1979)
EM400G	transmissie elektronen microscoop met goniometer stage, Philips
EM400T	transmissie elektronen microscoop met 'twin' lens, Philips
JSM 35C	scanning elektronen microscoop, JEOL
PSEM500	scanning elektronen microscoop, Philips
TRACOR TN2000	energie-dispersief röntgenmicroanalyse systeem, TRACOR

Symbolen en afkortingen

A	atoommassa	(kg/mol)
	absorptie	
B	achtergrond-intensiteit	(s^{-1})
BS	'Backscattering'	
C/R	verhouding van berekende en werkelijke concentratie	
C	concentratie	
C_0	begin-concentratie	
cps	counts per seconde	(s^{-1})

C.V.	'coefficient of variation'	
d	roosterafstand in het Bragg kristal	(m)
E	energie	(J)
E_c	kritische ionisatie energie	(J)
ED	energie-dispersief	
E_{eff}	gemiddelde effectieve ionisatie energie	(J)
EM	elektronenmicroscop	
E_o	versnelspanning	(V)
	kinetische energie van de elektronen	(J)
EP(X)MA	elektronensonde röntgenmicroanalyse	
F	fluorescentie	
F	ZAF-correctiefactor totaal of partieel	
G	geometrie-factor = $\text{Cos}(\Psi)/\text{Sin}(\gamma)$	
I	bundelstroom	(A)
K-ratio	verhouding van de piekintensiteiten van een element in preparaat en van het zuivere element	
KAP	kaliuimftalaat (WD-spectrometer kristal)	
LIF	lithium fluoride (WD-spectrometer kristal)	
O	oppervlakte	(m^2)
P	netto piekintensiteit	(s^{-1})
P/B	verhouding van piek en achtergrond-intensiteit	
PET	pentaerythritol (WD-spectrometer kristal)	
Q	ionisatie doorsnede	(m^2)
r	correlatiecoëfficiënt	
R	straal van het excitatievolume	(m)
S	de convergentie in ZAF-correctie	
	'stopping power'	
S.D.	standaard deviatie	
S.E.	'standard error'	
SEM	scanning elektronenmicroscop	
sp	'specimen', het preparaat	
st	standaard	
STEM	scanning transmissie elektronenmicroscop	
W	massa	(kg)
WD	'wavelength dispersive', golflengte-dispersief	
x	reikwijdte van bundelelektronen in materie	(m)
Z	atoomnummer	
	atoomnummer-effect	
ZAF	correctie voor atoomnummer-effect (Z), absorptie (A) en secundaire fluorescentie (F)	

Hoofdstuk 1. Algemene inleiding; Fysische principes en kwantificering in de röntgenmicroanalyse

1.1. Inleidende opmerkingen

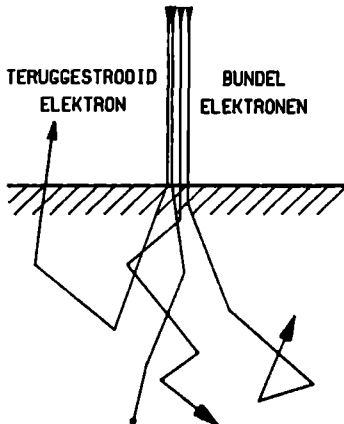
Elektronensonde röntgenmicroanalyse is een gevoelige analysemethode waarbij massafracties of absolute hoeveelheden van elementen aanwezig in een preparaat bepaald kunnen worden. De grote kracht van deze methode ligt in de mogelijkheid de informatie over de elementdistributie in het preparaat te correleren met de ultrastructuur van het preparaat. Zowel wat betreft de detectie van röntgenstraling als wat betreft de verwerking van de verkregen röntgenspectra zijn er de afgelopen jaren belangrijke ontwikkelingen geweest. Ook het aantal toepassingen van de elektronensonde röntgenmicroanalyse methode neemt snel toe. Het gehele vakgebied van de röntgenmicroanalyse is dan ook intussen zo omvangrijk geworden dat men reeds kan spreken van verschillende specialismen binnen dat gebied. Deze specialismen betreffen ondermeer de ontwikkeling van nieuwe röntgenstralingsdetectiemethoden, de ontwikkeling van nieuwe spectrumverwerkingsmethoden en de ontwikkeling van bepaalde prepareertechnieken. Een aparte plaats neemt de kwantificering (het berekenen van element-massafracties of absolute hoeveelheden) in, omdat het bij een analysetechniek hier in feite om gaat. Niettemin kan gesteld worden dat de ontwikkeling wat betreft de methodische kant van de kwantificering de laatste jaren traag verloopt. Nieuwe inzichten breken slechts langzaam door en opvallend is de vrijwel kritiekloze wijze waarop bestaande kwantificeringssoftware wordt gebruikt in nieuwe toepassingsgebieden.

In dit proefschrift wordt daarom een aantal kwantificeringsmethoden nader onderzocht en wordt nagegaan in hoeverre voor biologische analyseproblemen aanpassing van de bestaande methoden gewenst is. Teneinde de leesbaarheid van dit proefschrift te verbeteren wordt in deze inleiding een korte beschrijving gegeven van de fysische principes welke ten grondslag liggen aan de röntgenmicroanalyse. Vervolgens wordt ingegaan op enkele belangrijke detectiemethoden voor röntgenstraling en wordt een overzicht gegeven van een aantal belangrijke kwantificeringsmethoden. Uiteraard is het in het kader van dit proefschrift niet de bedoeling een complete verhandeling te schrijven over de achtergronden van de röntgenmicroanalyse. De lezer wordt daarvoor verwezen naar een aantal handboeken (Reed, 1975; Erasmus, 1978; Heinrich, 1981).

1.2. Fysische principes in de röntgenmicroanalyse

1.2.1. Interactie elektronen met materie

In een conventioneel transmissie elektronenmicroscop bezitten de bundel-elektronen een kinetische energie tussen ca 1 keV en 200 keV. In de hoogspannings elektronenmicroscop kunnen aanzienlijk hogere energieën voorkomen. Wanneer deze bundelelektronen materie binnendringen, worden deze verstrooid door botsingen, waarbij de elektronen door de atomen van het preparaat afgebogen worden. Een gedeelte van de elektronen ondergaat elastische botsingen waarbij geen kinetische energie verloren gaat. De elektronen worden alleen onder een bepaalde hoek afgebogen en kunnen zelfs worden teruggestrooid (zie Figuur 1). Het grootste deel van de elektronen echter ondergaat een groot aantal elastische botsingen waarbij ze telkens onder relatief kleine hoeken worden afgebogen. Aldus heeft het preparaat een divergerend effect op de elektronenbundel.

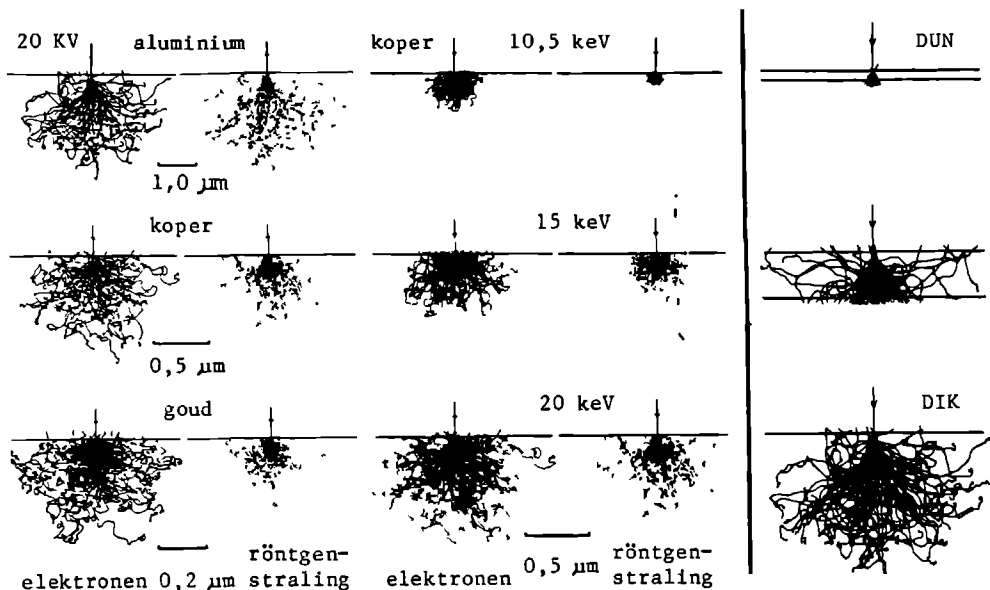


Figuur 1. Schematisch voorbeeld van de simulatie van het gedrag van bundelelektronen in materie.

Naast elastische botsingen zullen ook inelastische botsingen van de bundel-elektronen met de atomen in het preparaat optreden. Hierbij verliezen de elektronen een deel van hun kinetische energie. Dit heeft onder andere tot gevolg dat elektronen, die behoren tot de atomen van het preparaat, uit hun baan worden gestoten. In een voor een elektronenbundel oneindig dik preparaat verliezen de elektronen - na een meestal groot aantal elastische en inelastische botsingen - uiteindelijk hun oorspronkelijke kinetische energie geheel en komen 'tot stilstand'.

Bij de beschrijving van de interacties van bundelelektronen met materie zijn van belang de begrippen 'stopping power' en 'ionization cross section'. De stopping power, S , wordt gedefinieerd als het gemiddelde energieverlies van een bundelelektron door inelastische botsingen met atomen. S is afhankelijk van de oorspronkelijke kinetische energie van de elektronen, van de

elementsamenstelling van het preparaat en van de gemiddelde excitatie energie van de samenstellende elementen. De ionization cross section, Q , van een bepaalde elektronenschil van het atoom wordt gedefinieerd als het quotient van het aantal ionisaties van een bepaalde schil in het atoom per eenheid van afgelegde weg van het elektron in het preparaat en het aantal atomen in een volume-eenheid. Met het doel om de vorm en grootte te bepalen van het volume waarbinnen de bundelelektronen in het preparaat tot stilstand komen en dus hun kinetische energie verliezen, zijn computersimulaties gemaakt van het gedrag van elektronen in materie (Monte Carlo simulaties). Met deze berekeningen zijn voor een aantal gegeven omstandigheden wat betreft de samenstelling van het preparaat en de oorspronkelijke kinetische energie van de bundelelektronen, de trajecten weergegeven van een groot aantal elektronen. Figuur 2 toont hoe ver de bundelelektronen het preparaat binnendringen en waar de primaire röntgenstraling wordt opgewekt onder verschillende omstandigheden. Het ionisatievolume (= het volume waarbinnen de bundelelektronen de atomen van het preparaat kunnen ioniseren) wordt beïnvloed door de samenstelling van het preparaat en de oorspronkelijke kinetische energie van de elektronen. In Figuur 3 is aangegeven hoe de dikte van het preparaat wordt gedefinieerd.



Figuur 2. De trajecten van de bundelelektronen in het preparaat en de volumina waarbinnen de primaire röntgenstraling wordt opgewekt (zie Maurice, 1983).

Figuur 3. Definities van voor de bundelelektronen oneindig dikke en dunne preparaten.

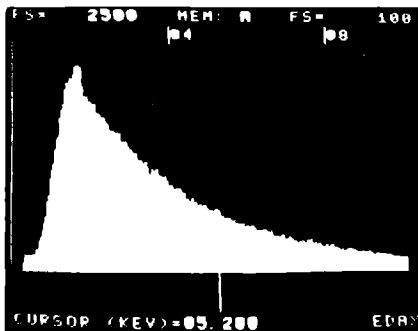
In een als dun te definiëren preparaat, vindt slechts een beperkte bundelverbreiding plaats. De elektronen verlaten het preparaat weer aan de onderzijde met eveneens slechts een beperkt verlies aan kinetische energie. Het ionisatievolume wordt voornamelijk bepaald door de dikte van het preparaat, de bundeldiameter en in mindere mate door de samenstelling van het preparaat. In een voor de bundelelektronen oneindig dik preparaat ontstaat het druppelvormige ionisatievolume, waarbij de grootste laterale diameter ordes van grootte groter is dan de oorspronkelijke bundeldiameter. Bij 'oneindig' dikke preparaten wordt het ionisatievolume niet meer bepaald door de dikte van het preparaat, maar juist door de samenstelling van het preparaat, de oorspronkelijke kinetische energie van de elektronen en de bundeldiameter (Fig. 2). In het gebied tussen 'oneindig' dik en zeer dun zal de elektronenbundel wel bundelverbreiding ondergaan maar is het preparaat toch zo dun dat een aantal elektronen het preparaat weer aan de onderzijde kan verlaten. Het ionisatievolume is hier zowel afhankelijk van de dikte van het preparaat, als van de samenstelling, de oorspronkelijke kinetische energie van de elektronen en de bundeldiameter.

Het excitatievolume is het volume waarbinnen de bundelelektronen nog voldoende kinetische energie bezitten om ionisaties teweeg te brengen van de meer naar binnen gelegen elektronenschillen van een bepaald atoom. De grootte van het excitatievolume wordt bepaald door het betrokken element en zal kleiner zijn dan het ionisatievolume omdat voor ionisatie van de valentieschil in het algemeen minder energie nodig is. Hieruit volgt dat bij analyse gesproken kan worden van een bepaald scheidend vermogen dat samenhangt met de grootte van het excitatievolume. Het zal duidelijk zijn dat dit scheidend vermogen bij dunne preparaten aanzienlijk gunstiger kan zijn dan bij dikke preparaten.

1.2.2. Emissie van röntgenstraling

Bundelelektronen kunnen op hun weg door de materie van het preparaat door de kern van een atoom worden afgeremd en afgebogen. Hierbij verliest het elektron een variabel, niet-discreet, deel van zijn kinetische energie. Deze energie wordt omgezet in een röntgenkwant met een energie tussen 0 en de kinetische energie van het elektron voor de botsing. Deze röntgenstraling wordt continuüm-, achtergrond-, of remstraling genoemd. In Figuur 4 is het energie-dispersieve continuümspectrum van koolstof weergegeven. De vorm van dit spectrum wordt bepaald door het gemiddeld atoomnummer van de materie in het preparaat, de oorspronkelijke kinetische energie van de bundelelektronen, de bundel-preparaat-röntgendetector geometrie en de dikte van het venster (zie

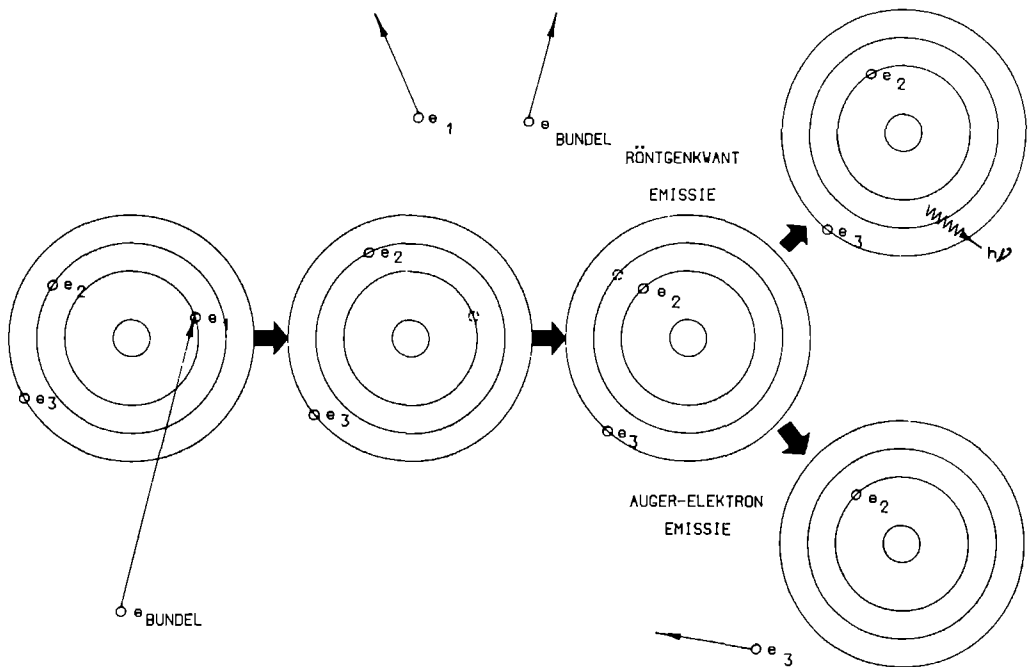
1.3.) van de röntgendetector. De intensiteit van de uitgezonden continuümstraling wordt behalve door bovengenoemde factoren ook nog bepaald door de grootte van de elektronenbundelstroom.



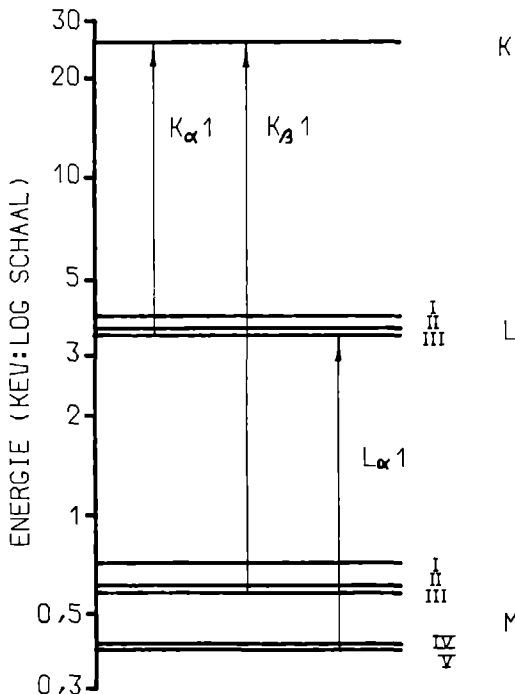
Figuur 4. Achtergrondspectrum van koolstof (versnelspanning 15 kV, analyse uitgevoerd op een Jeol 35C SEM).

Naast interactie met de atoomkernen kunnen bundelelektronen ook botsen met tot de elektronenmantel van het atoom behorende elektronen. Hierdoor kan het atoom worden geïoniseerd waarna stabilisatie volgt door opname van een vrij elektron. Verreweg het grootste deel van de op deze manier teweeg gebrachte ionisaties betreffen de valentie-elektronen omdat deze het zwakst gebonden zijn. Slechts in een gering deel van de ionisaties worden elektronen uit de meer naar binnen gelegen schillen (K en L schillen) uit hun baan gestoten. Het hierbij onstane 'gat' kan dan weer worden opgevuld door een elektron uit een meer naar buiten gelegen elektronenbaan (hoger energieniveau). Het verschil in energie tussen de twee bij deze overgang betrokken niveaus in de elektronenmantel is karakteristiek voor het betrokken element. Met deze vrijkomende energie kan een ander elektron uit de mantel worden vrijgemaakt of het kan worden omgezet in een röntgenkwant (zie Figuur 5). Indien een ander elektron wordt vrijgemaakt dan verkrijgt het elektron een kinetische energie die discreet is en element-karakteristiek. Hierop berust de spectrometrie met Auger-elektronen. Indien een röntgenkwant wordt uitgezonden dan heeft dit een energie die gelijk is aan de vrijkomende energie. Op de detectie van deze discrete en element-karakteristieke röntgenstraling berust de röntgenmicroanalyse. De verhouding tussen de kansen dat een Auger-elektron of een röntgenkwant wordt uitgezonden, wordt het fluorescentie rendement (ω), een element-karakteristieke fysische grootte, genoemd.

Een bundelelektron kan elektronen van verschillende energieniveaus uit hun baan stoten. Bovendien zijn er meestal verschillende overgangen mogelijk om een 'gat' op te vullen. Daarom zullen voor één element röntgenkwanten met verschillende discrete element-karakteristieke energieën worden uitgezonden (zie Figuur 6). Hierdoor ontstaat in theorie een lijnenspectrum, waarin bij



Figuur 5. De excitatie van elektronen in de binnenste schil van een atoom en de emissie van Auger-elektronen of röntgenkwanten.



Figuur 6. Een aantal mogelijke overgangen van elektronen in het atoom en de bijbehorende nomenclatuur van de element-karakteristieke röntgenkwant-emissies voor het element zilver.

bepaalde energieën röntgenkwanten worden uitgezonden afkomstig van die elementen die in het excitatievolume aanwezig zijn.

1.3. Detectie van röntgenstraling

1.3.1. Golflengte-dispersieve röntgenspectrometrie

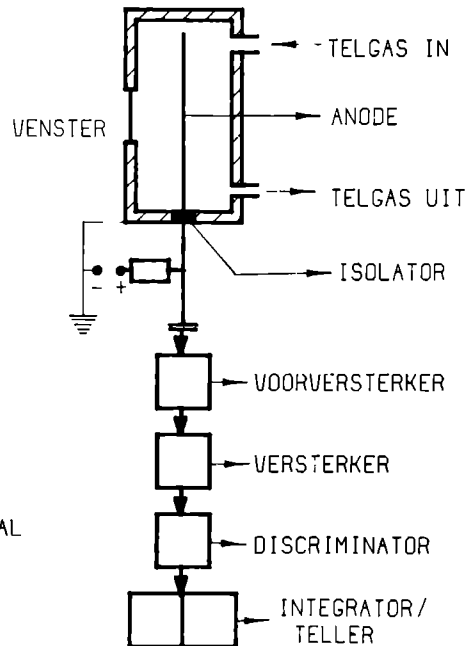
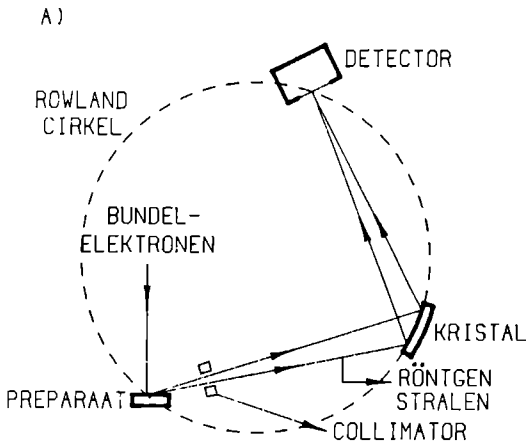
Het principe van golflengte-dispersieve röntgenspectrometrie berust op reflectie van de in het preparaat opgewekte röntgenstraling door een bepaald kristal onder een vaste hoek. In dit kristal vindt diffractie van röntgenstraling plaats volgens de wet van Bragg:

$$n \cdot \lambda = 2 \cdot d \cdot \sin \theta \quad (1)$$

waarin 'n' een natuurlijk getal is. Op deze manier functioneert het kristal als monochromator. Door verdraaiing van dit kristal zodat de hoek van inval verandert of door het gebruik van een kristal met een andere roosterafstand, kan straling met verschillende golflengtes in de richting van de detector worden gereflecteerd (zie Figuur 7a). Preparaat, kristal en detector voldoen hierbij tezamen aan een bepaalde geometrische situatie door zich alle drie te bevinden op de omtrek van een denkbeeldige cirkel (Rowland cirkel). Als reflecterend kristal worden stoffen gebruikt zoals pentaerythritol (PET), lithiumfluoride (LIF) en kalium ftalaat (KAP).

B)

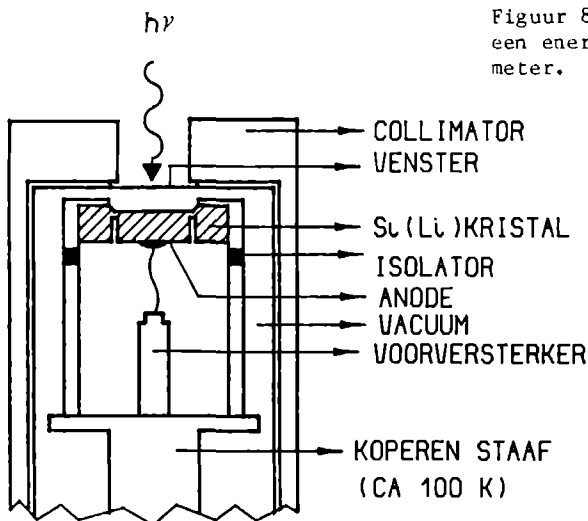
Figuur 7. Schematische voorstelling van een golflengte-dispersieve röntgenspectrometer (Fig. 7a) en de proportionele telbuis (Fig. 7b).



De röntgenstraling wordt gedetecteerd door middel van een proportionele telbuis (zie Figuur 7b). Straling komt de telbuis binnen door een dun gedeelte van de wand, het venster, dat meestal bestaat uit beryllium, mylar of formvar. In de telbuis bevindt zich een gas, meestal bestaande uit een edelgas (bijv. argon) en CO_2 of CH_4 . In dit gas worden door de ioniserende röntgenstraling ionparen gevormd, waarvan het aantal evenredig is met de oorspronkelijke kwantenenergie. In de telbuis bevindt zich verder een anode, terwijl de wand als kathode fungeert. Op deze manier wordt in het gas een grote toename bewerkstelligd van het aantal primair gevormde ionparen ('gas-vermenigvuldiging'). Uiteindelijk produceert elk binnentredend röntgenkwant een elektrische puls waarvan de grootte bepaald wordt onder andere door de kwantenenergie. Het aantal pulsen per tijdseenheid wordt gemeten en eventueel uitgezet als functie van de gemeten golflengte of energie van de röntgenkwanten. Door standaardisatie van de telsnelheid wordt in principe de kwantitatieve analyse uitgevoerd.

1.3.2. Energie-dispersieve röntgenspectrometrie

De energie-dispersieve röntgendetector bevat een silicium kristal waarin een gradiënt van lithium aanwezig is. Een dergelijke gradiënt kan alleen gehandhaafd worden indien het kristal wordt gehouden op 100 K. Om dit te bereiken wordt het kristal ingebouwd in een cryostaat die met vloeibare stikstof wordt gekoeld (zie Figuur 8). Om condensatie en contaminatie van het kristal te voorkomen wordt rondom een vacuüm gehandhaafd.



Figuur 8. Schematische voorstelling van een energie-dispersieve röntgenspectrometer.

Röntgenstraling treedt binnen door een dun gedeelte van de omhulling, het venster, dat meestal van beryllium wordt gemaakt. Moderne typen energie-dispersieve detectoren zijn soms voorzien van een mechanisme waarmee dit venster kan worden weggeklapt zodat straling ongehinderd op het detectiekristal kan invallen. De ioniserende röntgenstraling veroorzaakt in het kristal elektronen en elektronen-gat paren waarvan het aantal evenredig is met de oorspronkelijke kwantenenergie. Door een over het kristal aangelegde spanning ontstaat van elke binnenkomende kwant bij de anode een ladingspuls die vervolgens elektronisch wordt versterkt. De grootte van de uiteindelijke onstane elektrische puls is evenredig met de kwantenenergie. Kwanten van verschillende energie kunnen na elkaar worden gedetecteerd en de resulterende pulsen worden op grootte gesorteerd met een veelkanaalspulshoogteanalysator. Op deze manier wordt een röntgenspectrum in betrekkelijk korte tijd zichtbaar gemaakt, waarmee een kwalitatieve indruk van de samenstelling van een bepaald preparaat kan worden verkregen. Door standaardisatie van de netto piekintensiteiten en piek-achtergrond verhoudingen wordt in principe de kwantitatieve analyse uitgevoerd. In Tabel 1 is een vergelijking gemaakt van enkele aspecten van energie- en golflengte-dispersieve detectoren (zie Reed, 1975, voor een uitgebreid overzicht van de eigenschappen van deze detectoren).

Tabel 1. Vergelijking van enkele belangrijke eigenschappen van golflengte-dispersieve (WD) en energie-dispersieve (ED) detectoren. Bij vensterloze energie-dispersieve detectoren kan gedetecteerd worden van $Z=6$ tot 92.

	WD	ED
energieresolutie bij 5,9 keV	<10 eV	ca 140 eV
mechanische constructie	ingewikkeld	eenvoudig
detecteerbare elementen	$Z=4$ tot 92	$Z=11$ tot 92
achtergrondstraling	relatief laag	relatief hoog
spectrumacquisitie	sequentieel	parallel
efficiëntie	5 tot 20%	100% ($Z > 19$)

1.4. Kwantificering in de röntgenmicroanalyse

Na de acquisitie van röntgenstralingsintensiteiten, hetzij golflengte-dispersief, hetzij energie-dispersief, is het allereerst van belang vast te stellen of een vermeend element-karakteristiek signaal significant is ten opzichte van de achtergrondstraling (zie hiervoor bijvoorbeeld Heinrich, 1981). De voor deze significantie te formuleren criteria hangen nauw samen met de minimaal detecteerbare concentratie van een bepaald element. Bij de interpretatie van röntgenspectra ten behoeve van een kwalitatieve analyse is verder

het optreden van eventuele preparaatvreemde karakteristieke straling (bijvoorbeeld afkomstig van het gebruikte grid) en de mogelijkheid van interferentie (bijv. Pb M met S K) van belang (zie Chandler, 1978).

Bij de semikwantitatieve analyse worden netto piekintensiteiten en piek-achtergrond verhoudingen beoordeeld bijvoorbeeld bij de vergelijking van preparaten of elementen onderling. Het is hierbij noodzakelijk een indruk te verkrijgen van de achtergrond onder een bepaalde piek en hiervoor worden verschillende methoden gehanteerd afhankelijk van de vereiste nauwkeurigheid en de mogelijkheden die de spectra bieden (voor een overzicht zie Schamber, 1981). Bij de kwalitatieve en semikwantitatieve röntgenmicroanalyse wordt bij de beoordeling en de verwerking van de spectra in het algemeen geen rekening gehouden met het al of niet dik zijn van het preparaat. Dit aspect is uiteraard wel van belang bij het vaststellen van het scheidend vermogen van de analyse.

In de kwantitatieve analyse worden de na achtergrondaf trek verkregen netto piekintensiteiten of piek-achtergrond verhoudingen al of niet na standaardisatie via rekenkundige procedures verwerkt tot elementmassafracties of massa's. Bij deze rekenkundige procedures is de dikte van het preparaat wel van belang. In Tabel 2 is een overzicht gegeven van de belangrijkste kwantificeringsprocedures. Hieruit kan afgeleid worden dat de eigenschappen, van het preparaat en de beschikbaarheid van in fysisch en chemisch opzicht goed-gelijkende 'ideale' standaards de keuze van de kwantificeringsprocedure in belangrijke mate bepaalt. In de volgende hoofdstukken wordt nader ingegaan op verschillende van deze kwantificeringsmethoden.

1.5. Indeling van het proefschrift

In het eerste deel van dit proefschrift wordt de kwantificering in de röntgenmicroanalyse van dikke biologische preparaten behandeld (Hoofdstukken 2, 3, 4 en 5). In Hoofdstuk 2 wordt een overzicht gegeven van de literatuur op het gebied van de kwantificering in de röntgenmicroanalyse van dikke preparaten. In Hoofdstuk 3 volgt een vergelijking van de met ZAF-correctie verkregen resultaten wanneer goed gedefinieerde testgegevens worden verwerkt met een aantal verschillende ZAF-correctieformules. In Hoofdstuk 4 wordt een zelf ontworpen ZAF-correctie programma beschreven (BIOFLEX), dat bedoeld is om een aantal voor de biologische röntgenmicroanalyse specifieke problemen te onderzoeken. In Hoofdstuk 5 wordt een methode beschreven waarin de problemen die ontstaan door de analyse van een ruw oppervlak, grotendeels kunnen worden vermeden door het gebruik van een piek-achtergrond verhouding.

Tabel 2. Overzicht van de belangrijkste kwantificeringsmethoden in de röntgenmicroanalyse van biologische preparaten

preparaat	ideale standaard	niet-ideale standaard	
glad oppervlak	$C_{sp} = \frac{P_{sp}}{P_{st}} C_{st}$	ZAF-correctie van intensiteiten	2
DIK ruw oppervlak	$C_{sp} = \frac{(P/B)_{sp}}{(P/B)_{st}} C_{st}$ 1	ZAF-correctie van P/B ratio's	3
coupe	$C_{sp} = \frac{(P/B)_{sp}}{(P/B)_{st}} C_{st}$	continuüm methode of methode Linders	4
DUN 'particle'	$W_{sp} = \frac{P_{sp} M_{st}^2}{P_{st} M_{sp}^2} W_{st}$		5

Opmerkingen:

1. Zie Hoofdstuk 5
2. Zie Hoofdstukken 2, 3 en 4
3. Een computerprogramma, ontwikkeld op basis hiervan, is FRAME-P (cf. Small, et al., 1979)
4. Voor de continuüm methode zie Hall (1971); de methode Linders berust op een onafhankelijke massabepaling van het preparaat (zie Linders, et al., 1984)
5. Zie Hoofdstuk 8 en 9.

In het tweede deel van dit proefschrift wordt de kwantificering in de röntgenmicroanalyse van dunne biologische preparaten behandeld (Hoofdstuk 6, 7, 8 en 9). In Hoofdstuk 6 wordt ingegaan op het bereiden van microdruppels als standaard voor röntgenmicroanalyse. In Hoofdstuk 7 worden vervolgens dragermaterialen voor microdruppels en de verschillende röntgendetectiemethoden (ED of WD) met elkaar vergeleken. In Hoofdstuk 8 wordt de kwantificeringsmethode beschreven die in het algemeen gebruikt kan worden voor de röntgenmicroanalyse van elementen in zogenaamde 'particles'. In Hoofdstuk 9 tenslotte worden microdruppels en de in het voorgaande hoofdstuk beschreven kwantificeringsmethode toegepast in de analyse van calcium en magnesium in rattebloedplaatjes.

References

- Chandler, J.A. (1978). The application of λ -ray microanalysis in TEM to the study of ultrathin biological specimens- a review. In Electron Probe Microanalysis in Biology (Ed. D.A. Erasmus, Chapman & Hall, London) 37-93.
- Erasmus, D.A. (1978). Electron Probe Microanalysis in Biology (Chapman & Hall, London).
- Hall, T.A. (1971). The microprobe assay of chemical elements. In Physical Techniques in Biological Research, 2nd edition, vol 1A (Ed. G. Oster, Acad. Press, New York) 157-275.
- Heinrich, K.F.J. (1981). Electron Beam X-ray Microanalysis (Van Nostrand Reinhold, New York) 156-157.
- Linders, P.W.J., Van de Vorstenbosch, R.A., Smits, H.T.J., Stols, A.L.H. en Stadhouders, A.M. (1984). Absolute quantitative electron microscopy of thin biological specimens by energy-dispersive X-ray microanalysis and densitometric mass determination. Anal. Chim. Acta, 160, 57-67.
- Maurice, F. (1983). Microanalyse par sonde électronique et spectrométrie de rayon X: interactions électron-matière, émission X. In Microanalyse X en Biologie (Ed. C. Quintana en S. Halpen, Soc. franc. Microsc. Electr., Paris) 3-24.
- Reed, S.B.J. (1975). Electron Microprobe Analysis (Cambridge University Press, Cambridge) 72-173.
- Schamber, F.H. (1981). Curve fitting techniques and their application to the analysis of energy dispersive spectra. In: Energy Dispersive X-ray Spectrometry (Heinrich, K.F.J., Newbury, D.E. & Myklebust, R.L., U.S. Department of Commerce, Washington) 193-232.
- Small, J.A., Newbury, D.E. en Myklebust, R.L. (1979). Analysis of particles and rough samples by FRAME-P, a ZAF method incorporating peak-to-background measurements. In. Microbeam Analysis (Ed.: D.E. Newbury, San Francisco Press, San Francisco) 243-246.

In het eerste deel van dit proefschrift wordt nader ingegaan op een aantal aspecten met betrekking tot de kwantificering bij dikke biologische preparaten. Deze preparaten onderscheiden zich van dunne preparaten doordat deze de bundelelektronen volledig stoppen. Hierdoor is het ionisatievolume van de elektronen in het preparaat veel groter dan bij dunne preparaten. Dit betekent dat het grootste deel van de opgewekte röntgenstralen van relatief grote diepte komt en dat de opgewekte röntgenstralen op weg naar de detector een langere weg moeten afleggen door het preparaat. De samenstelling van de meestal organisch-chemische matrix van het preparaat heeft dan ook een belangrijke invloed op de röntgenstralingsintensiteiten. Omdat deze invloed in bepaalde gevallen de kwantificering kan bemoeilijken is het streven er in de biologische röntgenmicroanalyse in de eerste plaats op gericht de piekintensiteiten te ijken met een zogenaamde ideale standaard. Deze ideale standaard moet in chemisch en fysisch opzicht het preparaat zeer goed benaderen. De invloed van de matrix op de piekintensiteiten zijn dan voor preparaat en standaard dezelfde zodat het effect hiervan wegvalt in de kwantificering.

Indien men er niet in slaagt een ideale standaard toe te passen, zal met de invloed van de matrix op de piekintensiteiten rekening moeten worden gehouden. Dit mondt uit in zogenaamde matrix- of ZAF-correctie procedures, waarbij wordt gecorrigeerd voor een zogenaamd atoomnummer effect (Z), een absorptie effect (A) en een secundaire fluorescentie effect (F). Deze ZAF-correcties houden respectievelijk rekening met de invloed van matrix en analysecondities op het gedrag van de bundelelektronen en de opwekking van röntgenstralen (Z), op de absorptie van in het excitatievolume opgewekte primaire röntgenstralen (A) en op de opwekking en eventuele absorptie van door primaire röntgenstralen opgewekte secundaire röntgenstralen (F).

In de eerste drie hoofdstukken van dit deel (Hoofdstuk 2, 3 en 4) wordt ingegaan op de ZAF-correctie methode waarbij met name wordt behandeld welke implicaties er zijn wanneer ZAF-correctie wordt toegepast op biologische problemen. In het laatste hoofdstuk van Deel I (Hoofdstuk 5) wordt beschreven hoe een specifiek probleem in de kwantitatieve röntgenmicroanalyse van dikke biologische preparaten namelijk de ruwheid van het oppervlak, grotendeels kan worden omzeild door gebruik te maken van piek-achtergrond verhoudingen in plaats van netto piekintensiteiten.

QUANTITATION IN X RAY MICROANALYSIS OF BIOLOGICAL BULK SPECIMENS

A Boeckstein, A L H Stols and A M Stadhouders

Department of Submicroscopic Morphology, University of Nijmegen,
Medical School, Geert Grooteplein Zuid 24, Nijmegen, The Netherlands

Abstract

Electron probe microanalysis of biological bulk specimens, as compared to thin specimens, is limited by poor X-ray spatial resolution. On the other hand preparation methods for bulk specimens are often much simpler than for thin specimens. With respect to quantitation, however, numerous problems arise, such as poorly known composition of the matrix, local density differences, charging, mass loss, contamination, poorly defined surface topography, etc. The various quantitation methods, commonly used, include the use of ideal and non-ideal standards, the use of P/B-ratios, the calculation of ZAF-correction, and the use of so-called non-standard methods. The accuracy or reliability of the various methods has hardly been systematically investigated. It is shown that approximations from model systems will be necessary. Finally it is expected that the method used for particle analysis will be useful for the investigation of biological bulk specimens.

Introduction

In the field of electron probe X-ray microanalysis (EPMA) of biological objects, much attention has been given in recent years to the analysis of thin specimens. Although in most cases thin specimens indeed offer the best possibility to carry out meaningful quantitative analysis with the EPMA-technique, specimen preparation methods, especially the cryotechniques recommended, are very tedious and still far from perfect. Preparation methods for biological thick specimens, on the other hand, are often simpler and faster. The inherently poor X-ray spatial resolution of EPMA of thick specimens is in many instances not a serious drawback, for instance when relatively large biological compartments are to be analyzed, such as whole cells or intercellular spaces¹. Indeed in a number of studies the EPMA technique has been applied to thick specimens to solve a variety of biological problems. Various aspects of quantitation of thick biological specimens, however, have received little attention in the past. For this reason we pay attention in this review to the quantitative EPMA of biological thick specimens. We define a specimen to be a thick or 'bulk' specimen, when it is thick enough to decrease the kinetic energy of the beam electrons to the level of the critical ionization energy of a given shell (K, L or M) for the element under consideration.

We want to emphasize that we will not consider consequences of specimen preparation artifacts or artifacts of spectrum deconvolution. We will assume that correct values of net peak intensities and background counts of the specimens are available.

First we will elaborate on our definition of bulk specimens in relation to electron beam-specimen interactions. Then we will discuss specific problems of quantitative EPMA of biological bulk specimens and in a number of instances suggest ways to prevent or solve problems. Subsequently we will pay attention in some detail to various quantitation methods for bulk specimens as used in the literature. Our review ends with concluding remarks on quantitative EPMA of biological bulk specimens.

KEY WORDS Electron Probe X-ray Microanalysis, Biological Bulk Specimens, Quantitative Analysis, ZAF-correction Programs, Standards, P/B-ratios, Surface Topography, Matrix Substituting Element, Mass Loss

The whole field of quantitative EPMA has recently been reviewed by Russ², Lifshin³, Statham⁴, Fiori and Newbury⁵, and by Newbury⁶. Reviews on biological EPMA have been given by Coleman⁷, by Chandler⁸ and by Lechene and Warner⁹. Quantitative biological EPMA, mainly of thin specimens, has been reviewed by Hall^{10,11} and by Barbi¹². Roomans¹³ has reviewed the use of standards in quantitative biological EPMA.

List of Abbreviations and Symbols

A	Absorption
α	Spectrometer angle
B	Background intensity
β	The complement of the angle between the projection of the spectrometer axis on the horizontal plane and the tilt axis
BICEP	Program by Warner and Coleman ^{59,60} for thin biological specimens
BIOFLEX	Program by present authors for biological bulk specimens
C	Concentration
γ	Take-off angle
E	Energy
E_c	Critical ionization energy
E_0	Energy of beam electrons, accelerating voltage
ED	Energy dispersive
EPMA	Electron probe microanalysis
F	Fluorescence
FRAME-P	Program by Small et al ⁷⁴ for particles
$\phi(\rho z)$	Distribution of primary ionizations as a function of mass thickness
index i	Indicates the i -th element
K-ratio	Ratio of peak intensity of a certain element in a specimen to peak intensity for pure elemental standard
MAGIC-IV	Program by Colby ⁶¹ for bulk specimens
MIC	Program by Warner and Coleman ⁶⁰ for biological bulk specimens
MODEL	Program by Eshel ⁶² for biological specimens
P	Net peak intensity
ψ	Tilt angle
P/B	Ratio of net peak intensity to background intensity
PZAF	Program by Aden and Busek ⁷³ for particles
R	Radius of the sphere describing the excitation volume
ρ	Specific mass
S	Stopping power
x_r	Range of electrons penetrating matter
Z	Atomic number
ZAF	Combined effects of atomic number, absorption, and fluorescence
(Z^2/A)	Mean of atomic number squared over atomic weight

Electron Beam-Specimen Interaction

Penetration

In a specimen the electron beam will be broadened mainly as a consequence of elastic collisions of the electrons with atomic nuclei. As a consequence of inelastic collisions the kinetic energy of the beam electrons gradually decreases to zero unless the electrons have left the specimen earlier. Obviously there is a relation

between the phenomena of beam broadening and energy loss on the one side and the maximum penetration depth of the beam electrons on the other side. With so-called Monte Carlo calculations¹⁴ of the trajectories of beam electrons in matter, it is possible approximately to describe the shape of the X-ray excitation volume. Thus it has been calculated that in specimens with a low mean atomic number ($\bar{Z} = 13$), the excitation volume has a teardrop shape. For specimens with a higher \bar{Z} the excitation volume will be a half sphere¹⁵.

It is common to calculate the electron range in matter with the following equation

$$x_r = E_0 \int_0^0 \frac{dx}{dE} \int_0^E \frac{1}{\rho S} dE \quad (1)$$

where x_r = the electron range, ρ - the specific mass, S - the stopping power, E_0 = the accelerating voltage and E - the energy of the beam electrons.

By applying the 'Bethe formula' for the stopping power the electron range can be calculated (see e.g. Reed¹⁶). The electron range also indicates the maximum depth in the specimen for the excitation of primary continuum radiation. The element-specific primary X-ray line spectrum arises from a smaller volume, since the beam electrons must have a certain minimum kinetic energy equal to the critical ionization energy E_c , to be able to knock out a certain shell electron. Several formulae to calculate the maximum depth for the generation of element-specific primary X-rays have been published, a few of which are

Andersen and Hasler¹⁷ $x_1 = 0.064 \frac{E_0^{1.68} - E_{c1}^{1.68}}{\rho}$ (2)

Reed¹⁸ $x_1 = 0.048 \frac{E_0^{1.5} - E_{c1}^{1.5}}{\rho}$ (3)

Colby¹⁹ $x_1 = 0.033 \frac{E_0^{1.5} A_1}{\rho Z_1}$ (4)

where x_1 = maximum depth for X-rays from element 1 in μm ,

Z_1 = atomic number of element 1,
 A_1 = atomic mass of element 1, E_0 = accelerating voltage in kV, E_{c1} = critical ionization energy of element C_1 in kV and ρ = specific mass in g/cm^3 .

Formula (4) is only valid for those instances in which the overvoltage E_0/E_{c1} is more than 10. When the excitation volume has the shape of a half sphere the resolution can be defined by the radius R_1 of the sphere from which originated 99% of the primary generated element-specific X-rays¹⁶.

$$R_1 = 0.231 \frac{E_0^{1.5} - E_{c1}^{1.5}}{\rho} \quad (5)$$

Because of the fact that the excitation volume in biological material will have a teardrop shape,

Depth of generation of X-rays												
Accelerating voltage (kV)	10						20					
Type of radiation	Al K α			Ca K α			Al K α			Ca K α		
Specific Mass (kg/m ³)	200	1000	3000	200	1000	3000	200	1000	3000	200	1000	3000
Generation depth (m) according to												
Andersen and Hasler ¹⁷	15	2.9	1.0	13	2.5	0.83	49	9.7	3.2	46	9.2	3.1
- Reed ¹⁸	7.1	1.4	0.47	6	1.2	0.40	21	4.2	1.4	20	4.0	1.3
- Colby ¹⁹ *	-	-	-	-	-	-	31	6.2	2.1	-	-	-

Table 1 Maximum depths of generation of primary Al K α and Ca K α radiation for different accelerating voltages and values for the specific mass of the specimen
* Colby's formula is only valid for overvoltage $E_0/E_c > 10$

it is obvious that in this case there are at least two quantities needed to effectively describe the resolution. In the case of perpendicular incidence of electrons on the specimen we suggest using the maximum depth for the generation of element-specific primary X-rays as a measure of the *depth resolution*, and the maximum diameter of the broadened beam as a measure of the *lateral resolution*. If this suggestion is adopted, the term spatial resolution should not be used anymore (as we will do further on). When the specimen is tilted the situation becomes complicated. Now the maximum depth for the generation of X-rays as measured perpendicular to the specimen surface should be used as the depth resolution, and the size of the projection of the excitation volume on the specimen surface as the lateral resolution.

In the formulae 2-5 a value for the specific mass of the specimen must be assigned to ρ . For frozen-hydrated soft biological tissues the specific mass will be about 1000 kg/m³. In freeze-dried material with an initial water content of 75%-85%, the specific mass will drop to about 250-150 kg/m³. Freeze-dried tissue that has been embedded in resins will have a specific mass of about 1100 kg/m³ taking into account a shrinkage of 20% (v/v)²⁰. The specific mass of hard tissues usually is considerably higher. For example dentine is assumed to have a specific mass approximately equal to apatite (3100-3300 kg/m³). Using typical values for the accelerating voltage and the specific mass we calculated with the formulae 2, 3 and 4 values for the maximum depth for the generation of primary Al K α and Ca K α X-rays, see Table 1.

In order to make the ionization volume profile visible, Possin and Norton²¹ irradiate layers of polymethylmethacrylate with 5 and 10 kV electrons. The absorbed ionization energy strongly enhances the solubility of the polymer in a suitable developer. Typical dimensions of such a profile for an accelerating voltage of 10 kV and a specific mass of the polymer of about 1200 kg/m³ are a depth of about 1.7 μ m and a lateral width of about 2 μ m. In order to estimate the maximum depth of generation of primary Al K α

X-rays in biological specimens Zs-Nagy et al²² and Wroblewski et al²³ mount sections of known nominal thickness on an aluminium support. They measure the Al K α X-rays emerging from the support as a function of thickness. For polymer sections they find a maximum depth of about 3 μ m for 10 kV and a depth of about 6 μ m for 20 kV.²² Zs-Nagy et al²², and Wroblewski et al²³, also analyze freeze-dried tissue sections and find a maximum penetration depth of about 5 μ m using 10 kV and a depth of about 12 μ m for 20 kV accelerating voltage.

Charging
Charging can be described as a surplus of (negative) charge in the specimen. Charging of a specimen occurs when the total beam current initially is larger than the total current which can leave the specimen by common processes. At the start of the electron irradiation, incident beam electrons will form an internal space charge. As a consequence the mean penetration depth of beam electrons will be decreased.²⁴ In general the occurrence of charging is associated with a redistribution, as a function of depth, of the primary ionizations. The kinetic energy of the beam electrons is then decreased by both inelastic scattering and electrostatic repulsion.^{25,26} Obviously this will influence the depth resolution as well as the lateral resolution.

It is important to realize that all ZAF-correction formulae have been derived for primary ionization distribution curves based on inelastic and elastic scattering phenomena only. Buchner and Stienen²⁴ remark that ZAF-correction formulae must be adjusted when the electrical conductivity decreases below 10^{-8} (Ω cm)⁻¹.

Loss of mass

Loss of mass occurs when molecules and/or fragments of molecules disappear from the specimen into the vacuum of the probe instrument. Loss of mass is governed by the dissipation of the energy of beam electrons in the specimen, which, together with the poor thermal conductivity of the specimen, causes the breaking of chemical bonds. Radiation damage and mass loss have recently been reviewed by Cosslett²⁷, and Glaeser and Taylor²⁸. Mass loss can lead to an

altered elemental composition in the analyzed volume and to a modification of surface topography. When occurring, these consequences of mass loss will have a large influence on quantitation. Edie and Glick²⁹ have studied the 'dynamic counting rate' during EPMA of unstable specimens. They find that after some time has elapsed the analysis actually is performed on the bottom of a pit. Moreover the specific mass appears to be locally increased as a consequence of the electron irradiation.

Contamination

Contamination occurs when molecules and fragments of molecules are deposited on the specimen. These deposits originate either from compounds present in the vacuum of the instrument or from the specimen itself and its surface coating. One of the annoying effects of contamination in EPMA is the appearance of additional peaks in the spectrum (e.g. Si K α). Contamination can also mean that after a certain time interval the analyzed volume contains matter of a different elemental composition. Moreover contamination can change the surface topography. For reviews on contamination, see Reimer³⁰ and Fourie³¹.

Specific Problems of Biological Bulk Specimen

In this section we shall review the optimization of specimen preparation and analytical procedures with especial reference to quantitative analysis of biological bulk specimens.

Penetration

Characteristic for soft biological tissue is that the electron penetration depth is large, resulting in a poor X-ray lateral and depth resolution. Resolution can be improved in a number of ways. Firstly one can decrease the penetration depth considerably (by approximately a factor 5) by studying frozen-hydrated or epoxy-resin embedded specimens instead of freeze-dried specimens. Secondly, the choice of the accelerating voltage is important. Swift³², for instance applies a very low accelerating voltage (3 kV) in the analysis of sulphur in hair to ensure that the majority of the X-rays are not generated beyond a certain depth. Therefore it may be useful to deviate from the rule of thumb to analyse at an overvoltage E_0/E_c of 2-3. Another method to decrease the mean penetration depth of the electrons is to tilt the specimen towards the beam. Thus Zs-Nagy et al.²² studied Na and K in liver cells nuclei, using a tilt angle of 45°.

Charging

In general biological specimens are poor conductors of electricity. The charging which can possibly occur poses a problem in quantitation since both size and shape of the excitation volume change and the electron beam can jump across the specimen due to electrostatic repulsion. Several methods can be applied to prevent or diminish charging or to minimize its effects. Firstly conducting layers can be deposited onto the specimen surface. The pros and cons of coating and sputtering have been reviewed by DeNee and Walker³³ and Echlin³⁴. Carbon or aluminium are often used as conducting materials, but

Marshall³⁵ concludes from his work on frozen hydrated Malpighian tubules (-145°C) that chromium is more effective in the elimination of charging.

It is often mistakenly assumed that a conducting layer is effective in eliminating all charging. Fuchs et al.^{26,36} studying charging phenomena in ice layers, have observed that internal space charging occurs even when a carbon coating is present. A possible disadvantage of conducting layers, not particularly important for EPMA, however, is that the image resolution may be deteriorated. Therefore methods have been developed to improve the electrical conductivity throughout the specimen by a chemical reaction. An example of such a reaction which may be suitable in X-ray microanalysis, is osmium vapour fixation. Other treatments suggested are mostly of the wet-chemical type and will undoubtedly influence the concentration distribution and the quantitation of weakly bound elements. For a review of these methods see Murphy³⁷. A recent development is the charge eliminating method, proposed by Crawford³⁸, which is applied during analysis in the microscope. In this method the surface charging is eliminated by bombardment of the specimen with a beam of lithium ions with an energy of a few eV. Crawford³⁸ states that his method will not damage the specimen and that the use of lithium will not interfere with X-ray microanalysis because thin layers only are 'deposited'. It is unknown whether this method can eliminate internal space charging.

As for the analytical conditions (i.e. specimen temperature, time of analysis, accelerating voltage and beam current, specimen-detector geometry) it is obvious that accelerating voltage and beam current have an influence on charging. For quartz Buchner and Stienen²⁴ find an increase of charging with increasing beam current and/or increasing accelerating voltage. Fuchs et al.²⁶ report that charging in ice layers, present on an aluminium supporting layer, can be eliminated completely by application of a carbon coating and by limiting the ice layer thickness to at most twice the penetration depth of the electrons.

Another important analytical condition in relation to charging is the specimen temperature. During the last years contradictory findings have been published concerning this point. Marshall³⁵ investigates carbon coated frozen hydrated specimens (20% albumin standards) and concludes that charging becomes more serious when the specimen temperature decreases from -65° to -105°C. However, Ledbetter³⁹, studying frozen hydrated plant tissue, does not find charging even in uncoated specimens. This is probably related to the very low beam current he uses. Ledbetter uses 5-100 pA, whereas Marshall³⁵ is using 500 pA. Zs-Nagy et al.²² also are not troubled by charging in their analyses of uncoated freeze-dried liver. These authors do not specify the current they have used. Wittry and Wu⁴⁰ study charging in frozen-hydrated specimens of GaAs and extrapolate their findings to the analysis in ice. They argue on theoretical grounds that under certain conditions such specimens can be investigated without a conducting layer and without charging. In our opinion it is important to consider

electrical conductivity aspects when choosing a standard, since it is possible that internal space charging can be similarly produced in a suitable standard so that its effect on quantitation is cancelled out.

It is perhaps possible in the future to take into account the effects of internal space charging in applying ZAF-correction. To this end it is necessary that $\rho(\rho z)$ -curves for poorly conducting materials are available. In this respect the Monte Carlo approach may be useful.

Loss of mass, contamination

As emphasized above, biological material is very sensitive to electron beam irradiation with electron energies > 1 keV. Structures can be damaged and chemical bonds can be broken, but in quantitative EPMA of biological bulk specimens this type of damage in itself is of minor importance. It is important, however, when certain volatile components disappear from the specimen, and when certain components disappear faster than to others. It is obvious that in this case mass and composition of the sample may be changed, thus influencing the quantitation. Radiation damage has been studied especially in high resolution transmission electron microscopy and many methods to prevent damage have been investigated here. For reviews, see Cosslett²⁷, and Glaeser and Taylor²⁸. The embedding of freeze-dried material in epoxy resin or keeping the specimen in the frozen-hydrated state, may probably help to prevent volatile radiation products leaving the specimen. The application of a metal coating may be of importance since this improves the thermal conductivity of the specimen. One of the most important preventive measures, however, is the radical lowering of the specimen temperature before and during the analysis. Several investigators keep their frozen-hydrated specimens below about -145°C to prevent even superficial freeze-drying of the specimen (Fuchs et al.³⁶).

Another important way to prevent damage and mass loss is the lowering of the beam current density, which of course is accompanied by the disadvantage of a proportionally decreasing X-ray yield. Hohling et al.⁴¹ find for doubly coated thin specimens that a beam current density of $10 \text{ nA}/\mu\text{m}^2$ does not cause any measurable mass loss. Using thin specimens Hall and Peters⁴², state that $5 \text{ nA}/\mu\text{m}^2$ gives an acceptable X-ray yield. We do not know if the situation for EPMA of biological bulk specimens is as bright as for thin specimens. It is very doubtful whether it is possible to simulate the specimen mass loss by choosing an appropriate standard (c.f. Hall and Peters⁴²). In the prevention of contamination the quality of the vacuum in the microscope is of great importance. Values of $< 1.2 \times 10^{-5}$ Pa have been recommended⁴³. In general it is strongly advisable to cool the specimen environment with a cold trap surrounding the specimen as completely as possible. If in that case the specimen itself is also cooled this can give a further contribution to prevent contamination.

Surface topography

Originally, or as a consequence of the applied preparation method (e.g. freeze fracturing) the surface of biological bulk specimens will not be flat. Mass loss and contamination can also

modify surface topography. This obviously influences quantitation because a non-flat surface leaves the shape of the excitation volume poorly defined, since tilt angle and take off angle are not known exactly.

It is possible to minimize the effect of a non-flat surface on quantitation by choosing the appropriate analytical conditions. If the excitation volume is an order of magnitude larger than is the roughness of the surface, the effect of this roughness will be relatively small. In this respect the density of the specimen, the accelerating voltage and the X-ray energy to be analyzed are important. Furthermore the effect of variations in the specimen-detector geometry (see Fig. 1) will be smaller if a high take-off angle can be realized. Finally one can minimize the influence of specimen roughness on the results by using P/B-ratios instead of net peak intensities (see Wroblewski et al.²³). Both Small et al.⁴⁴ and Statham and Pawley⁴⁵ have studied the effect of the poorly defined surface topography of glass particles on the results and they find that the P/B-ratios are relatively insensitive for variations in shape or size of the particles.

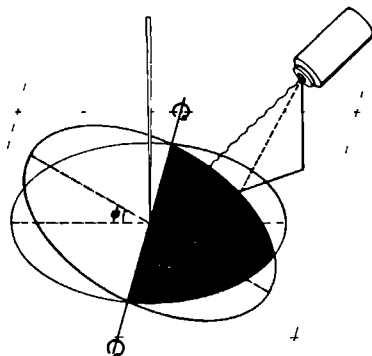


Fig. 1. The specimen-spectrometer geometry α = the spectrometer angle, ψ = the tilt angle γ = the take-off angle, β = the complement of the angle between the projection of the spectrometer axis on the horizontal plane and the tilt axis

Local density

In a wet or a frozen-hydrated biological specimen local density variations generally will be small. In freeze-dried specimens, however, differences can be larger. For this reason Ingram et al.²⁰ embed their freeze-dried specimens in an epoxy resin. Another example of establishing a matrix with the same density throughout the specimen is the impregnation of dental enamel with potassium iodide (Frank et al.⁴⁶), after the extraction of organic matter.

Additional density variations can occur when the biological material is fixed with heavy elements. Ingram and Ingram⁴⁷, e.g. fix their freeze-dried specimen with osmium (VIII) oxide vapour,

before embedding. In analyzing their specimen in the linescan mode they correct for local density variations by using the continuum X-ray signal as a measure of the local density. Furthermore, they show that the backscattered electron signal⁴⁸ can be used instead of the continuum X-ray signal.

Poorly Known Matrix Composition

In biological specimens the mass fractions of the light matrix elements H, C, N and O usually are relatively large. When carrying out a ZAF-correction the influence of these elements on quantitation is important. Accurate knowledge of the mass fractions of the matrix elements is then required. However, with EPMA these light elements are difficult to analyze, and with other techniques only approximate overall information can be obtained, for instance as mass fraction ratios.

Several commercial ZAF-correction programs offer the possibility of specifying one element which can be determined by difference. Therefore it goes without saying that one will choose as the element to be determined by difference the most abundant matrix element which is often carbon. However, we will show that with this approach errors of up to 15% in the ZAF-corrected concentrations can be introduced.

Quantitation Methods For Biological Bulk Specimens

Initially the EPMA-technique has found application mainly in materials science. As a consequence, the preparation and quantitation methods from materials science, were adopted in the early biological application of the technique. Investigators preferred to work with flat-polished specimens and they looked for standards which, regarding composition and physical properties, resembled the specimen as closely as possible. If such a standard was not available, corrections were carried out for the effects of the differences in composition and physical properties.

Net Peak Intensities, P/B-ratios

Since initially EPMA has been performed with wavelength-dispersive spectrometers only, it is clear that net peak intensities were used as the starting data for quantitation. After the introduction of energy-dispersive X-ray systems, the use of P/B ratios for quantitation was increased, especially for thin specimens. The P/B ratio is the ratio of the net peak counts divided by the continuum radiation counts in a defined region⁷ originating from the specimen only. This means that a good estimate of the extraneous background radiation is needed. This, however, can meet with serious difficulties.⁴⁹ An advantage of using P/B-ratios is that results are relatively unaffected by local variations of the take-off angle. Moreover, when using P/B-ratios, an inherent 'correction' for beam current fluctuations occurs. In 1968 Marshall and Hall⁵⁰ have given a first start for a special biological quantitation method. They proposed the use of P/B ratios instead of the net peak intensities. Although their theory has been developed for thin specimens, P/B-ratios are also used in EPMA of bulk specimens by Cobet and Traub⁵¹. These authors have tested the equation

$$C_{1 \text{ specimen}} = a (P/B)_1 - b \quad (6)$$

In this equation the constants a and b have been derived by using bulk standards of dried polyacrylamide, in which known concentrations of certain elements were present. Zs-Nagy et al²² examine the validity for biological bulk specimens of the following equation

$$C_{1 \text{ specimen}} = a (P/B)_1 \frac{Z^2/A}{Z^2/A} \quad (7)$$

They use crystals of salts like sodium citrate to determine the constant a. In their ZAF-correction procedure Wroblewski et al²³ and Statham⁵² use a ratio of the P/B-ratios for a particular element, from both the specimen and the standard, to get an initial estimation of the concentration. Standards, commonly used in quantitation, can be divided into ideal standards and 'non-ideal' standards, respectively.⁴⁷ In an ideal standard the effects of the interaction of the beam electrons and of the primary generated X-rays with the specimen, are of the same kind and magnitude in specimen and standard. Therefore ZAF-corrections are not necessary. On the other hand, with non-ideal standards corrections must be carried out. Quantitation with ideal standards is very simple.

$$C_{1 \text{ specimen}} = C_{1 \text{ standard}} \frac{P_{1 \text{ specimen}}}{P_{1 \text{ standard}}} \quad (8)$$

in which C = mass fraction, P = net peak intensity and 1 = index for analyzed element. For hard tissues like dentine, ideal standards are often minerals like apatite. For soft tissues gelling solutions of proteins (gelatin, albumin) with salts are often used. Such standards can then be treated similarly to the specimen, including cryofixation, freeze-drying, embedding in resins, etc. Recently, resin soluble organic compounds, containing one of the transition metals or light elements (e.g. Na, P, S, Cl, K) have been developed for use in standards.^{53,54,55} Thus ideal standards can be prepared for analysis of resin embedded specimens. Zierold and Schafer⁵⁶ have developed an interesting method for preparing an ideal standard for non-embedded bulk specimens. Investigating skeletal muscle fiber types, they use muscular tissue in which the membranes were made permeable for ions, as a standard. This tissue is then permeated with an electrolyte solution of known composition.

One of the advantages of non-ideal standards can be an actual high mass fraction of the element under investigation. The time of analysis can then be relatively short while maintaining good counting statistics. Another aspect of importance is that many standards are usually quite homogeneous. As an example of the use of a non-ideal standard we mention the work of Halse⁵⁷, who analyzed iron in teeth, using biotite as a standard. She noted differences in the calculated Fe-concentration, computed with and without ZAF-correction.

ZAF-correction

In a ZAF-procedure corrections are applied for

- loss of kinetic energy of beam electrons (stopping power S)
- partial backscattering of beam electrons
- absorption of primary generated X-rays
- generation and subsequent partial absorption of secondary X-rays (X-ray fluorescence)

These four effects will have different magnitudes in a specimen and a non-ideal standard. For computation of the ZAF-correction factors the elemental composition of the specimen and the standard must be known. For the unknown it is therefore necessary to make initial estimates of all elemental concentrations. For a part of the elements present in the specimen this can be done by analyzing a suitable standard and applying equation (8). For the elements present in a biological specimen which usually are not analyzed (e.g. C, N, O), good estimations of their mass fractions must be available. ZAF-corrections for each of the elements present can then be computed, and then new estimates of the concentrations are calculated according to

$$C_{1, \text{corrected}} = F_{1, \text{ZAF}} C_{1, \text{initial estimation}} \quad (9)$$

in which C = mass fraction, F_{ZAF} = total ZAF-correction factor, λ^2 = index for the element for which the correction is applied

We should like to introduce the notion 'direct ZAF correction' when the unknown is directly compared with the (non-ideal) standard, followed by ZAF-correction. As an example of what we would like to call an 'empirical (ZAF)-correction' we will briefly mention the approach of Ingram and Ingram⁴⁷, and of Maroudas⁵⁸. Ingram and Ingram⁴⁷ have studied Na and K in mouse kidney slices. They first compare measurements on non-ideal standards such as KCl and NaCl crystals with measurements on ideal freeze-dried resin embedded albumin standards. From this they derive empirical correction factors for the elements under investigation. These factors are subsequently used in the analysis of mouse kidney tissue with KCl and NaCl-crystals as standards. Maroudas⁵⁸ analyzes Ca and S in articular cartilage using CaF₂ and Cu₂S as standards. By comparing these non-ideal standards with CaSO₄ in a gelatin-matrix, the correction factors are calculated. Biological ZAF-programs

Warner and Coleman^{59,60} have developed a complete correction program, BICEP, originally meant for thin biological specimens present on a thick support. Though BICEP is also suitable for bulk specimens, the authors recommend the use of their program MIC for bulk specimens. The correction scheme of this program is based on Magic IV from Colby⁶¹. These authors have studied the effect of the composition of the organic matrix Z < 10 on the calculated concentrations of elements with 10 < Z < 21. Their method consists of simulating the composition of the organic matrix by C or N or O. They compute for these cases the mutual relative differences in the calculated concentrations. Max. μm

differences of about 10% are found for elements such as Na and Mg.

Eshel⁶² has developed a biological correction program, MODEL, based on BICEP. With this program he studies the influence of neglecting an element with 10 < Z < 21 in the calculations. He takes into account the in vivo concentration ranges and concludes that errors up to 8-9% can be introduced in the calculated concentrations of the other elements with 10 < Z < 21.

The present authors have developed a ZAF-correction program, BIOFLEX, especially designed for quantitative EPMA of biological bulk specimens.

Features of this program are

- Input of mass fractions of all light elements from the matrix with Z < 10 is possible
- The sum of the mass fractions of the elements Z < 10 can be treated as a variable, whereas their individual mass fractions can be entered as ratios.

With BIOFLEX we have investigated which of a number of commonly used formulae for ZAF-corrections yields the most accurate results. We have compared two absorption correction formulae, two backscattering correction formulae, two stopping power correction formulae and three formulae for the mean ionization potential (a quantity needed for the stopping power correction). The 24 alternative ZAF-correction procedures, which thus arise, have mutually been compared. We have used a large number of sets of EPMA-data from binary systems (composition, K-ratio measured, tilt angle and take-off angle, accelerating voltage, etc.). These data were taken from Love et al.^{63,64} We have restricted our study to systems consisting of elements with Z < 31. An important improvement in ZAF-correction accuracy was achieved, using the absorption correction formula of Bishop⁶⁵ instead of the formula of Philibert⁶⁶, combined with the formula of Duncumb and Reed⁶⁷ instead of the formula of Berger and Seltzer⁶⁸ for the mean ionization potential. We have used the best ZAF-correction alternative in our further studies with BIOFLEX. In these studies we have made use of approximations of the intensities of the elements in the specimen with Z > 10, and we have supposed for the specimen matrix the following: (1) $Z - 6.31$ for freeze-dried tissue, and (2) $Z - 6.96$ for frozen hydrated tissue. These latter figures are taken from reference 69.

Firstly the effect of 'substitution' of all of the elements H, C, N and O of the organic matrix by one element with Z < 10 has been studied. For these cases the differences in the calculated concentrations of elements with 10 < Z < 21 relative to a matrix of natural composition have been determined. The results are presented in figures 2 - 5. From these results we conclude that for the substitution of the matrix of freeze-dried soft biological tissue nitrogen is the optimal choice. For frozen-hydrated tissue, the choice of oxygen appears to be optimal. It must be added that in spite of these efforts, errors larger than 10% can occur. For instance, in the latter case, using 30 kV, 40° tilt angle and a 63° take-off

angle, the error in the calculated sodium concentration is about 15% (cf Fig. 4). These results emphasize the importance of specifying the matrix composition as accurately as possible in applying ZAF-correction.

We have also checked with BIOFLEX the consequences of a poorly defined surface topography for the peak intensities. To this end we have determined how the ZAF-corrected concentration of element 1 (C_1) changes with a change in tilt angle (ψ , compare Fig. 1). The way the quotient ($\Delta C_1 / \Delta \psi$) depends on the spectrometer angle (α) was also determined. The results are shown in figures 6 & 7. We conclude that the effect of the tilt angle variations can be decreased by a factor of about 5 by raising the spectrometer angle from 10° to 60° .

In a similar way we have studied the effect of small variations in the accelerating voltage on the calculated concentrations. A variation of 6% in the accelerating voltage caused a 2% difference in the concentration (see Boekestein et al.⁷⁰, compare also Myklebust and Newbury⁷¹).

Concluding Remarks

From our literature study we would like to conclude that few systematic studies have been performed to investigate the reliability of quantitative EPMA on biological bulk specimens. There is a particular need for studies in which EPMA is performed in parallel with established quantitative methods, carried out on a micro-scale.

Regarding the quantitation aspects described above, it is remarkable that most investigators do realize the effects of electron beam broadening and penetration and of mass loss on their results, but do not pay attention to aspects of internal space charging and the poorly defined surface topography. For instance, it is often assumed that charging has not occurred when the ED-spectrum on the high energy side ends at the energy of the incident beam electrons. When an adequately conducting coating is present, it is obvious that electrostatic repulsion will not occur before the electrons have passed the coating, so that X-rays of the maximum possible energy are generated.

It appears that the number of quantitative EPMA studies with non-ideal standards is rather small. This may be due not only to the increasing possibilities to prepare ideal standards, but also to the complexity of a ZAF-procedure. The empirical approach, as used by Ingram et al.⁴⁷, can be a good alternative. Furthermore, it has been found that the application of a ZAF-correction in many cases is not needed in biological X-ray microanalysis (Sumner⁷²). In a number of studies of biological bulk specimens, quantification is not done by calculating concentrations or concentration ratios, but by correcting net peak intensities for a limited number of effects, e.g. spectrometer efficiency. In these studies no corrections are carried out for atomic number, absorption, and fluorescence effects. We think that although this type of work can be very worthwhile, these studies should not be considered to pertain to the field of

quantitative EPMA.

An important development with possible applications to biological bulk specimens is the quantitative EPMA of solid particles. In this analysis it appears that net peak intensities vary considerably with the exact local position of the electron beam because the shape of the particles is very irregular. Therefore Armstrong⁷³ and Aden and Busek⁷⁴ developed a relatively large program, PZAF, to correct the peak intensities for the effects of the size and the shape of the particle. Small et al.⁷⁵ and Statham and Pawley⁴⁵ have found, however, that the P/B-ratio varies much less with the position of the beam on the particles than the peak intensity does. They found that when a particle and a bulk specimen have the same composition the following equation holds.

$$\begin{aligned} P/B_{\text{particle}} &= P/B_{\text{bulk}} \cdot P'_{\text{particle}} = \\ P_{\text{bulk}} &= P/B_{\text{particle}} \cdot B_{\text{bulk}} \end{aligned} \quad (9)$$

B_{bulk} can be computed if the background is measured on a standard. P'_{particle} is subsequently used in a ZAF-correction procedure, e.g. Frame-P. This method will be of great importance for the quantitative EPMA of biological bulk specimens because these specimens often have a rough surface. Ratio and no-standards methods⁷⁶ have hardly been applied in quantitative EPMA of biological bulk specimens. In these methods the measured net peak intensity of one element is divided by the intensity of the pure element theoretically expected (Russ⁷⁷). In this way K-ratios are calculated which subsequently can be processed in a normal ZAF-correction procedure. Few or no standards are needed so the method is fast and the number of specimen exchanges in the microprobe is minimized, which can be advantageous. However, the accuracy of the method in the analysis of biological bulk specimens is hardly assessed. Furthermore it is not clear which formula can best be used for the ionization cross section (Q), a quantity needed in the theoretical peak calculation (Newbury and Myklebust⁷⁸). Moreover the spectrometer efficiency (in ED-studies) has to be known.

Finally it must be realized that in biological EPMA multi-element standards can be easily prepared, facilitating the much easier type of EPMA with ideal standards.

Acknowledgement

The authors would like to thank Mr. G. Elemans, Mr. P. Suthoff, and Dr. F. Smolders, of the Department of Medical Information Processing of the St. Radboud Hospital of Nijmegen, Medical School, for their assistance in operating the PDP 11/45 computer. Dr. M. van 't Hoff is gratefully acknowledged for his advice and help in the application of statistical tests. Ms. C. van Hoek is gratefully acknowledged for providing us with data of the EDAX BEP program. The authors wish also to express their appreciation to Dr. P.T. Mier for reading the manuscript.

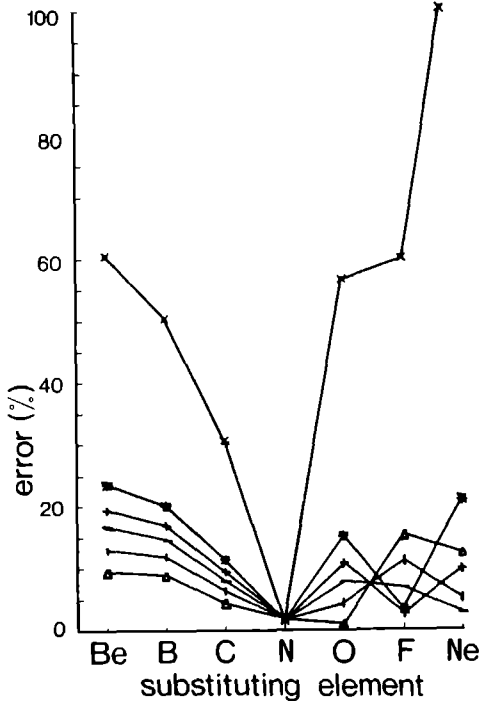


Fig. 2. Relative error in the ZAF-corrected concentrations when the organic matrix of "freeze-dried liver" ($\bar{Z}=6.31$) is substituted by one element with Z lower than 11. Conditions applied are E_0 30 kV; ψ 40°, γ 63°. X=Na, *P; +S, -Cl; |K, Δ=Fe.

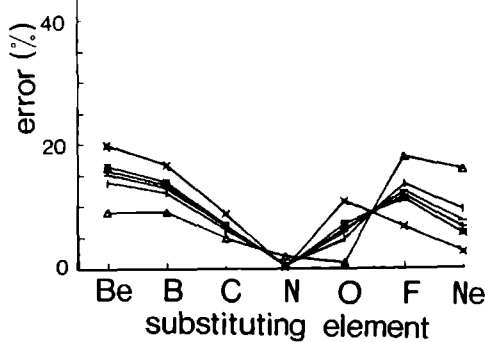


Fig. 3. Relative error in the ZAF-corrected concentrations plotted against Z when the organic matrix of "freeze-dried liver" ($\bar{Z}=6.31$) is substituted by one element with Z lower than 11. Conditions applied are E_0 10 kV; ψ 80°, γ 46°. For the meaning of the symbols see Fig. 2.

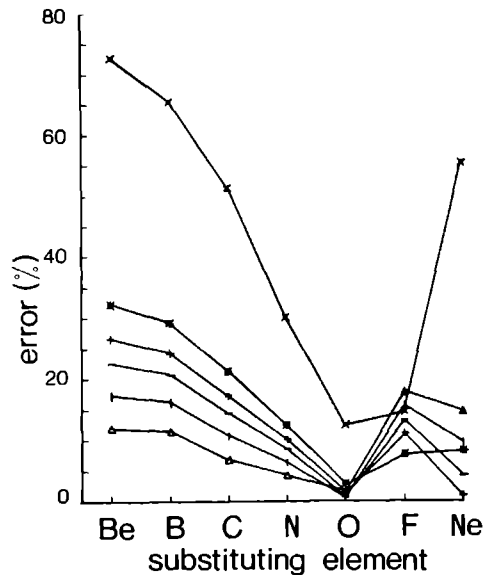


Fig. 4. Relative error in the ZAF-corrected concentrations plotted against Z when the organic matrix of "frozen hydrated liver" ($\bar{Z}=6.96$) is substituted by one element with Z lower than 11. Conditions applied are E_0 30 kV; ψ 40°, γ 63°. For the meaning of the symbols see Fig. 2.

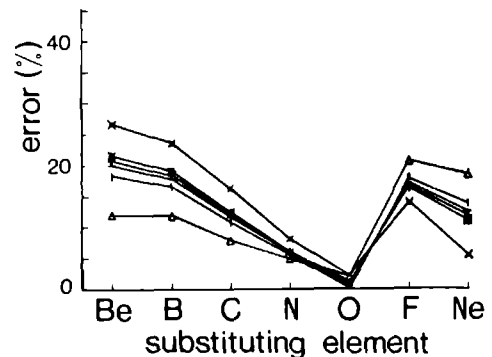


Fig. 5. Relative error in the ZAF-corrected concentrations plotted against Z when the organic matrix of "frozen hydrated liver" ($\bar{Z}=6.96$) is substituted by one element with Z lower than 11. Conditions applied are E_0 10 kV; ψ 80°, γ 46°. For the meaning of the symbols see Fig. 2.

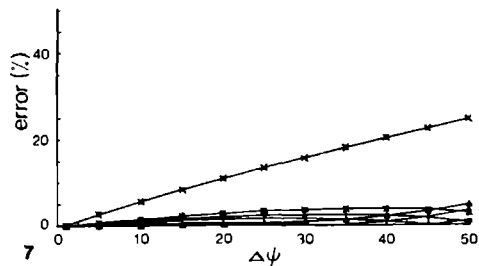
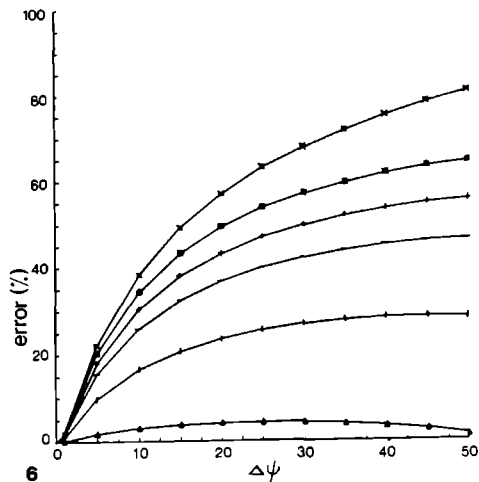


Fig. 6. Relative error (as a function of $\Delta\psi$) introduced in the ZAF-corrected concentrations by differences $\Delta\psi$ between the real local tilt angle and the tilt angle used in the ZAF-correction. The specimen is "frozen hydrated" liver ($Z=6.96$). Conditions applied are: E_0 : 30 kV, ψ : 0° ; γ : 11° . For the meaning of the symbols see Fig. 2.

Fig. 7. Relative error (as a function of $\Delta\psi$) introduced in the ZAF-corrected concentrations by a difference $\Delta\psi$ between the real local tilt angle and the tilt angle used in the ZAF-correction. The specimen is "frozen hydrated liver" ($Z=6.96$). Conditions applied are: E_0 : 30 kV, ψ : 0° ; γ : 61° . For the meaning of the symbols see Fig. 2.

Finally the authors want to thank Mrs Birgitta Hachmang-Rissenbeek and Ms. Annelies Schreurs for typing the manuscript.

References

1. K. Zierold. Versuche zur quantitativen Röntgen-Mikroanalyse an Gefrierbrüchen biologischer Proben. Beitr. Elektronenmikroskop. Direktabb. Oberfl. 9, 1976, 85-102.
2. J.C. Russ. X-ray Microanalysis in the Biological Sciences. J. Submicr. Cytol. 6, 1974, 55-79.
3. E. Lifshin. Quantitative Microprobe Analysis with Energy Dispersive Detectors - A Status Report. Adv. in X-ray Analysis 19, 1976, 113-152.
4. P.J. Statham. Quantitative Chemical Analysis with E.D.S. Systems. In: 13th Annual Conference of the Microbeam Analysis Society, Ann Arbor, 1978, paper no. T2.
5. C.E. Fiori & D.E. Newbury. Artefacts observed in Energy Dispersive X-ray spectrometry in the Scanning Electron Microscope. SEM/1978/I, SEM Inc., AMF O'Hare, IL. 60666, 401-422.
6. D.E. Newbury. Microanalysis in the Scanning Electron Microscope: Progress and Prospects. SEM/1979/II, SEM Inc., AMF O'Hare, IL. 60666, 1-20.
7. J.R. Coleman. X-ray Analysis of Biological Samples. SEM/1978/II, SEM Inc., AMF O'Hare, IL. 60666, 911-926.
8. J.A. Chandler. Principles of X-ray Microanalysis in Biology. SEM/1979/II, SEM Inc., AMF O'Hare, IL. 60666, 595-606.
9. C.P. Lechene & R.R. Warner. Microbeam Analysis in Biology. Academic Press, New York 1979.
10. T.A. Hall. The Microprobe Assay of Chemical Elements. In: Physical Techniques in Biological Research, 2nd ed. Ed.: G. Oster, Academic Press, New York, 1971, 1A, 157-275.
11. T.A. Hall. Methods of Quantitative Analysis. J. Microscopie Biol. Cell. 22, 1975, 271-282.
12. N. C Barbi. Quantitative Methods in Biological X-ray Microanalysis, SEM/1979/II, SEM Inc., AMF O'Hare, IL. 60666, 659-672.
13. G.M. Roomans. Standards for X-ray microanalysis of Biological Specimens. SEM/1979/II, SEM Inc., AMF O'Hare, IL. 60666, 649-658.
14. G. Shinoda, K. Murata & R. Shimizu. Scattering of Electrons in Metallic Targets. In Quantitative Electron Probe Microanalysis. National Bureau of Standards, Washington, 1968, 155-187.
15. J.I. Goldstein & H. Yakowitz. Practical Scanning Electron Microscopy, Electron and Ion Microprobe Analysis. Plenum Press, New York & London, 1975, 57.
16. S.J.B. Reed. Electron Microprobe Analysis. Cambridge University Press - Cambridge, 1975, 211-217.
17. C.A. Andersen, & M.F. Hasler. Extension of Electron Microprobe Techniques to Biochemistry by the Use of Long Wavelength X-rays. In: 4th International Congress on X-ray Optics and Microanalysis. Eds.: R. Castaing, P. P. Deschamps & J. Philibert. Hermann, Paris, 1966, 310-318.
18. S.J.B. Reed. Spatial Resolution in Electron Probe Microanalysis. In: 4th International Congress on X-ray Optics and Microanalysis. Eds.: R. Castaing, P. Deschamps & J. Philibert. Hermann, Paris, 1966, 339.

19. J.V. Colby Quantitative Microprobe Analysis of Thin Insulating Films. In *Advances in X-ray Analysis*, 11, Eds J. Newkirk, G. Mallett & H. Pfeiffer. Plenum Press, New York, 1968, 287-305.
20. F.D. Ingram, M.-J. Ingram & C.A.M. Hogben. An Analysis of the Freeze-Dried Plastic Embedded Electron Probe Specimen Preparation. In *Microprobe Analysis as Applied to Cells and Tissues* eds. T. Hall, P. Echlin & R. Kaufmann. Academic Press, New York & London, 1974, 119-146.
21. G.E. Possin & J. T. Norton. Spatial Distribution of 5 and 10 Kilovolt Electron Beam Ionization in Solids. *SEM/1975*, IIT Research Institute, Chicago, IL. 60616, 457-464.
22. I. Zs.-Nagy, C. Pierni, C. Guilli et al. Energy Dispersive X-ray Microanalysis of the Electrolytes in Biological Bulk Specimens. *J. Ultrastruc. Res.* 58, 1977, 22-33.
23. R. Krowblewski, G.M. Roomans, E. Jansson et al. X-ray Microanalysis of Human Muscle Biopsies. *Histochem.* 55, 1978, 281-292.
24. A.R. Buchner & A.P.M. Stienen. Einfluss der elektrischen Leitfähigkeit der Probe auf die Korrekturberechnung bei der quantitativen Mikrosondenanalyse. *Mikrochim. Acta* 1976 II, 635-652.
25. J.D. Brombach. Electron-Beam X-ray Microanalysis of Frozen Biological Bulk Specimen Below 130 K, II. The Electrical Charging of the Sample in Quantitative Analysis. *J. Microsc. Biol. Cell.* 22, 1975, 233-238.
26. W. Fuchs, J.D. Brombach & W. Trosch. Charging Effect in Electron-Irradiated Ice. *J. Microsc.* 112, 1978, 63-74.
27. V.E. Cosslett. Radiation Damage in the High Resolution Electron Microscopy of Biological Materials: a Review. *J. Microsc.* 113, 1978, 113-129.
28. R.M. Glaser & K.A. Taylor. Radiation Damage relative to Transmission Electron Microscopy of Biological Specimens at Low Temperature - a Review. *J. Microsc.* 112, 1978, 127-138.
29. J.W. Edie & P.L. Glick. Electron Irradiation Products from Organic Materials and Implications for Microanalysis of Biological Sections. In 14th Annual Conference of the Microbeam Analysis Society, San Francisco Press, San Francisco, 1979, 81-84.
30. L. Reimer & M. Wachter. Contribution to the Contamination Problem in Transmission Electron Microscopy. *Ultramicroscopy* 3, 1978, 169-174.
31. J.I. Fourie. A Theory of Surface-Originating Contamination and a Method for its Elimination. *SEM/1979/II*, SEM Inc., AMF O'Hare, IL. 60666, 87-102.
32. J.A. Swift. Minimum Depth Electron Probe X-ray Microanalysis as a Means for Determining the Sulphur Content of the Human Hair Surface. *Scanning* 2, 1979, 83-88.
33. P.B. DeNee & E.R. Walker. Specimen Coating Technique for the SEM - A Comparative Study. *SEM/1975*, IIT Research Institute, Chicago, IL 60616, 225-232.
34. P. Echlin. Sputter Coating Techniques for Scanning Electron Microscopy. *SEM/1975*, IIT Research Institute, Chicago, IL. 60616, 217-224.
35. A.T. Marshall. Electron Probe X-ray Microanalysis of Frozen-Hydrated Biological Specimens. *Microsc. Acta* 79, 1977, 254-266.
36. W. Fuchs, B. Lindemann & J.D. Brombach. Instrumentation and Specimen Preparation for Electron Beam X-ray Microanalysis of Frozen Hydrated Bulk Specimens. *J. Microsc.* 112, 1978, 75-87.
37. J.A. Murphy. Non-Coating Techniques to Render Biological Specimens Conductive. *SEM/1978/II*, SEM Inc., AMF O'Hare, IL. 60666, 175-194.
38. C.K. Crawford. Charge Neutralization Using Very Low Energy Ions. *SEM/1979/II*, SEM Inc., AMF O'Hare, IL. 60666, 31-46.
39. M.C. Ledbetter. Practical Problems in Observation of Unfixed, Uncoated Plant Surface by SEM. *SEM/1976/II*, IIT Research Institute, Chicago, IL. 60616, 453-460.
40. D.B. Vittry & C.J. Wu. The Charging of Semi-Insulating Specimens in Electron Microprobe Instruments. *SEM/1975*, IIT Research Institute, Chicago, IL. 60616, 441-446.
41. H.J. Hohling et al., cited by T.A. Hall & B.L. Gupta. Beam-Induced Loss of Organic Mass under Electron-Microprobe Conditions. *J. Microsc.* 100, 1974, 177-188.
42. T.A. Hall & P.D. Peters. Quantitative Analysis of Thin Sections, and the Choice of Standards. In *Microprobe Analysis as Applied to Cells and Tissues*, Eds. T. Hall, P. Echlin & R. Kaufmann. Academic Press, New York, London, 1974, 229-237.
43. C. Lechene. Electron Probe Microanalysis of Bulk Frozen Hydrated Biological Samples. In 14th Annual Conference of the Microbeam Analysis Society, San Francisco Press, San Francisco, 1979, 59-60.
44. J.A. Small, K.F.J. Heinrich, C.E. Fiori et al. The production and Characterization of Glass Fibers and Spheres for Microanalysis. *SEM/1978/I*, SEM Inc., AMF O'Hare, IL. 60666, 445-454.
45. P.J. Statham & J.B. Pawley. A New Method for Particle X-ray Microanalysis Based on Peak to Background Measurements. *SEM/1978/I*, SEM Inc., AMF O'Hare, IL. 60666, 469-478.
46. R.M. Frank, M. Capitant & J. Goni. Electron Probe Studies of Human Enamel. *J. Dent. Res.* 45, 1966, 672-682.
47. F.D. Ingram & M.-J. Ingram. Quantitative Analysis with the Freeze-Dried, Plastic Embedded Tissue Specimen. *J. Microscopie Biol. Cell.* 22, 1975, 193-204.
48. F.D. Ingram & M.-J. Ingram. Backscattered Electron Signal for Background Monitoring with Biological Tissue Samples. In 9th Annual Conference of the Microbeam Analysis Society, Ottawa, 1974, paper no. 11.
49. A.G.S. Janossy & D. Neumann. Quantitative X-ray Microanalysis. Microcrystal Standards and Excessive Background. *Micron* 7, 1976, 225-229.
50. D.J. Marshall & T.A. Hall. Electron-Probe X-ray Microanalysis of Thin Films. *Brit. J. Appl. Phys.* 2, 1968, 1651-1656.
51. U. Cobet & F. Traub. Untersuchungen an speziellen biologischen Geweben mit der Elektronenstrahlmikroskonde. *Exp. Techn. Physik* 19, 1971, 479-480.
52. P.J. Statham. A ZAF-Procedure for Microprobe Analysis Based on Measurements of Peak-to-Background Ratios. In 14th Annual Conference of the Microbeam Society, San Francisco Press, San Francisco, 1979, 247-253.

53. G.M. Roomans & H.L.M. van Gaal. Organometallic and Organometalloid Compounds as Standards for Microprobe Analysis of Epoxy Resin Embedded Tissue. *J. Microsc.* 109, 1977, 235-240.
54. G.M. Roomans. Quantitative X-ray Microanalysis of Halogen Elements in Biological Specimens. *Histochem.* 65, 1979, 49-58.
55. A.R. Spurr. Choice and Preparation of Standards for X-ray Microanalysis of Biological Materials with Special Reference to Macrocyclic Polyether Complexes. *J. Microscopie Biol. Cell.* 22, 1975, 287-302.
56. K. Zierold & D. Scafer. Quantitative X-ray Microanalysis of Diffusible Ions in the Skeletal Muscle Bulk Specimen. *J. Microsc.* 112, 1978, 89-93.
57. A. Halse. An Electron Microprobe Investigation of the Distribution of Iron in Rat Incisor Enamel. *Scand. J. Dent. Res.* 80, 1972, 26-32.
58. A. Maroudas. X-ray Microprobe Analysis of Articular Cartilage. *Conn. Tiss. Res.* 1, 1972, 153-163.
59. R.R. Warner & J.R. Coleman. A Procedure for Quantitative Electron Probe Microanalysis of Biological Material. *Micron* 4, 1971, 61-68.
60. R.R. Warner & J.R. Coleman. Quantitative Analysis of Biological Material Using Computer Correction of X-ray Intensities. In: Microprobe Analysis as Applied to Cells and Tissues. Eds. T. Hall, P. Echlin & R. Kaufmann. Academic Press, New York & London, 1974, 249-268.
- *61. J.W. Colby. Magic IV-a New Improved Version of Magic. In 6th National Conference on Electron Probe Analysis, Pittsburgh, 1971, paper no. 17.
62. A. Eshel. Quantitative Electron Probe Microanalysis of Biological Specimens. I, A Theoretical Analysis of some Variables involved. *Micron* 5, 1974, 41-49.
63. G. Love, M.G.C. Cox & V.D. Scott. Assessment of Philibert's Absorption Correction Models in Electron-Probe Microanalysis. *J. Phys. D.: Appl. Phys.* 8, 1975, 686-702.
64. G. Love, M.G.C. Cox & V.D. Scott. Assessment of Bishop's Absorption Correction Model in Electron-Probe Microanalysis. *J. Phys. D.: Appl. Phys.* 9, 1975, 7-13.
65. H.E. Bishop. The Prospects for an Improved Absorption Correction in Electron Probe Microanalysis. *J. Phys. D.: Appl. Phys.* 7, 1974, 2009-2020.
66. J. Philibert. A Method for Calculating the Absorption Correction in Electron-Probe Microanalysis. In: 3rd. International Congress on X-ray Optics and X-ray Microanalysis, eds.: H.H. Pattee, V.E. Cosslett & A. Engstrom, Academic Press, New York, 1963, 379-391.
67. P. Duncumb & S.J.B. Reed. The Calculation of Stopping Power and Backscatter Effects in Electron Probe Microanalysis. In: Quantitative Electron Probe Microanalysis. National Bureau of Standards, Washington, 1968, 133-154.
68. M.J. Berger & S.M. Seltzer. In: Studies of Penetration of Charged Particles in Matter. National Research Council Publ. 1133. Natl. Acad. Sciences, Washington DC, 1964, 205.
69. Wissenschaftliche Tabellen, 7th ed., J.R. Geigy A.G., Basel, Switzerland, 1968, 513-519.
- *70. A. Boekestein, G.M. Roomans, A.L.H. Stols & A.M. Stadhouders. ZAF-Correction Procedures in Electronprobe X-ray Microanalysis of Biological Bulk Specimen. In 13th Annual Conference of the Microbeam Analysis Society. Ann Arbor, 1978, paper no. 17.
71. R.L. Myklebust & D.E. Newbury. The Use and Abuse of a Quantitative Analysis Procedure for Energy-Dispersive X-ray Microanalysis. In: 14th Annual Conference of the Microbeam Analysis Society, San Francisco Press, San Francisco, 1979, 231-237.
72. A.T. Sumner. Quantitation in Biological X-ray Microanalysis with Particular Reference to Histochemistry. *J. Microsc.* 114, 1978, 19-30.
73. J.T. Armstrong. Methods of Quantitative Analysis of Individual Microparticles with Electron Beam Instruments. SEM/1978/I, SEM Inc., AMF O'Hare, IL 60666, 455-468.
74. G.D. Aden & P.R. Busek. Rapid Quantitative Analysis of Individual Particles by Energy-Dispersive Spectrometry. In: 14th Annual Conference of the Microbeam Analysis Society, San Francisco Press, San Francisco, 1979, 254-258.
75. J.A. Small, D.E. Newbury & R.L. Myklebust. Analysis of Particles and Rough Samples by Frame P, a ZAF Method Incorporating Peak-to-Background Measurements. In: 14th Annual Conference of the Microbeam Analysis Society, San Francisco Press, San Francisco, 1979, 243-246.
76. A.G.S. Janossy, K. Kovac & I. Toth. Parameters for the Ratio Method by X-ray Microanalysis. *Anal. Chem.* 51, 1979, 491-495.
- *77. J.C. Russ. A Fast, Self-Contained, No-standard Quantitative Program for EDS. In: 13th Annual Conference of the Microbeam Analysis Society, Ann. Arbor, 1978, paper no. 46.
78. D.E. Newbury & R.L. Myklebust. Monte Carlo Calculations of Absolute X-ray Generation from Solid Targets. In: 14th Annual Conference of the Microbeam Analysis Society, San Francisco Press, San Francisco, 1979, 51-53.

Discussion with Reviewers

J.C. Russ: Most ZAF programs can use as the "element by difference" any combination of elements, such as C-H-N-O, provided their ratios can be specified. Indeed the author does this himself in the program he later describes. The statement that only a single element is possible is not correct, and probably reflects the fact that in most materials analyses situations there is only one important missing element (e.g. O in minerals, C in steels).

Authors: We do admit that among the many ZAF-correction programs developed by individual investigators there are several programs which offer the opportunity to enter as the element by difference combinations of elements in fixed ratios (see review by Beaman and Isasi⁷⁹). However, the commercial ZAF programs we had at our disposal did not have such a possibility.

C.E. Fror: In the authors section "local density" the method proposed by Ingram and Ingram⁴⁸ does not seem to correct for local density but rather for local average atomic number.

*Past MAS proceedings also available from San Francisco Press.

Furthermore, it should be noted that Ingrams method may not work for E_0 much below about 7 keV as the backscatter coefficient tends to 0.5 for all Z as E_0 decreases below about 5 keV⁸⁰

J C Russ Background or continuum intensity is proportional to density, as the author states, and also to average atomic number. Since for many of the standards the author discussed, the standard and unknown have different atomic number, an adjustment such as that proposed by Hall¹⁰ must be made. The same problem arises in using P/B ratio as an indication of concentration for rough or particulate samples. If the particle is of different Z than the substrate, or the roughness is related to concentration differences, the background will change and alter the ratio.

Authors The Ingrams apply their method in order to obtain a valid measure of the off-peak background at each point of analysis. In their measurements the background varied partly because of density variations and partly because of variations in the average atomic number. The specimens under consideration always contained about 80% of epoxy resin. They did not use a P/B ratio in their quantitation procedure. Therefore an atomic number correction on their background measurements was unnecessary. From the work of Darlington and Cosslett⁸⁰ it can be deduced that at low accelerating voltage the backscatter coefficient tends to 0.5 for all Z values, but also that even at 2 kV (which for biological EPMA is an absolute minimum) the differences between the backscatter coefficients for different Z are distinct. Ingram did carry out his experiments mostly at 10 kV. When in the analysis of particles or rough surfaces, the P/B ratio cannot be measured on a flat polished sample of the same composition, an atomic number correction of the background measurements can be carried out as recently proposed by Small and coworkers⁸¹.

G M Roomans The binary systems used for the comparison of the ZAF-correction alternatives do not in the least resemble a typical biological specimen. Can your results be extrapolated to biological specimens? Couldn't a correction alternative that was inferior for those binary systems be more suitable for biological specimens? Have you tested how well BIOFLEX performs on biological systems?

Authors We tested BIOFLEX with 199 sets of EPMA data from binary systems consisting of elements with atomic number below 31. Almost all these data were taken from the compilation by Love et al.^{63,64} Among these there were also some systems consisting of C or O with another element. We believe that correction formulae performing well for these systems will be optimal for ZAF-correction in biological bulk specimen analysis. To test BIOFLEX on real biological specimens will require the absence of internal space charging, mass loss, etc.

C E Fiori In formulating a definition of observed X-ray spatial resolution do you propose to neglect the effects of specimen self absorption and the distribution in depth of the characteristic X-rays? For a given X-ray energy it

would seem necessary to know where in the excitation volume the bulk of X-rays which are successfully detected arise. Observed X-ray spatial resolution can be considerably less than that predicted by an electron range equation. Would the authors please comment on this?

Authors With our definitions of depth and lateral resolution, instead of spatial resolution, we propose to define the region in the specimen where the primary characteristic X-rays are emitted. We admit that for a number of analysis situations an experimental check of these definitions with detected X-rays will be quite difficult. In those cases the use of an observed X-ray spatial resolution is more practical.

R B Bolon I am troubled by the way in which the data in figures 2 through 5 show a minimum error for all elements using either oxygen or nitrogen for the balance of the unmeasured light elements. Could this be related to how the standard or matrix of natural composition was determined? What was this standard and how was it characterized? Can you elaborate more as to the significance of these observations?

Authors From the data in Fig 2-5 and from Table 2 it can be concluded that there is a relation between the mean atomic number of the organic matrix and the optimal choice for the element calculated by difference. The matrix compositions indicated in this table have been used in the calculations with BIOFLEX both for the standard and the specimen. Thus it was assumed that the standard was ideal. In the case of a standard which does not resemble the specimen so closely the errors will be larger, because the overall ZAF-correction is larger.

	H	C	N	O	\bar{Z}
freeze-dried liver	7.67	52.57	10.18	29.58	6.31
frozen hydrated liver	10.04	15.39	2.86	71.71	6.96

Table 2. Approximate composition and the mean atomic number of the matrix $Z < 10$ in weight % of freeze-dried and frozen hydrated liver. Data based on⁶⁸

H Fuchs Could the authors please describe some properties of their computer program (e.g. programming language, computer requirements, number of elements which can be handled at one time, computation time for one set of data)?

Authors The program has been written in Fortran IV and can be run in a partition of 9.6 K bytes in a PDP 11/45 computer. BIOFLEX can handle data from elements with $10 < Z < 30$. Standards can be used for 6 elements. We have no figures on the computation time for one set of data. For one set on the average a few seconds is probably sufficient.

H Fuchs Is there any correction for charging in the authors' program?

C P Lechene The authors state rightly that it is often assumed that charging has not occurred when the ED spectrum on the high energy side

ends at the energy of the incident beam electrons. What would the author suggest to appreciate the existence and magnitude of internal space charging?

Authors Our program does not contain a correction for charging. We think that before a correction for charging can be implemented in a ZAF-procedure, more experiments will be needed to determine the depth distribution of primary ionizations in the specimen. We think that the method proposed by Fuchs et al.²⁶ is a good technique to measure the magnitude of internal space charging.

G M Roomans You do not mention any backscatter correction. Does BIOFLEX include this correction - if so, in what form?

Authors BIOFLEX includes the backscattering correction. Several alternatives have been compared. For the present study the backscattering correction formula as recently proposed by Love et al.^{82,83} has been used.

G M Roomans Could you state the reason why some ZAF-correction alternatives performed better than others? How large were the actual differences between the various correction alternatives?

Authors We have found (publication in preparation) that Bishop's absorption correction formula⁶⁵ performs significantly better than Philibert's⁶⁶ formula based on his simplified model. One of the reasons for this finding presumably is the unrealistic $\rho(\rho z)$ -curve on which this Philibert model is based. When the corrected concentrations (C) were divided by the actual concentrations (A), the mean C/A-ratios did not differ significantly from 1 for most of the alternatives of BIOFLEX. However, the programs EDAX 7EP, 8EP, and TRACOR 10D/37 showed a C/A-ratio significantly different from 1.

C P Lechene At 30 kV substitution of oxygen for the organic matrix still leaves an error for sodium of approximately 15%. What would the author propose in his program to reduce this error?

Authors The occurrence of such high errors as the one mentioned is a particularly strong argument for complete specification of the organic matrix in ZAF-correction. In BIOFLEX we have the possibility to enter the complete composition of the matrix as mass fractions or as mass fraction ratios. In the latter case the program works with a variable total organic mass fraction.

H Fuchs Did the authors also use a P/B-ratio method as proposed by P J Statham⁵² and if so, what are the results as compared to the optimized ZAF-correction procedure as presented?

Authors Until now we have not applied the method as proposed by Statham. We want to emphasize again that especially for biological but specimens the use of P/B-ratios offers several advantages.

G M Roomans Aren't the results you describe on the variation of the spectrometer angle just a way of telling the reader that uncertainties cause a larger error when the absorption correction is

large than when it is small?

Authors Yes, we believe that our results are due to differences in absorption, but there will also be an effect of secondary fluorescence.

R B Bolon In Table I you show that there are significant differences in the depth of generation of X-rays when calculated with the equations of Andersen and Hasler¹⁷, Reed¹⁸ and Colby¹⁹. In your opinion which is the most accurate and useful for biological samples?

Authors We don't know. In any case Colby's formula has the disadvantage that it has no theoretical ground for overvoltages larger than 10.

G M Roomans Have you investigated the effect of neglecting the correction for secondary fluorescence?

Authors No.

R B Bolon You describe sample contamination and the problem of loss of mass. What about the problem of additional mass such as the growth of carbon contamination during a long data counting interval? Can this be significant? If so can it be corrected for when analyzing small structures?

Authors We believe that the effect on quantitation of mass gain due to contamination can become quite significant. To correct this effect seems to be impractical, because little will be known about the shape, thickness, and composition of the mass added. Prevention of mass gain should be the ultimate goal.

References

- 79 D R Beaman & J A Isasi: A Critical Examination of Computer Programs Used in Quantitative Electron Microprobe Analysis. Anal Chem 42, 1970, 1540-1568
- 80 E H Darlington & V E Cosslett: Backscattering of 0.5-10 keV Electrons from Solid Targets. J Phys D: Appl Phys 5, 1972, 1969-1981
- 81 J A Small, K F J Heinrich, D E Newbury & R L Myklebust: Progress in the Development of the Peak-to-Background Method for the Quantitative Analysis of Single Particles with the Electron Probe SEM/1979/II, SEM Inc., AMF O'Hare, IL 60666, 807-816
- 82 G Love, M G C Cox & V D Scott: A Versatile Atomic Number Correction for Electron Probe Microanalysis. J Phys D: Appl Phys 11, 1978, 7-21
- 83 G Love & V D Scott: Evaluation of a New Correction Procedure for Quantitative Electron Probe Microanalysis. J Phys D: Appl Phys 11, 1978, 1969-1976

SHORT NOTE

A COMPARISON OF ZAF-CORRECTION METHODS IN QUANTITATIVE X-RAY MICROANALYSIS OF LIGHT-ELEMENT SPECIMENS *

A BOEKESTEIN ** A M STADHOUDERS A L H STOLS and G M ROOMANS ***

Department of Submicroscopic Morphology, University of Nijmegen Medical School, Nijmegen, The Netherlands

Received 27 June 1983

1 Introduction

In quantitative electron probe X-ray microanalysis of bulk specimens, a so called ZAF correction is often applied. Several mathematical expressions for each of the parts of this ZAF correction can be found in the literature [1,2]. Generally these expressions have been developed for specimens consisting of heavier elements. They contain assumptions and approximations of which the validity has been tested only for those heavier elements. In biological specimens, there is a need to quantify one or more elements with atomic number higher than 10 in a matrix consisting mainly of light elements ($Z < 10$) that are generally not measurable with energy dispersive X-ray microanalysis. It is doubtful whether all alternative expressions in the ZAF correction could be applied to such situations.

Since it is difficult to obtain biological bulk specimens that are sufficiently accurately characterized and homogeneous for the critical assessment of ZAF-correction procedures, and, in addition, these specimens might suffer mass loss which would further complicate the assessment, test data were taken from binary systems (from a compilation by Love and coworkers [3,4]), that contained at least one relatively light element and no elements with $Z < 30$. The possibility of extrapolat-

ing our findings on these binary systems to biological specimens will be discussed.

Commercially available ZAF-correction programs supplied by the manufacturers of X-ray microanalysis equipment also display a bias towards heavy-element specimens common in the materials sciences. In view of the increasing interest in quantitative analysis of biological bulk specimens, a study of the suitability of these commercial ZAF programs for analysis of light-element specimens seemed of interest.

2 Methods

ZAF correction equations For the backscatter correction, the equation of Love et al [5] was used. For the stopping power correction either the equation of Bethe and Ashkin [6] or that of Love et al [5] was used. Values for the mean ionization potential were calculated with the formulae of Bloch, Duncumb and Da Casa or Sternheimer (see Heinrich [7] for a review on this subject). Since the Sternheimer equation is only valid for $Z > 12$, the equation of Duncumb and Da Casa was used for $6 < Z < 12$. For the absorption correction either the equation of Philibert [8] based on his simplified model, or the equation of Bishop [9] was used. In both, values for the Lenard coefficient and the h -factor were used as proposed by Love et al [3,4]. Mass absorption coefficients were taken from Heinrich [10]. Correction for secondary fluorescence was carried out according to Reed [11]. No continuum fluorescence correction was applied.

* Address for all correspondence: A. Boekestein, Sleedoorn 3, 6581 VX, Maiden, The Netherlands.

** Present address: Technical and Physical Engineering Research Service, Wageningen, The Netherlands.

*** Present address: Wenner Gren Institute, Stockholm, Sweden.

Commercial ZAF programs Three commercially available ZAF programs were tested: the 7EP and 8FP ZAF programs of EDAX (Prairie View, IL USA) mainly based on FRAME B and described by Russ [12] and the 10D/37 version of the ZAF program of TRACOR Northern (Madison WI USA), mainly based on MAGIC IV [13].

Test data Data from a series of binary systems taken from a compilation by Love et al. [3], yielding 195 data sets, were used to compare the correction procedures. The systems consisted of elements with $Z < 31$, and virtually all systems contained at least one element with $Z < 17$. One of the elements in each binary system was calculated "by difference". For the other element, the K-ratio, i.e. the ratio between the measured peak intensity of the element in the specimen and the peak intensity of a pure reference, was known. All test data have been critically evaluated by Love [4] regarding their reliability, and suspicious data were omitted.

Statistical analysis The ZAF-corrected concentration (C) was divided by the real concentration (R) to give the ratio C/R . C/R ratios were calculated for each ZAF program and each set of

test data, mean C/R and the standard deviation around 1 were calculated for each ZAF program.

The C/R results were further evaluated with the Friedman test [14] and the Wilcoxon test. With the Friedman test the ZAF programs were arranged according to decreasing mean rank number of the C/R results. The rank number was obtained in the following way: each of the analysis problems has 15 solutions after correction by all ZAF programs examined. The program giving the best answer to that particular problem is assigned rank number 1, etc. The mean rank number was obtained after all analysis problems were ranked. This means that the lower the mean rank number of the ZAF program, the better its average performance.

3. Results and discussion

The result of the statistical analysis of the various ZAF-correction alternatives is summarized in table 1. The three commercial programs yielded a mean C/R value significantly different from 1. A

Table 1
Statistical results for the comparison of the ZAF correction accuracy of 12 different ZAF programs and 3 commercially available ZAF programs

ZAF program	Stopping power correction ^{a1)} using the formulae of		Absorption correction using the formulae of	Friedman test ^{b)}	C/R	SD ^{c)}
TRACOR 10D/37				4	0.987 ^{d)}	0.059
EDAX 7EP				11	1.010 ^{e)}	0.069
EDAX 8FP				10	1.024 ^{d)}	0.061
1	Bethe	Bloch	Bishop	5	0.998	0.057
2	Bethe	Duncumb	Bishop	2	0.994	0.056
3	Bethe	Sternheimer	Bishop	15	1.000	0.064
4	Love	Bloch	Bishop	1	0.996	0.055
5	Love	Duncumb	Bishop	3	0.993	0.051
6	Love	Sternheimer	Bishop	12	0.997	0.056
7	Bethe	Bloch	Philibert	9	1.003	0.072
8	Bethe	Duncumb	Philibert	6	1.000	0.065
9	Bethe	Sternheimer	Philibert	14	1.004	0.072
10	Love	Bloch	Philibert	7	1.001	0.068
11	Love	Duncumb	Philibert	8	0.998	0.068
12	Love	Sternheimer	Philibert	13	1.000	0.075

^{a1)} See text for explanation

^{b)} $p < 0.001$

^{c)} Standard deviation around 1

^{d)} $p < 0.01$

^{e)} $p < 0.05$

C/R value close to 1 is in itself, however, not sufficient indication that a particular ZAF program is accurate. Program 12, with a "correct" mean C/R value, has a relatively large standard deviation around 1, indicating inferior performance. On the other hand, the TRACOR program has a C/R value significantly different from 1, but a relatively small standard deviation. For examining and comparing the accuracy of ZAF-correction programs we propose therefore to use also a different method: the Friedman test.

In the last column of table 1, the ZAF programs are arranged according to their Friedman test rank number: a lower number indicates a better overall performance. The worst performance is shown by those programs that contain the Sternheimer value for the mean ionization potential (ZAF programs 3, 6, 9, 12 and the two EDAX programs). On the average, programs containing the Bishop absorption correction (programs 1-6) perform better than those containing the Philibert correction program (program 7-12).

The three commercial programs were compared more rigorously with the Wilcoxon test. No significant differences were found between the 7EP and 8EP programs of EDAX, but TRACOR's ZAF program was found to perform better than both EDAX's programs ($0.01 < p < 0.05$).

Our results suggest that the EDAX programs could be improved for analysis of specimens with a low atomic-weight matrix, by substituting the Sternheimer equation for the mean ionization potential for that of Bloch or Duncumb and Da Casa. The TRACOR 10D/37 program might be improved by the use of Bishop's method of absorption correction instead of that of Philibert. Similar criticism could be directed against other commercial programs not tested in this study, e.g. that of KEVEX, based on MAGIC V, which uses the Philibert absorption correction and the Sternheimer value for the mean ionization potential.

According to Love and coworkers [4], Bishop's method of absorption correction combines the best features of the full Philibert method for elements with $Z < 12$ and the simplified Philibert method

for $Z > 12$. Especially if the absorption is high, Bishop's method is superior to the Philibert method. The test specimens used in this study did not completely resemble biological specimens, even though they contained relatively light elements. However, the considerations about the choice of the absorption correction are likely to apply also to biological specimens, where the absorption may be high, e.g. in the case of Na or Mg, and Bishop's method is to be preferred. In a ZAF program to be used for biological microanalysis, there is evidently no place for the Sternheimer formula.

A factor which was not investigated in this study is the necessity of including a correction for continuum fluorescence. This omission affects, however, all alternatives in the same way and does not invalidate the comparison. In the materials sciences the correction is generally felt to be negligible, it is not included in most of the commercially available ZAF programs.

4. Conclusion

Bearing in mind that our study was restricted to a finite number of test data, we conclude that in ZAF corrections of specimens of the type investigated in this study

- (1) The differences between the results obtained using the stopping power correction of Bethe and that of Love et al. are not significant, the equation of Bloch or that of Duncumb and Da Casa for the mean ionization potential gives significantly better results than that of Sternheimer.
- (2) The absorption correction of Bishop performs significantly better than that of Philibert.

It is evident from our study that the requirements for ZAF-correction methods for quantitative analysis of bulk specimens containing a light-element matrix (such as biological specimens) are different from the ZAF-correction programs commercially available "for general use". Moreover, the use of such unsuitable ZAF-correction methods leads to significantly deviant results. The use of different types of ZAF corrections for different types of specimens should therefore be considered

Acknowledgements

We would like to thank Mr. G. Elemans, Mr. P. Sutthof and Dr. F. Smolders (Department of Medical Information Processing, St. Radbouds Hospital, University of Nijmegen) for their help in operating the PDP 11/45 computer. We also gratefully acknowledge the advice and assistance of Dr. M. van 't Hoff in the application of the statistical tests.

Miss C. van Hoek kindly provided us with the data of the EDAX 8EP program.

References

[1] P.M. Martin and D.M. Poole, *Met. Rev.* 150 (1971) 19
[2] S.J.B. Reed, *Electron Microprobe Analysis* (Cambridge University Press, Cambridge, 1975)
[3] G. Love, M.G.C. Cox and V.D. Scott, *J. Phys.* D8 (1975) 686

[4] G. Love, M.G.C. Cox and V.D. Scott, *J. Phys.* D9 (1976) 7
[5] G. Love, M.G.C. Cox and V.D. Scott, *J. Phys.* D11 (1978) 7
[6] H. Bethe and J. Ashkin, in *Experimental Nuclear Physics*, I (Wiley, New York, 1953) p. 252
[7] K.F.J. Heinrich, *Electron Beam X-Ray Microanalysis* (Van Nostrand, New York, 1981) p. 231
[8] J. Philibert, in *X-Ray Optics and X-Ray Microanalysis*, Eds. H.H. Pattee, V.E. Cosslett and A. Engstrom (Academic Press, New York, 1963) p. 379
[9] H.E. Bishop, *J. Phys.* D7 (1974) 2009.
[10] K.F.J. Heinrich, in *The Electron Microprobe*, Eds. T.D. McKinley and D.B. Wittry (Wiley, New York, 1966) p. 296
[11] S.J.B. Reed, *Brit. J. Appl. Phys.* 16 (1965) 913.
[12] J.C. Russ, *EDAX Editor* 5 (3) (1975) 1
[13] J.W. Colby, in *Proc. 6th Natl. Conf. on Electron Probe Analysis* (Electron Probe Analysis Society of America, Pittsburgh, PA, 1971) paper 17
[14] S. Siegel, *Non-Parametric Statistics* (McGraw-Hill, New York, 1956).

QUANTITATIVE BIOLOGICAL X-RAY MICROANALYSIS OF BULK SPECIMENS. AN ANALYSIS OF
INACCURACIES INVOLVED IN ZAF-CORRECTION

A. Boekstein^{*1}, A. M. Stadhouders², A. L. d. Stols² and G. M. Roomans³

1. Technical and Physical Engineering Research Service,
Wageningen, The Netherlands
2. Department for Electron Microscopy, University of Nijmegen,
The Netherlands
3. Wanner-Gren Institute, Stockholm, Sweden

(Paper received February 9 1983, complete manuscript received July 12 1983)

Abstract

In this paper the need for a biological approach to ZAF-correction is elucidated. Programming details are given for the composition of a ZAF-correction program, specifically designed for biological specimens. BIOFLX was written and set up as a working program to investigate two specific inaccuracies involved in quantitative X-ray microanalysis of biological bulk specimens. These are the poorly known composition of the organic matrix of the specimen as well as the poorly known specimen-beam spectrometer geometry. The outcome of our calculations, which is based on hypothetical (but representative) data, indicates that the organic matrix composition should be specified in elemental mass fractions. Moreover it was found that a poorly known geometry will give errors in concentrations of about 1 - 2%.

KEY WORDS: ZAF-correction, X-ray microanalysis, quantitative analysis, biological bulk specimens, tilt angle, organic matrix, backscattering correction, BIOFLX, normalization, analysis conditions.

* Address for correspondence
A. Boekstein, Postbus 356, 6700 AJ Wageningen,
The Netherlands Phone No. (08370) 19143.

Introduction

In quantitative X-ray microanalysis, correction procedures become necessary when primary generated X-ray intensities from standard and specimen are not, to the same extent, affected by a number of phenomena, such as X-ray absorption. Several computer programs for the processing of X-ray spectra have been developed to handle such correction procedures and these are usually supplied by the manufacturer of the X-ray analysis equipment. It appears that such ZAF- or matrix correction programs are basically similar, irrespective of the manufacturer, with only differences in details regarding the actual correction formulae used.

In general, commercially available ZAF-programs use approximative formulae for several physical constants, such as the mass attenuation coefficients, in order to save memory space. However, such procedures decrease the overall accuracy and slow down the computation speed in spectrum processing. An alternative would be to provide the computer program with complete data files with all the physical constants. When combined with a more restricted purpose of the ZAF-program, for instance to light element specimens, this approach could mean an improvement both in accuracy and in speed of analysis. The ZAF-program should then be restricted to specimens such as organic and biological specimens consisting only of relatively light ($Z < 31$) elements.

It is well known, however, that ZAF-correction practice is based on materials science specimens that consist mainly of relatively heavy elements (Martin and Poole, 1971). Therefore, commercially available ZAF-programs are biased towards heavy element specimens. In spite of this they are, however, often presented as general purpose programs. This has resulted in new development of correction formulae in recent years following the increased interest in light element analysis (Love et al., 1978). For biological specimens consisting primarily of a light matrix of H, C, N and O and some other relatively light elements ($11 < Z < 31$), recent efforts have been made to develop new methods for the ZAF-correction (Boekstein et al., 1980a).

A special ZAF-correction program for biological specimens is necessary basically because biological specimens differ from metallurgical specimens both chemically and physically. Biological specimens have almost unavoidably a relatively rough surface and they generally exhibit charging in the bulk of the specimen (Fuchs et al , 1978, Marshall, 1980). Their mean atomic number is below 10 in most cases and - most important - the local matrix composition can generally not be measured. Even the average composition of the matrix is only poorly known although it contributes more than 80% of the mass in most cases. Also, existing programs are not very suitable for biological problems because the composition of the organic matrix cannot generally be specified. Many programs only offer the opportunity to specify one remaining element to be calculated 'by difference'.

This paper describes a ZAF-correction program, called BIOFLEX, which is specifically designed for biological X-ray analysis problems. With this program the magnitude of an appreciable inaccuracy, due to the approximation of the whole organic matrix by only one element, is demonstrated. Furthermore, the program is used to demonstrate the inaccuracies involved in the ZAF-correction when the local tilt angle of the specimen is not accurately known.

Description of BIOFLEX

Goals

The most important demand on a biological ZAF-program is that the composition of the standard and the elements present in the specimen can be specified completely. With regard to the organic matrix it is also necessary to specify the matrix composition in the form of concentration ratios because in most cases the ratios are better defined than are the absolute concentrations. Furthermore it should be possible to specify the analytical conditions both for the standard and for the specimen because they may be different, to some extent, due to charging and surface roughness (Bockstein et al., 1980a). Normalization of the concentrations to 100% in ZAF-corrections should be possible in different ways depending on the nature of the specimen involved and the available data.

A survey of BIOFLEX

BIOFLEX was developed in Fortran IV with RSX 11D as the operating system for a PDP 11/45 computer (Digital Equipment Corporation). The program was built in overlay structure and had a length of 10K bytes. Physical constants were provided in data files and recently developed formulae for light element analysis were used when possible. BIOFLEX contains extended possibilities for user interaction and it is possible to automate the sequential processing of X-ray microanalysis data. The user may choose different routes in the program and output can be given in tables or graphs. In figure 1 a block diagram of the program is given.

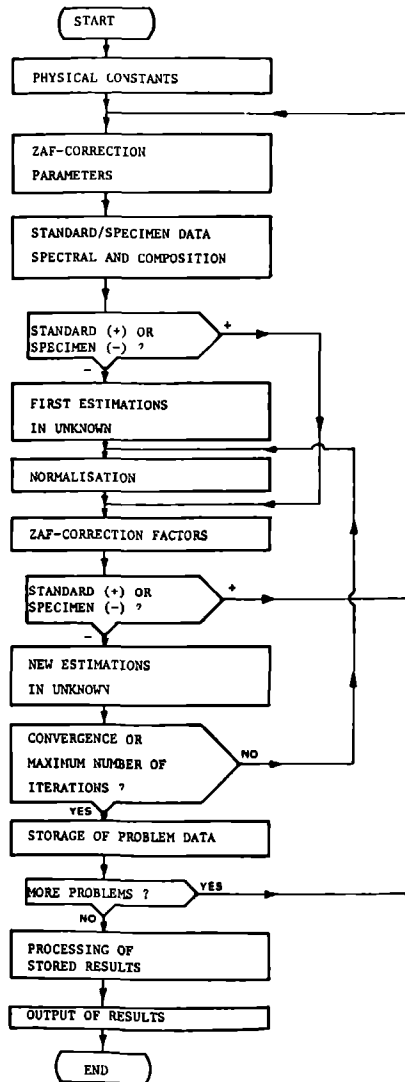


Figure 1. Simplified block diagram of the ZAF-correction program BIOFLEX

Physical constants

Physical constants for the first 30 elements of the periodic system have been entered as data arrays. Electron backscatter coefficients and fluorescence yields were taken from Bishop (1966). Mass attenuation coefficients were taken from Heinrich (1966) and absorption edge jump ratios were taken from Reed (1975).

ZAF-correction parameters

A number of parameters which determine the maximum number of iteration, the normalization method, graphical output format, etc. can be specified by the user. In addition the correction formulae to be used for the different parts in the ZAF-correction can be specified.

Standard data

After the number of standard data sets have been entered the program asks for the λ -ray take-off angle, the specimen tilt angle, the accelerating voltage and the concentrations or concentration ratios. Then the net peak intensities of the elements present in the analyzed micro-volume and the corresponding atomic numbers to be referred to have to be entered. Finally an identification number can be attached to this set of data.

After a certain standard data set has been processed, the calculated ZAF-correction factors (see below) and the relevant input standard data are stored. For one analysis problem standardization can be achieved for six elements. Data can be entered interactively. Data can also be present in a so-called 'indirect file' and read automatically by the computer. With this feature large amounts of data can be processed without interaction with the user.

Table 1. ZAF-correction formulae with BIOFLX

stopping power correction:	Bethe (1930) or Love et al. (1978)
mean ionisation potential:	Bloch or Duncumb & Da Casa or Sternheimer
backscattering correction:	Love et al. (1978) or Boeckstein et al. (1983) (this paper)
absorption correction:	Philibert (1963) or Bishop (1974) (see also Love et al. (1975, 1976)
secondary fluorescence:	Reed (1965)

Table 1. ZAF-correction formulae included in BIOFLEX. In total 24 different combinations are possible.

Correction factors (see table 1)

To enable the ZAF-program to calculate ZAF-correction factors for a particular specimen an estimate of the elemental concentrations in the specimens should be given, because the correction factors are directly dependent on these concentrations. Therefore an iterative procedure is included in order to calculate final values for correction factors and elemental concentrations in the specimens.

Stopping power correction BIOFLX can be used with two different formulae to calculate the stopping power correction, namely those taken from Bethe (1930) and from Love et al. (1978). In order to obtain values for the mean ionisation potential in these formulae, experimentally fitted expressions generally were used. Of these the formulae of Bloch, Duncumb and Da Casa and Sternheimer were included in BIOFLEX (see Heinrich (1981) for an extensive review on this subject).

According to Reed (1975) the effective electron energy (E_{eff1}) for element 1 was calculated as:

$$E_{eff1} = \frac{2V + E_1}{3} \quad (1)$$

where V = the accelerating voltage

E_1 = the critical absorption energy of element 1 emission of X-rays of a certain energy

Electron backscattering correction. The correction for electron backscattering in BIOFLEX was calculated with the formula of Love et al. (1978), which includes a specimen tilt correction.

We derived a simpler formula for this correction (F_{BS1}) by fitting a simplified first

order Springer polynomial expression to data for the electron backscatter factors of Duncumb and Reed (1968) for 0° tilt angle and of Reed (1971) for 45° tilt angle:

$$45^\circ: 1/F_{BS1} = \sum_j C_j (.9483 - .0089Z_j + .0886E_1/V + .0068E_1Z_j/V) \quad (2)$$

$$0^\circ: 1/F_{BS1} = \sum_j C_j (1.017 - .0078Z_j - .0002E_1/V + .0072F_1Z_j/V) \quad (3)$$

where C_j = concentration of element j
 Z_j = atomic number
 E_1 = critical absorption energy
 V = accelerating voltage

X-ray absorption correction. BIOFLEX can calculate the correction for absorption of X-rays according to Bishop (1974) or according to the simplified formula of Philibert (1963). Both formulae use values for the Lenard coefficient and the so-called 'h-factor' according to Love et al. (1975, 1976). The effect of tilting the specimen is taken into account by multiplying the total mass attenuation factor of the specimen with a geometry factor, G :

$$G = \frac{\cos(\text{tilt angle})}{\sin(\text{takeoff angle})} \quad (4)$$

Secondary fluorescence correction. The correction for secondary fluorescence was carried out essentially according to Reed (1965). Lenard coefficients were calculated as in Love et al. (1976). For the effect of the tilt angle the geometry factor was used (see above). A correction for continuum fluorescence was not applied for practical reasons. Most commercial ZAF-programs do not contain this correction because the calculations involved are quite complicated while the correction is in many cases relatively small. Nevertheless, the correction can become important (Warner and Taylor, 1981; Roomans, 1981).

First estimations of the unknown concentrations

If a standard peak is measured for an element present in the specimen, a first estimation C_{01} is calculated according to:

$$C_{01} = C_{\text{standard}_1} \frac{\text{Peak}_{\text{specimen}_1}}{\text{Peak}_{\text{standard}_1}} \quad (5)$$

For elements without a measurable peak present in the specimen (e.g., carbon, nitrogen and oxygen in many cases) concentrations or concentration ratios must be given.

Normalisation

With BIOFLEX normalization of the concentrations can be achieved in four different ways, depending on the specific analysis problem (table 2). The first method is used for biological specimens with an organic matrix constituting a large part of the total mass, with known ratios between the concentrations of the elements in that matrix. The second method is used if one element is chosen as the one which can be calculated 'by difference'.

The third method can be used for those cases with known concentration, for some elements (for example when the organic matrix of biological specimens is known). The fourth method is a general normalization.

New estimations of the concentrations in the specimen

After the total ZAF-correction factor F_{tot} has been calculated for the elements to be measured in the specimen, new estimations are made according to:

$$C_i = C_{01} \frac{I_{\text{tot specimen}}}{I_{\text{tot standard}}} \quad (6)$$

These new estimations are normalized once more for the next iteration in the ZAF-correction program, except after the last iteration. For normalisation method 2 it is obvious that normalisation of the concentrations is always carried out.

Convergence

In most cases in ZAF-correction the calculated concentrations converge to certain values from one iteration to the next. Therefore most programs contain a so-called convergence criterion which causes the program to stop when the concentrations after two subsequent iterations do not differ more than a given value. In BIOFLEX the convergence (S) is calculated according to:

$$S = \frac{|C_{\text{old}} - C_{\text{new}}|}{C_{\text{old}}} \cdot 100\% \quad (7)$$

The iteration stops if $S \cdot (\text{number of elements}) < 0.1$. In addition the user can specify the maximum number of iterations allowed.

Table 2. Normalisation Methods

	<u>formula</u>	<u>validity</u>	<u>application</u>
1.	$C_i = \text{ratio}_i \cdot (1 - \sum_{j=1}^{30} C_j)$	$i = 1 \text{ to } 10$	biological specimens, known ratios in matrix
2.	$C_i = 1 - \sum_{j=1}^{30} C_j$	$i = 1 \text{ to } 30$ $i \neq j$	element by difference
3.	$C_i = \frac{C_i}{\sum_{j=1}^{30} C_j} \cdot (1 - \sum_{k=1}^{10} C_k)$	$i = 11 \text{ to } 30$	biological specimens, known matrix
4.	$C_i = \frac{C_i}{\sum_{j=1}^{30} C_j}$	$i = 1 \text{ to } 30$	general normalisation method

Table 2. Normalisation methods in ZAF-correction with BIOFLEX ZAF-correction program

Storage of problem data and output of results

The analytical conditions, the correction formulae used, the last convergence S , the used number of iterations, the calculated concentrations and the total and partial ZAF-correction factor ratios between the standard and the specimen are stored in arrays for the analysis problem processed. Problem data and calculated results can be reproduced for the user in tables or graphs. Also specific calculations can be performed on the results of a number of processed problems.

Scope

BIOFLEX can be used both for metallurgical as well as biological analysis problems with the exclusion of specimens containing elements with atomic numbers higher than 30. For one analysis problem up to six standards can be specified. Standards may contain more than one element. The organic matrix of biological specimens must be specified as concentrations of the light elements or as their concentration ratios. The analytical conditions for the standard may be different from those for the specimen, although this is not advisable from the point of view of keeping the magnitude of the ZAF-correction as low as possible. In addition the user can specify the normalization method and various ZAF-correction parameters like the choice of the ZAF-correction formulae. Spectral input data for BIOFLEX are net peak intensities which can be obtained either by wavelength dispersive or by energy dispersive X-ray microanalysis.

Results and discussionComparison of ZAF-correction formulae

In order to test BIOFLEX we compared the results of BIOFLEX calculations with a number of analysis problems as compiled by Love et al. (1975, 1976). Their specimens consisted of well-defined binary systems of which one element was measured against a pure element standard, the other being calculated 'by difference'.

Love et al. (1976) tested the problem data for reliability and suspected data were omitted from the test. We included in our test only specimens containing elements with atomic numbers below 31 and compared the results given for different combinations of ZAF-correction formulae set up with BIOFLEX. Moreover we compared these results with the results given by a number of commercial ZAF-programs on the same analysis problems (see table 3). From these studies we concluded that the best combination of ZAF-correction formulae was achieved with the stopping power formulae of Bethe (1930) or Love et al. (1978) with the mean ionization potential as given by Duncumb and Da Casa (see Heinrich, 1981). The backscattering correction may be taken from Love et al. (1978), including a tilt correction. Alternatively, the simple formulae (2) or (3) are used with the restriction that these formulae are limited to fixed tilt angles. The absorption correction should be taken from Bishop (1974) (see Love et al., 1976). Moreover we concluded that BIOFLEX performed better than did the commercial programs when applied to these binary system problems.

The conclusions of this part of the study were based on the comparison of mean relative errors in the ZAF-corrected concentrations, the standard deviation around unity for the relative errors obtained with one particular ZAF-correction alternative, and the so-called Friedman ranking test (Siegel, 1956). In further studies with BIOFLEX the optimal combination of ZAF-correction formulae was used.

The organic matrix in ZAF-correction

Of the many problems encountered in quantitative X-ray microanalysis of biological bulk specimens, the poor knowledge of the organic matrix is probably the most prominent problem (Soekestein et al., 1980a). This poor knowledge of the concentrations of H, C, N and O can yield significant errors in biological ZAF-corrections because these matrix elements constitute a major part of total mass in the specimen. Moreover, commercial ZAF-procedures offer only a limited possibility to take into account the organic matrix of the biological specimen. In many cases it is possible only to calculate one element 'by difference'. Therefore we carried out a ZAF-correction in two ways: (1) By simulating the whole organic matrix of the specimen by one element only, to be calculated 'by difference' and (2) By specifying the whole organic matrix completely as concentrations or concentration ratios. The two resulting answers were compared and this allowed an estimation of the difference between these two approaches which could indicate an error in the ZAF-corrected concentrations.

For the composition of a hypothetical biological specimen typical concentrations were chosen as specified in table 4. These concentrations resemble closely the chemical composition of liver as calculated from data given by Documenta Geigy (1968). In order to estimate the real concentrations in a specimen we had to specify the specimen preparation technique used. Therefore we assume in one case freeze-drying, which results ideally in a replacement of the water in the specimen ultimately by vacuum. In the other case we assume that the specimen was kept in the frozen-hydrated state (Lechene et al., 1979). It is clear that due to the presence of a large amount of water in the latter case the mean atomic number of the specimen will be higher (see table 4).

For the standards we assume an organic matrix similar to the specimens. In addition we assume that the same elements were present in the standards as were present in the specimens with concentrations in the standard of about twice the concentrations in the specimens. In other words, the standards could be regarded as 'ideal'. Recent publications of Roomans and van Gaal (1977), Roomans (1979), Zierold (1981) and Fiori and Blackburn (1982) have shown that such ideal standards generally can be prepared.

Table 3. ZAF-correction program accuracy

ZAF program* ⁶	stopping power correction* ¹		absorption correction	Friedman test* ²	rel.error	S.D.* ³
Tracor 10D/37				4	0.987 * ⁵	0.059
EDAX 7EP				13	1.010 * ⁴	0.069
EDAX 8EP				12	1.024 * ⁵	0.061
1	Bethe	Bloch	Bishop	7	0.998	0.057
2	Bethe	Duncumb	Bishop	4	0.994	0.056
3	Bethe	Sternheimer	Bishop	17	1.000	0.064
4	Love	Bloch	Bishop	3	0.996	0.055
5	Love	Duncumb	Bishop	5	0.993	0.051
6	Love	Sternheimer	Bishop	10	0.997	0.056
7	Bethe	Bloch	Philibert	11	1.003	0.072
8	Bethe	Duncumb	Philibert	8	1.000	0.065
9	Bethe	Sternheimer	Philibert	16	1.004	0.072
10	Love	Bloch	Philibert	9	1.001	0.068
11	Love	Duncumb	Philibert	10	0.998	0.068
12	Love	Sternheimer	Philibert	15	1.000	0.075
13	Bethe	Duncumb	Bishop	1	0.998	0.051
14	Love	Bloch	Bishop	2	1.000	0.050

Table 3: statistical results for the comparison of the ZAF-correction accuracy of 17 different ZAF programs. (* 1) See text for explanation, (* 2) $p < 0.001$, (* 3) standard deviation around 1, (* 4) $p < 0.05$, (* 5) $p < 0.01$, (* 6) backscattering correction according to Love et al. (1978) in programs 1-12. In programs 13 and 14 formula (3) is used.

Table 4. Composition of biological 'model' specimen

Specimen	H	C	N	O	Na	P	S	Cl	K	Fe
dried ($\bar{Z} = 6.31$)	7.36	50.42	9.76	28.37	0.34	0.93	0.90	0.48	1.00	0.07
matrix	7.67	52.57	10.18	29.58						
hydrated ($\bar{Z} = 6.96$)	9.91	15.19	2.82	70.76	0.10	0.27	0.44	0.14	0.29	0.01
matrix	10.04	15.39	2.86	71.71						

Table 4: Composition (expressed as mass fractions) of biological 'model' specimen with freeze-dried or frozen-hydrated matrix assumption.

Calculated for liver and derived from Documenta Geigy (1968).

Net peak intensities for the elements with atomic numbers higher than 10 present in standards and specimens were entered into the computer memory. With regard to the analytical conditions we assume a number of possible combinations of accelerating voltage, tilt and takeoff angles (see table 5).

In table 5 the relative differences in the ZAF-corrected concentrations of a number of light elements upon substitution of the organic matrix by one element with $Z < 11$ are summarized. It is evident that for 'frozen-hydrated' matrices oxygen is the best choice with a maximum relative difference ('error') of 13% for the worst combination of conditions examined (30 kV accelerating voltage and 11° takeoff angle). For 'frozen-dried' matrices nitrogen was the best choice, with oxygen as second best with a maximum relative difference for nitrogen as substituting element of 2.6% for the worst combination of analytical conditions examined (10 or 30 kV and 11° takeoff angle). In figure 2 the dependence of these relative differences on the element chosen for substitution is shown for different combinations of analytical conditions. From these observations it is clear that the optimal choice for substitution of the organic matrix by one element is determined strongly by the preparation method (freeze-drying the specimen or keeping it frozen-hydrated) and that this optimal choice deviates from the mean atomic number of the matrix (table 4). This illustrates that there is no mean chemical matrix

that can be used universally in quantitative X-ray microanalysis of biological specimens.

The use of non-ideal standards which can be avoided in most cases (Roomans, 1979) will result in a larger ZAF-correction which could have a larger, more pronounced effect on the relative differences noted. In view of the magnitude of the differences, we consider it to be necessary to specify the complete organic matrix as concentration ratios in the ZAF-correction of biological specimens. Even if the matrix composition cannot be given accurately this procedure is better than replacement with only one element. In the description of BIOFLEX it is shown that this implies only a minor modification of the normal ZAF-procedure.

Tilt angle inaccuracy in ZAF-correction

In the ZAF-correction three analytical conditions always have to be entered: the accelerating voltage, the tilt angle, and the takeoff angle. Of these the tilt angle and the takeoff angle are often the most inaccurately known, especially in biological X-ray microanalysis. Several factors may cause the local beam-specimen-spectrometer geometry to be inaccurate. The natural surface of many biological specimens is rough and cannot be polished for evident reasons (Hess, 1960). Further on the local situation on the specimen can be disturbed by radiation damage due to the electron beam or to heat caused by poor thermal conductivity (Possin and Norton, 1975).

Table 5. Effect of organic matrix substitution on ZAF-corrected concentrations

accelerating voltage (kV)	10				30				
	0		40		0		40		
specimen tilt angle									
X-ray takeoff angle	10.5	60.5	35.5	63.0	10.5	60.5	35.5	63.0	
frozen-hydrated matrix	Na	10.82	2.29	3.38	1.52	12.68	12.53	13.02	12.40
	P	0.93	2.11	1.61	1.96	12.13	3.68	4.80	2.80
	K	2.14	2.84	2.53	2.60	4.46	0.55	0.11	0.51
	Fe	3.00	3.06	2.95	2.95	0.96	1.85	1.46	1.55
freeze-dried matrix	Na	2.12	2.43	2.16	2.22	1.41	1.45	1.23	1.29
	P	2.49	2.53*	2.30	2.30	1.64	1.81	1.56	1.59
	K	2.60*	2.55*	2.38*	2.38*	2.13	1.93	1.68	1.65
	Fe	2.55*	2.53*	2.47*	2.47*	2.17	1.90*	1.69*	1.66*

Table 5: Calculated minimal percentage differences in the ZAF-corrected concentrations of light elements (column 1) upon substitution of the organic matrix by one element $Z < 11$ only. For frozen-hydrated: oxygen; for freeze-dried: nitrogen. Differences are calculated by comparison with the ZAF-procedure in which all the concentrations in the organic matrix are specified.

* Oxygen yielded a lower difference.

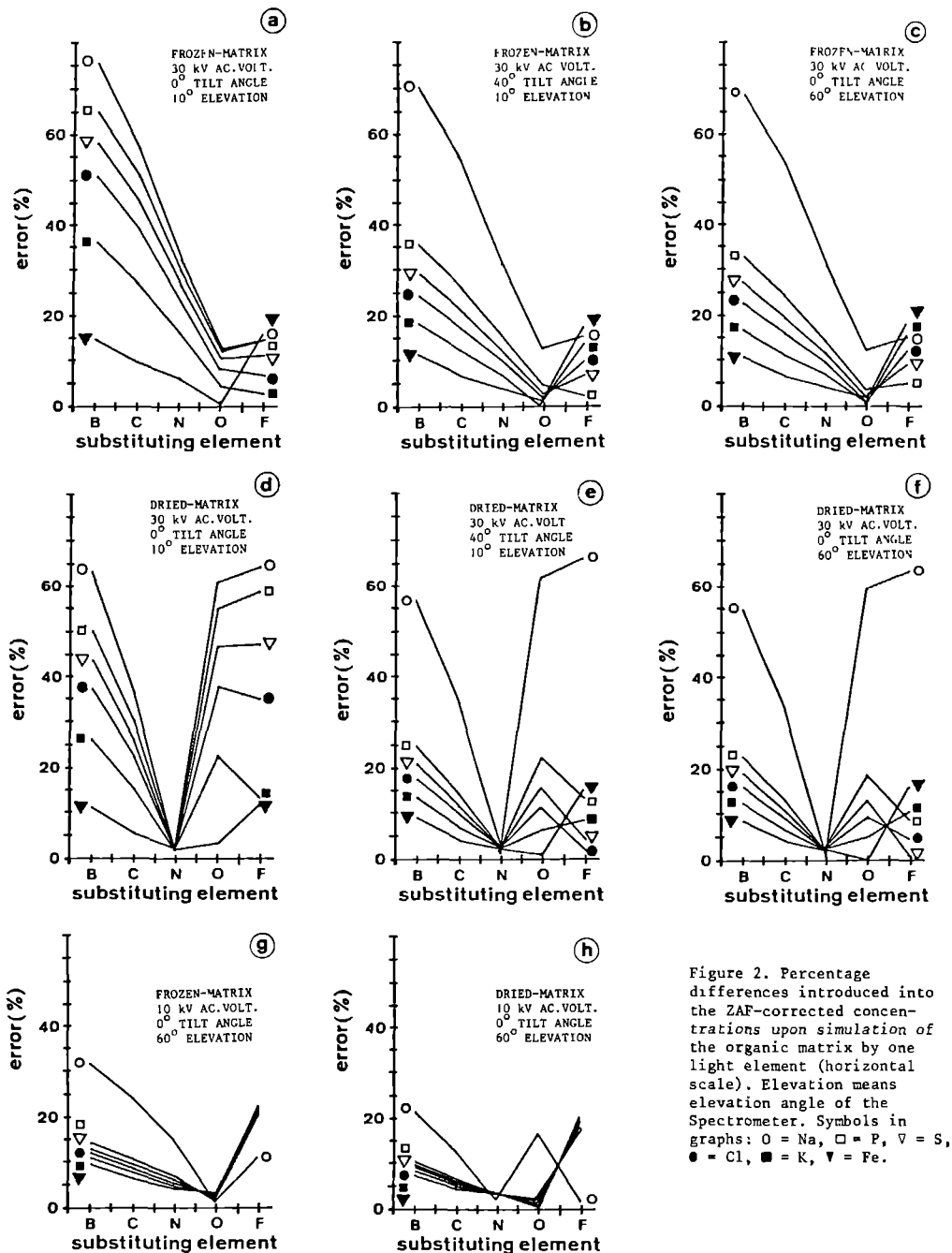


Figure 2. Percentage differences introduced into the ZAF-corrected concentrations upon simulation of the organic matrix by one light element (horizontal scale). Elevation means elevation angle of the Spectrometer. Symbols in graphs: O = Na, □ = P, ▽ = S, ● = Cl, ■ = K, ▼ = Fe.

We simulated the poor knowledge of the local geometry on the surface of a biological specimen by assuming a deviation of the nominal specimen tilt angle which reflects the real existing local tilt angle. For these two conditions (nominal and real tilt angle) ZAF-corrections were executed with BIOFLEX and the corrected concentrations were mutually compared and translated to relative differences ('errors') resulting from a certain inaccuracy in the tilt angles.

The compositions of specimen and standard are summarized in table 4. A number of combinations of analytical conditions were investigated (see table 6) whereas for the difference between the real and the nominal tilt angle a number of values were taken (see figure 3).

The effect of a difference between the nominal tilt angle and the real tilt angle is shown in figure 3. Differences varied between 1° and 50°. The situation for 1° tilt angle error can be regarded as a minimum for the resulting differences because 1° is an optimistic estimation for the inaccuracy in the nominal setting of the tilt angle. Our results indicate that, depending on the analytical conditions, the errors vary up to 2.4% for this 'zero' effect. In general, differences in the ZAF-corrected concentrations increase with increasing tilt angle 'error'. For the higher tilt angles in combination with larger tilt angle 'errors', however, the observations seem to be somewhat unpredictable (figure 3a). However, this finding can be explained when the actual takeoff angle is calculated for these specific situations. It can be shown that in some specific geometrical situations the takeoff angle

decreases with increasing tilt angle, which means that the absorption correction and the correction for secondary fluorescence are governed by two opposite effects.

For further evaluations we restricted our data to the relative differences in the ZAF-corrected concentrations for a 10° error in the specimen tilt angle (see table 6). It can be seen that differences introduced in the ZAF-corrected concentrations can reach highly unacceptable values of almost 40% for certain combinations of analytical conditions. However, for optimally chosen analytical conditions the introduced differences can be limited to 1.5%. These conditions are: the lowest accelerating voltage examined in this study (10 kV), a moderate tilt angle (20°) and a high spectrometer of elevation angle (60°), examined in this study. It is clear from our studies that the combination of a high elevation angle with a high tilt angle is a bad choice which may be explained by the actual takeoff angle as calculated.

The data presented in table 6 for the freeze-dried and the frozen-hydrated matrix (table 4) indicate that the organic matrix of the specimen has only a minor influence on the differences introduced for the ideal standard case. In most cases the differences are generally somewhat higher for frozen-hydrated specimens and the explanation can probably be deduced from a larger ZAF-correction for the frozen-hydrated matrix due to the presence of large amounts of oxygen instead of carbon.

From other studies (Boekstein et al., 1980b) it became evident that the use of a peak-background ratio instead of a net peak intensity, in the

Table 6. Effect of tilt angle inaccuracy on ZAF-corrected concentrations

specimen tilt angle	0		20		40		60			
	10	60	10	60	10	60	10	60		
detector elevation angle										
kV matrix										
10 freeze-dried matrix	Na	29.05	1.45	10.36	0.66	3.95	1.27	8.61	11.55	
	S	5.14	0.08	0.78	0.53	1.71	2.35	12.23	12.58	
	Fe	0.12	0.02	0.11	0.14	0.59	0.61	3.68	3.68	
	frozen-hydrated matrix	Na	33.53	2.02	13.61	1.20	6.28	0.71	6.69	10.74
		S	6.75	0.13	1.22	0.52	1.59	2.44	12.51	12.97
		Fe	0.18	0.02	0.11	0.15	0.65	0.67	3.89	3.91
30 freeze-dried matrix	Na	38.33	5.60	24.12	5.39	20.65	5.40	16.31	4.21	
	S	26.78	1.19	8.84	0.39	2.81	1.61	9.42	11.88	
	Fe	2.77	0.02	0.04	0.64	2.20	2.53	12.86	13.04	
	frozen-hydrated matrix	Na	38.38	5.97	24.26	5.89	21.81	6.28	20.64	6.70
		S	30.45	1.57	11.12	0.73	4.36	1.28	8.22	11.41
		Fe	3.06	0.01	0.09	0.68	2.30	2.67	13.31	13.51

Table 6: Relative differences introduced in the ZAF-corrected concentrations of certain light elements for a tilt angle inaccuracy of 10°.

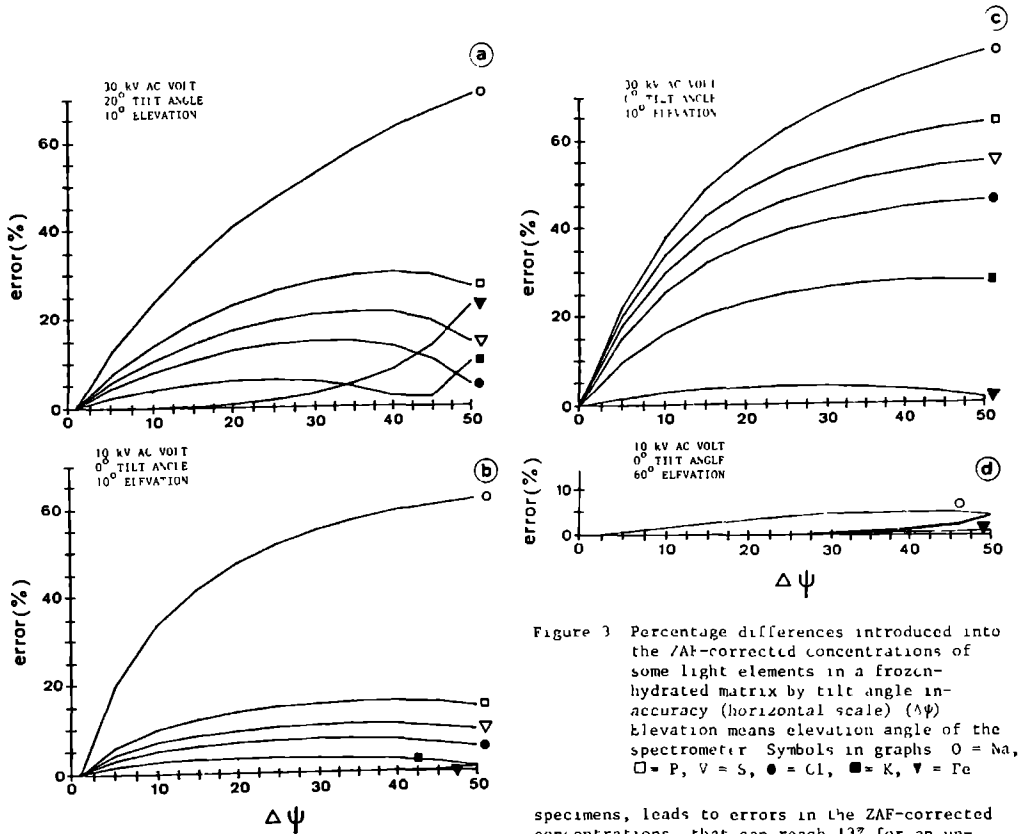


Figure 3 Percentage differences introduced into the ZAF-corrected concentrations of some light elements in a frozen-hydrated matrix by tilt angle inaccuracy (horizontal scale) ($\Delta\psi$) Elevation means elevation angle of the spectrometer. Symbols in graphs ○ = Na, □ = P, ▽ = S, ● = Cl, ■ = K, ▼ = Fe

analysis of rough surfaces with a poorly defined tilt angle, could mean a considerable improvement in analysis accuracy (Roomans, 1981; Small et al, 1979, Statham, 1978, 1981).

Conclusions

In this paper we have described the necessity for a special biological approach to the ZAF-correction. The main arguments are: (1) The biological matrix is complex and poorly known although it constitutes in most cases over 80% of the mass, (2) There are specific inaccuracies involved in biological ZAF-correction which have to be investigated and (3) ZAF-correction formulae can be optimized for light element analysis as is substantiated by the work of Love et al. (1975, 1978).

We have described our ZAF-program BIOFLEX which was originally designed as a working program to investigate specific inaccuracies involved in the ZAF-correction for biological specimens. From studies with BIOFLEX it appeared that it is better to specify the complete organic matrix. Choosing one light element with atomic number below 10 in order to substitute the whole matrix in organic

specimens, leads to errors in the ZAF-corrected concentrations, that can reach 13% for an unfortunate combination of analytical conditions. It cannot be excluded that this value can even be higher for other specimens. A considerable decrease in the errors can be achieved by choosing other analytical conditions but the fact remains that an error results of a few percent. This error can be avoided by specifying the matrix composition completely.

Tilt angle inaccuracies cannot be avoided in most cases, only the effects on the ZAF-corrected concentrations can be reduced by choosing appropriate analytical conditions. The resulting error of a few percent is systematic and adds to the overall inaccuracy of quantitative biological bulk specimen X-ray microanalysis.

Acknowledgements

The authors would like to thank Messrs. G. Elemans, P. Sutthoff, and Dr. F. Smolders of the Medical Information Department of the Radboud hospital in Nijmegen for encouraging discussion regarding programming the ZAF-correction and for the computer facilities. Dr. M. van 't Hoff of the Mathematical and Statistical Analysis Department of the University of Nijmegen has carried out the

statistical tests for the comparison of ZAF-correction programs. Mrs. C. van Hoek kindly provided us with data of the EDAX 8EP program. The help of Mrs. J.G.G. Kamps-van den Brakel in typing the manuscript and of Messrs. F.C. van Korlaar, H.G. Florie and F. Thiel in preparing the figures is gratefully acknowledged.

References

- Bethe H. (1930). Zur Theorie des Durchgangs schneller Korpuskularstrahlen durch Materie, *Ann. Phys.*, *Ipz.*, **5**, 325-400.
- Bishop HE. (1966). In *Optique des Rayons X et de Microanalyse*, R.Castaing et al. (eds.), Hermann, Paris, 153-158.
- Bishop HE. (1966). The prospects for an improved absorption correction in electron probe microanalysis, *J. Phys. D*, **7**, 2009-2020.
- Boekstein A, Stols AH and Stadhouders AM. (1980a). Quantitation in X-ray microanalysis of biological bulk specimens, *Scanning Electron Microsc.* 1980; **II**: 321-334.
- Boekstein A, van Kerkhof-Peters E and Stadhouders AM. (1980b). The use of peak to background ratios in the electron probe X-ray microanalysis of biological bulk specimens, in: *Electron Microscopy 1980*; **III**, P.Brederoo and V.E.Cosslett (eds.), EUREM foundation, Leiden, 74-75.
- Documenta Geigy Wissenschaftliche Tabellen 7th edition, Geigy A G., Basel, 1968, 302-383
- Duncumb P, Reed SJB. (1968). The calculation of stopping power and backscattering effects in electron probe microanalysis, in: *Quantitative Electron Probe Microanalysis*, K.F.J.Heinrich (ed.), Natl. Bur. Stand., Washington D.C., 133-154
- Fiore C, Blackburn DH. (1982). Low Z glass standards for biological X-ray microanalysis, *J.Microsc.*, **127**, 223-226.
- Fuchs W, Brombach JD and Trösch W. (1978). Charging effect in electron-irradiated ice, *J. Microsc.*, **112**, 63-74.
- Heinrich KFJ. (1966). X-ray absorption uncertainty, in: *The Electron Microprobe*, T.D.McKinley et al. (eds.), J.Wiley & Sons, New York, 296-377.
- Heinrich KFJ. (1981). Electron-beam X-ray Microanalysis, Van Nostrand, New York, 229-232.
- Hess FD. (1980). Influence of specimen topography in microanalysis, in: *X-ray Microanalysis in Biology*, M.A.Hayat (ed.), University Park Press, Baltimore, 241-262.
- Lechene CP, Bonventre JV and Warner RR. (1979). Electron probe analysis of frozen-hydrated bulk tissue, in: *Microbeam Analysis*, C P.Lechene and R.R.Warner (eds.), Acad. Press, New York, 409-426.
- Love G, Cox MGC and Scott VD. (1975). Assessment of Philibert's absorption correction models in electron-probe microanalysis, *J.Phys. D*, **8**, 686-702.
- Love G, Cox MGC and Scott VD. (1976). Assessment of Bishop's absorption correction model in electron-probe microanalysis, *J.Phys. D*, **9**, 7-13.
- Love G, Cox MGC and Scott VD. (1978). A versatile atomic number correction for electron probe microanalysis, *J.Phys. D*, **11**, 7-21.
- Marshall AT. (1980). Frozen-hydrated bulk specimens, in: *X-ray Microanalysis in Biology*, M.A.Hayat (ed.), University Park Press, Baltimore, 167-196.
- Martin PM and Poole DM. (1971). *Electron Probe Microanalysis: The relation between intensity and concentration*, *Metall.Rev.*, **5**, 19-47.
- Philibert J. (1963). A method for calculating the absorption correction in electron probe microanalysis, in *X-ray Optics and X-ray Microanalysis*, H.H.Pattee et al. (eds.), Acad. Press, New York, 379-391.
- Possin GE and Norton T (1975). Spatial distribution of 5 and 10 Kilovolt electron beam ionization in solids, *Scanning Electron Microsc.* 1975; 457-464
- Reed SJB. (1965). Characteristic fluorescence corrections in electron-probe microanalysis, *Br.J.appl.Phys.*, **16**, 913-926.
- Reed SJB. (1977). The backscattering correction for quantitative electron probe microanalysis with electrons incident at 45°, *J.Phys D*, **4**, 1910-1912.
- Reed SJB. (1975). *Electron Microprobe Analysis*, Cambridge University Press, Cambridge, 198-287.
- Roomans GM and van Gaal H. (1977). Organometallic and organometalloid compounds as standards for microprobe analysis of epoxy resin embedded tissue, *J.Microsc.*, **109**, 235-240.
- Roomans GM (1979). Standards for X-ray microanalysis of biological specimens, *Scanning Electron Microsc.* 1979, **II**: 649-657.
- Roomans GM (1981). Quantitative electron probe X-ray microanalysis of biological bulk specimens, *Scanning Electron Microsc.* 1981; **II**: 345-356.
- Siegel S. (1956). *Non-parametric Studies*, McGraw-Hill, New York.
- Small JA, Newbury D and Mckleburn R. (1979). Analysis of particulate and rough samples of FRAE-P, a ZAF-method incorporating peak-background measurements, in: *Proc. 14th Congress of the Microbeam Analysis Society*, San Francisco Press, San Francisco, 243-246.
- Statham P. (1978). A new method for particle X-ray microanalysis based on peak to background measurements, *Scanning Electron Microsc.* 1978, **I**. 469-478.
- Statham P. (1981). X-ray microanalysis with Si(Li) detectors, *J.Microsc.*, **123**, 1-24.
- Warner RR, Taylor DA. (1981). The continuum fluorescence correction in biological tissue, in: *Microprobe Analysis of Biological Systems*, T.Hutchinson (ed.), Acad. Press, New York, 197-211.
- Zierold K. (1981). X-ray microanalysis of tissue culture cells in SEM and STEM, *Scanning Electron Microscopy 1981*; **II**: 409-418.

Discussion with reviewers

F.D. Ingram: A seldom measured, but readily accessible parameter is average atomic number. If a calibration curve of average atomic number was plotted against backscattered electron coefficient, it would be possible to obtain average atomic number at each point of analysis. Would this parameter help to more accurately determine matrix composition?

Authors Determination of the electron back-scatter coefficient would help in assessment of the average atomic number of the microvolume which is analyzed, but there is doubt whether the average atomic number must be used in simulation of the organic matrix in biological ZAF-correction (compare table 4 and figure 2). Nevertheless, in material, varying largely in composition and hence average atomic number, it would help in finding the optimal element to simulate the matrix composition.

F.D. Ingram: In the last set of figures you show the error involved in not accurately knowing the tilt angle. Should this be considered a weakness of the ZAF-correction scheme, or is it not demonstrating the difficulties associated with working with systems that do not have stable, known geometries, independent of the method adopted for quantification?

Authors: The introduced errors do not show a weakness of the ZAF-correction scheme, but can be regarded as inherent to biological specimens in applying a ZAF-correction. For other quantification methods the errors may be different depending on the formulae used. In our opinion we can only quantify the errors like we did and try to minimize them by choosing the right analytical conditions.

K. Zierold: Can the BIOFLEX-program be used to calculate the hydration state of an unknown partly hydrated specimen, e.g. by comparison with continuum measurements in appropriate standards?

A.T. Marshall: For testing the effect of organic matrix composition on the ZAF-correction you use a hypothetical biological specimen. How do you derive net peak intensities for this test?

Authors: For the net peak intensities we assume values which are of the same order of magnitude as the peak intensities for the same elements in the standard. BIOFLEX cannot deal with complete spectra; the continuous background must be removed previously. BIOFLEX cannot be used to calculate the hydration state of an unknown partly hydrated specimen.

K. Zierold: Is the same model composition of elements (table 4) appropriate for the analysis of different compartments (e.g. cytoplasm, nucleus, extracellular space)?

Authors: The data shown in table 4 reflect the average composition of liver. For the purposes of this study these data are sufficient. For the quantitative analysis of different compartments in the cells the local composition must be estimated, and this will also be dependent on the preparation method followed.

J.C. Russ: I note that the test presented in table 3 apparently uses predominantly inorganic samples. It is not surprising that the Duncumb-Da Casa mean ionization potential performs well for these, having been derived "Backwards" specifically to minimize mean errors in computed composition for such samples, for low Z elements. There is no fundamental justification for the rather wild behavior of this function at low Z, however, and it is dangerous to transport the model to different types of materials, especially

when internal charging in some organic samples may produce serious alterations.

K. Zierold In frozen-hydrated specimens a space charge affects the shape of the excitation volume and the effective excitation energy of the primary electrons (text reference Fuchs et al. 1978). How do you take into account the space charge problem?

Authors. The bulk charging phenomena have been disregarded in this study because data are lacking to incorporate the charging effect in the ZAF-correction formulae. Because of the complexity of the charging problem and the unstable character of the analysis performed under such circumstances, efforts should be directed towards elimination of bulk charging. We feel that incorporation of the effect into the ZAF-correction formulae is a very long term solution.

F.D. Ingram: Would it be reasonably accurate in the case of freeze-dried tissue embedded in plastic to replace the whole matrix with carbon for simplicity?

Authors. Many plastics used for embedding freeze-dried material also contain oxygen and not only carbon and hydrogen. Therefore it is not obvious that the mean atomic number of freeze-dried material is lowered upon embedding. As can be seen in table 4 the mean atomic number of freeze-dried material is 6.3. For this type of material we found nitrogen the best choice for simulation of the organic matrix in ZAF-correction. Therefore we would suggest this element (nitrogen) to be used for simulation of the organic matrix of plastic embedded specimens as well.

F.D. Ingram: Is BIOFLEX available for distribution? If so, how might one obtain a listing or copy?

Authors: A listing can be obtained through the authors upon request.

K. Zierold: Is it possible to calculate the actual tilt angle of the microarea on a rough specimen surface by means of stereomicro-analysis, e.g. by comparing two spectra obtained at different tilt angles from the same microarea with the curves in figure 3?

Authors: In theory this seems to be possible, but one needs more curves than the number of curves shown in figure 3 and they should be derived for the appropriate matrix composition and analytical conditions.

F.D. Ingram: Does BIOFLEX have the capability for working with thin or moderately thick samples, or is it limited to bulk sample analysis?

Authors: BIOFLEX has been developed for bulk specimens only.

F.D. Ingram: Can your correction scheme handle heavy metal stains, such as Os, in biological materials?

Authors: Heavy metal stains like Os cannot be dealt with in our correction scheme because we can only process data for atomic numbers below 31.

Surface roughness and the use of a peak to background ratio in the X-ray microanalysis of bio-organic bulk specimens

by A. BOEKESTEIN, F. THIEL, A. L. H. STOLS,* E. BOUW and A. M. STADHOUDERS,*
*Technical and Physical Engineering Research Service, Wageningen, and *Department of Electron Microscopy, University of Nijmegen Medical School, Nijmegen, The Netherlands*

KEY WORDS P/B-ratio, X-ray microanalysis, bulk specimens, surface roughness, quantitative analysis, background subtraction, peak intensity, biological microanalysis, scanning electron microscopy, energy dispersive analysis, tilt angle, epoxy resin.

SUMMARY

The use of a net peak intensity and of a peak to background (P/B)-ratio of sulphur and chlorine is examined in the X-ray microanalysis of a 2.4% w/w S bulk standard in Spurr's epoxy resin. In calculating the P/B-ratio, the background intensity is calculated for the same energy region as for the net peak. Analyses were carried out on the flat top of the standard and on the slope running down from the top on the side not facing the X-ray detector. The results obtained for the peak to local background ratios from the top and the slope yielded a relatively small mean deviation (11%) while net peak intensities ultimately were reduced to 7% or less of the initial value for the flat top. This indicated that a peak to local background ratio is to be preferred in the quantitative analysis of bulk specimens which have poorly defined local tilt and takeoff angles. A second advantage is the inherent correction for beam current fluctuations.

INTRODUCTION

In quantitative X-ray microanalysis of thin biological specimens (i.e. transparent to the beam electrons) both net peak intensities as well as peak to background (P/B) ratios are used in order to quantify the spectral information on elemental composition (Hall, 1975). In the quantification of bulk specimens, in general, the net peak intensity is used ever since the beginning years of electron probe microanalysis (early fifties). However, in the last decade the advantages of using a P/B ratio instead of a net peak intensity, especially in biological bulk specimen X-ray microanalysis, are increasingly recognized (Statham, 1981; Echlin *et al.*, 1982). As early as 1971 Cobet & Traub found empirical relations between the P/B ratio and the concentration of a certain element in methacrylate standards. Zs-Nagy *et al.* (1977) showed the same results for measurements on organic crystals. Statham & Pawley (1978) and Small *et al.* (1979) approached the use of P/B ratios for bulk specimens more theoretically and developed a special method to analyse irregularly-shaped specimens. Wroblewski *et al.* (1978) and Statham (1979) used the ratio of the P/B ratio of an element in the specimen to the P/B ratio of the same element in the standard, as starting data for a ZAF-correction.

In biological bulk specimen X-ray microanalysis the use of a P/B ratio can be advantageous because one of the inaccuracies involved is the poorly defined surface topography (Boekestein *et al.*, 1980a, b). The specimen preparation techniques for X-ray microanalysis will include

© 1984 The Royal Microscopical Society

techniques to create a well-defined surface topography, but in many cases, especially in biological X-ray microanalysis, they are rarely successful (Hess, 1980). In order to diminish the effects of surface irregularities it is possible to spread the analysis across a large surface, an order of magnitude larger than the size of the irregularities themselves. It is obvious that this solution leads to a very serious restriction of the applicability of X-ray microanalysis to biological specimens.

A different solution can be to create a large X-ray takeoff angle by tilting the specimen or by providing a large spectrometer elevation angle on the electron microscope column. With this solution the penetration depth of the beam electrons can be diminished and or the X-ray path length in the specimen can be decreased.

In this study the effect of a poorly defined surface topography of an organic bulk specimen on the variation of net peak intensity and P/B ratio, is investigated. It is demonstrated that the use of a P/B ratio in biological bulk X-ray microanalysis can lead to more accurate results.

MATERIALS AND METHODS

The specimens consisted of Spurr's epoxy resin (Spurr, 1969) with known amounts of dissolved organometallic compounds (Roomans & Van Gaal, 1977). Bis-(dibutylthiocarbamate) zinc was used as a standard for S (2.4% , w/w S in Spurr). The epoxy resin block was mounted with carbon paste (Leit-C, Neubauer Chemikalien) on an aluminium specimen stub (Fig. 1) and subsequently coated with carbon by evaporation. In Fig. 2 part of the relatively flat top of the epoxy resin block is shown with the edge across which the measurements were carried out (arrow).

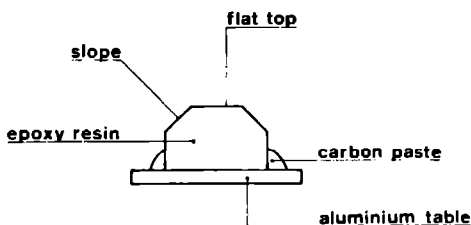


Fig. 1. The standard specimen: 2.4% , w/w S in Spurr's epoxy resin.

X-ray microanalysis was carried out in the Jeol 35C scanning electron microscope, equipped with an LaB_6 -gun and with an EDAX energy dispersive X-ray detection system (model 9100 65). The spectrometer elevation angle was 10° and the spectrometer azimuth was 45° as defined before (Boeckstein *et al.*, 1980a). The SEM was operated at 5, 10, 15, 20 and 25 kV accelerating voltage respectively. The (nominal) tilt angle setting of the specimen was 10° . The beam current was measured before and after each analysis and appeared to be constant. The analysis live time was 100 s, with exception of the locations across an edge, where we used longer analysis times. X-ray spectra were recorded of locations with clearly differing local tilt and takeoff angles separated from each other by $25\ \mu\text{m}$ on the specimen surface. In Fig. 3 the analysis situation has been drawn schematically.

Net peak intensities and P/B ratios were determined with the software provided for by EDAX (version 2.2, part A). This software calculates a background underneath the peak with a modified Kramer's function (EDAX PV9100 software manual) on the basis of user-defined background points. For most spectra two background points at each side of the S and Cl K peaks are sufficient to create a smooth background shape underneath the peaks. For a few spectra showing heavily absorption artefacts a background shape has been created by defining an intermediate point between the S and Cl K peaks. The EDAX software automatically calculates the

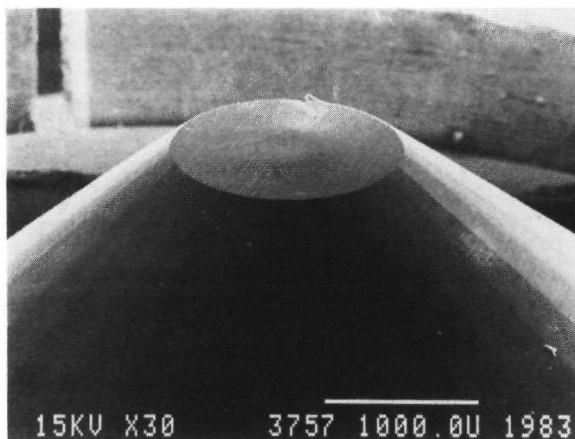


Fig. 2. The flat top of the S-standard with the slope not facing the X-ray detector (left) and the edge (arrow) across which the measurements were carried out.

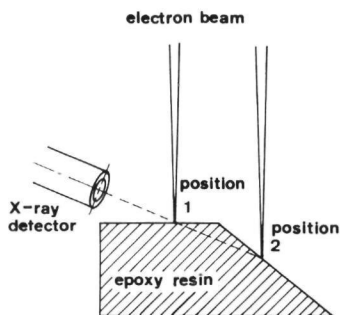


Fig. 3. Schematic presentation of the analysis situation.

peak and the background underneath the peak for an energy region 1.2^* (full width at half peak maximum).

The homogeneity of the standards was assessed with thin sections examined in the Philips STEM 400T equipped with an EDAX energy dispersive detector. The analysis showed no differences in the S and Cl count rate exceeding statistical accuracy for ten different analyses.

RESULTS

In Fig. 4 a spectrum is shown from the S standard with an additional peak of Cl, which is a known contamination of Spurr's resin. These spectra were obtained from the flat top of the specimen (see Fig. 3). In Fig. 5 a spectrum is shown obtained from the same specimen on a different location on the slope not facing the energy dispersive detector. It can be seen that the shape of the continuous background has changed considerably especially in the light-element region (below 3 keV).

The net peak intensities and peak to local background ratios for S and Cl measured on the

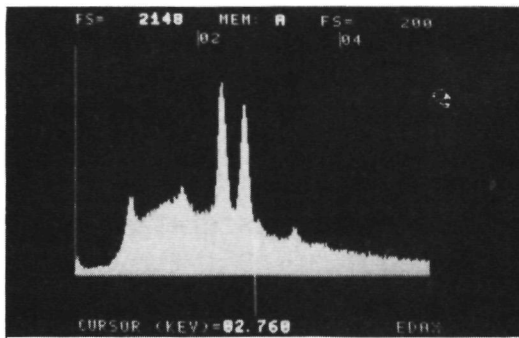


Fig. 4. An energy dispersive X-ray spectrum of the flat top of a 2.4% w/w S bulk standard.

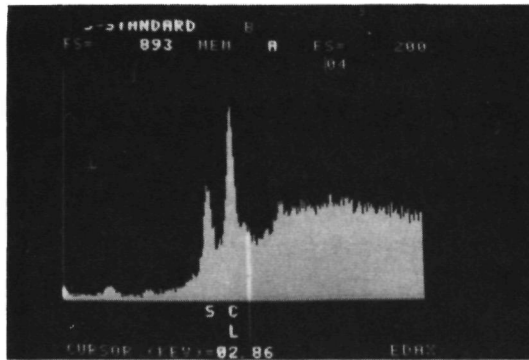


Fig. 5. An energy dispersive X-ray spectrum of a location on a 2.4% w/w S bulk standard on the slope not facing the X-ray detector.

flat top of the specimen are summarized in Table 1. Relative to these measurements the results of the analysis on locations on the slope of the specimen were calculated (Table 2). The results for sulphur for three different accelerating voltages are shown. For chlorine similar results were obtained. In Table 3 the results of the measurements on the slope are summarized.

Table 1. Peak and peak to local background ratios of sulphur and chlorine with coefficients of variation (SD %) for a number of measurements on the flat top of the standard specimen. Peak intensities are expressed as counts per second. The analysis live time was 100 s. *n* is number of measurement.

V(kV)	n	Sulphur				Chlorine			
		P	SD (%)	P/B	SD (%)	P	SD (%)	P/B	SD (%)
5	5	8.67	2.9	0.66	3.7	3.67	15.3	0.30	13.7
10	4	76.84	2.4	2.20	1.7	75.45	1.0	2.16	1.2
15	4	108.46	1.5	2.70	1.8	138.79	0.5	3.36	1.8
20	4	108.39	2.1	2.80	0.8	151.38	2.4	3.77	2.7
25	4	105.33	3.7	3.06	1.1	147.42	1.7	3.99	1.3

Table 2. Percentage changes in the sulphur K peak intensities and peak to local background ratios for a number of locations on the slope of the standard specimen not facing the X-ray detector. Changes were calculated from the mean values in Table 1

Location	Percentage changes in	
	Peak	P/B
5 kV		
1	-7 93	+2 28
2	-37 22	+11 06
3	-56 24	+28 94
4	-74 29	+12 73
5	-83 39	+14 09
6	-93 39	+23 64
15 kV		
1	-18 29	+10 44
2	-64 40	+14 03
3	-84 57	-0 56
4	-92 53	-3 59
5	-96 64	-6 44
6	-98 03	-8 18
7	-99 10	-14 10
25 kV		
1	-41 91	+5 99
2	-80 72	-1 41
3	-93 30	+2 68
4	-98 35	+24 08

Table 3. Mean percentage changes in peak to local background ratios of S and Cl K peaks for a number of measurements (n) on the slope of the standard specimen not facing the X-ray detector. Changes were calculated from the mean values in Table 1. SD is the standard deviation of the mean

V (kV)	n	Percentage changes in peak to local background ratios			
		S		Cl	
		Mean	SD	Mean	SD
5	6	+7 58	16 03	+1 35	18 80
10	7	-11 05	4 70	+5 22	7 38
15	7	+1 20	9 39	-0 35	11 20
20	5	-2 30	10 12	-3 30	9 03
25	4	-4 21	11 77	-1 09	3 54

DISCUSSION

From the results obtained it can be concluded that a change in the local tilt and take-off angle can have a dramatic effect on the shape of the continuous background and on the recorded net peak intensities especially in the light element region below 3 keV which is important for biological microanalysis (cf. Figs. 4 and 5). Therefore it is essential in calculating a P/B-ratio to relate the net peak to the background below the peak because in that case continuous and characteristic radiation lie in the same energy band which means that an equal part will be absorbed in the matrix of the specimen between detector and point of X-ray generation. It is therefore important that the continuous radiation consists of true specimen background.

From the data presented in Table 1 it can be concluded that the variation in the peak intensities can only to a limited extent be ascribed to counting statistics (e.g. Cl measurements for 5 kV). The variation exceeding counting statistics may be explained in part by the contribution of scattered electron beam to the background intensity, but it can be noticed that especially in the range 15, 20 and 25 kV accelerating voltage, P/B values show a slight increase while peak intensities stay almost constant. This indicates that there is no increase in the background intensity while the electron backscattering effect should be responsible for an increase in background intensity. This implies that we can ignore the backscattering effect for the purposes of our study. The reproducibility of the results for 10, 15 and 20 kV is 1-2%, and this figure

can be ascribed to radiation damage (Possin & Norton, 1975 (because the epoxy resin specimens were not cooled), to the probably small effect of backscattered beam, to the way in which the background intensity underneath the peak was calculated and to small beam fluctuations. Although there are more sophisticated methods to calculate the background intensity, we believe that the method followed yields results accurate enough to draw conclusions on the use of peak to local background ratios in comparison with net peak intensities upon beam-specimen-detector geometry changes. The background subtraction method can be compared with 'blanking' of a spectrum by an ideal background standard or with computer-assisted non-linear background interpolation (Boekestein *et al.*, 1980b). This way of background subtraction can handle peak overlap situations whenever the contribution of neighbouring peaks to the top of a particular peak is negligible. Small peaks do not offer specific difficulties but will show a poor accuracy and reproducibility because of counting statistics even if the background is accurately determined (see the results for Cl at 5 kV in Table 1). Propagation of errors from net peak intensities to P/B values can affect accuracy of course, but nevertheless the reproducibility of P/B values can be better, compared to net peak intensities due to inherent corrections. The inaccuracy of the background subtraction method followed in the study due to counting statistics is estimated less than 5%, when the background points are carefully chosen (see methods). 15 kV appears to be optimal for analysis and we conclude that the reproducibility of the background subtraction method followed is within 2%, for 15 kV. From the standard deviation values it is concluded that the peak to local background ratio is at least an even reproducible spectral signal as is the net peak intensity. In Table 2 it can be seen that even for a location where more than 90% of the net peak intensity is lost due to absorption the peak to local background ratio only deviates at most 29% from the mean value for the flat top (for many locations the deviation is even less than 15%). Further it can be noticed that the decreasing effect on the net peak intensities is stronger for higher accelerating voltages. This can be explained by the larger penetration depths for these voltages yielding larger X-ray absorption path lengths in the epoxy resin.

From Table 3 it can be concluded that the (1 standard deviation) range of changes in the peak to local background ratios is for sulphur -13%, to -9%, and for chlorine -10%, to +11%. These values are within the range of accuracies common to biological microanalysis.

The stable character of the P/B ratio obtained from rough surfaces, implies that there is enough reason to look for empirical relations between the P/B ratio and the concentration of an element. Cobet & Traub (1971) and Zs-Nagy *et al.* (1977) thus provided a quantification method for their specific applications. Another advantage of the P/B ratio method would be the insensitivity to electron beam current fluctuations.

From this study it is evident that in X-ray microanalysis of bio-organic bulk specimens with a poorly defined local tilt and take-off angle, the use of a P/B ratio is to be preferred. The background should then be taken right beneath the characteristic peak. Quantification may be carried out by measuring empirical standard curves of 'ideal' standards versus the concentration.

REFERENCES

- Boekestein, A., Stols, A.L.H. & Stadhouders, A.M. (1980a) Quantitation in X-ray microanalysis of biological bulk specimens. *Scanning Electron Microscopy*, 11, 321-334.
- Boekestein, A., van Kerkhof-Peters, F. & Stadhouders, A.M. (1980b) The use of peak to background ratios in the electron probe X-ray microanalysis of biological bulk specimens. In *Electron Microscopy*, 3 (Ed. by P. Brederoo and V. E. Coslett), pp. 74-75. Seventh European Congress on Electron Microscopy Foundation, I. eiden.
- Cobet, U. & Traub, F. (1971) Untersuchungen an speziellen biologischen Geweben mit der Elektronenstrahlmikrosonde. *Exp. Techn. Physik*, 19, 479-480.
- Echlin, P., Lai, C.E. & Hayes, T.L. (1982) Low temperature X-ray microanalysis of the differentiating vascular tissue in root tips of *Lemna minor*. *J. Microsc.* 126, 285-306.
- Hall, T.A. (1975) Methods of quantitative analysis. *J. Microscopy Biol. Cell* 22, 271-282.
- Hess, F.D. (1980) Influence of specimen topography on microanalysis. In *X-ray Microanalysis in Biology* (Ed. by M. A. Hayat), pp. 241-262. University Park Press, Baltimore.
- Possin, G.E. & Norton, J.F. (1975) Spatial distribution of 5 and 10 kilovolt electron beam ionization in solids. *Scanning Electron Microscopy*, 457-464.

- Roomans, G M & Van Gaal, H L M (1977) Organometallic and organometalloid compounds as standards for microprobe analysis of epoxy resin embedded tissue *J Microsc* **109**, 235-240
- Small, J A, Newbury, D E & Myklebust, R I (1979) Analysis of particles and rough samples by Frame P, a ZAF method incorporating peak-to-background measurements In *Microbeam Analysis* (Ed by D E Newbury), pp 243-246 San Francisco Press, San Francisco
- Spurr, A R (1969) A low-viscosity epoxy resin embedding medium for electron microscopy *J Ultrastruct Res* **26**, 31-43
- Statham, P J (1979) A ZAF-procedure for microprobe analysis based on measurements of peak-to-background ratios In *Microbeam Analysis* (Ed by D E Newbury), pp 247-253 San Francisco Press, San Francisco
- Statham, P J (1981) X-ray microanalysis with Si(Li) detectors *J Microsc* **123**, 1-24
- Statham, P J & Pawley, J B (1978) A new method for particle X-ray microanalysis based on peak to background measurements *Scanning Electron Microscopy*, **1**, 469-478
- Wroblewski, R, Roomans, G M, Janssen, E & Edstrom, L (1978) X-ray microanalysis of human muscle biopsies *Histochemistry*, **55**, 281-292
- Zs-Nagy, I, Picti, C, Gulli, C, Bertoni-Freddari & Zs-Nagy, V (1977) Energy dispersive X-ray microanalysis of the electrolytes in biological bulk specimen *J Ultrastruct Res* **58**, 22-33

In het tweede deel van dit proefschrift wordt ingegaan op de kwantificering bij dunne preparaten. Zoals in Hoofdstuk 1 is uiteengezet is het ionisatievolume van de bundelelektronen bij deze preparaten meestal zeer klein in vergelijking met het ionisatievolume bij dikke preparaten. Dit betekent dat verschijnselen als absorptie van röntgenstraling en het opwekken van secundaire röntgenstralen minder van belang zijn. De ingewikkelde correctie methoden zoals die bij dikke preparaten worden gebruikt kunnen dan ook bij dunne preparaten meestal achterwege blijven. Toch is ook hier het streven erop gericht een ideale standaard te vinden voor elk specifiek analyseprobleem. Indien dit echter niet lukt, kan meestal toch betrouwbaar gekwantificeerd worden bereikt door gebruik te maken van relatief eenvoudige correctieformules.

In het algemeen wordt bij dunne preparaten gewerkt met piek-achtergrond verhoudingen omdat preparaat en standaard vrijwel altijd verschillend dik zijn. Netto piekintensiteiten zijn sterk afhankelijk van de dikte van het preparaat. Bij gebruik van een piek-achtergrond verhouding wordt automatisch gecorrigeerd voor de geanalyseerde massa (dikte). Gezien de aard van de preparaten worden meestal geen absolute massahoeveelheden bepaald maar massafracties voor de elementen aanwezig in bepaalde gedeelten van de (aangesneden cel) compartimenten.

In die gevallen waarin het analyseprobleem een bepaald duidelijk begrensd geheel compartiment (particle) betreft, kan een methode worden toegepast waarbij uitgegaan wordt van netto piekintensiteiten en waarbij absolute massahoeveelheden worden berekend. Een dergelijke analyse vereist een standaard die ook een duidelijk 'particle' karakter heeft. Zogenaamde microdruppels (volume $> 1 \text{ pl}$) zijn voor dit doel geschikte standaards, die bovendien op relatief eenvoudige manier en met de meest uiteenlopende samenstellingen te bereiden zijn.

In Hoofdstuk 6 wordt de bereiding van microdruppel-standaards beschreven en in de Hoofdstukken 7 en 8 respectievelijk de röntgenmicroanalyse en de kwantificering met microdruppels. In Hoofdstuk 9 tenslotte wordt de in de voorgaande hoofdstukken beschreven methode toegepast op de bepaling van het magnesium en calcium gehalte van bloedplaatjes van de rat.

Samenvatting

In dit hoofdstuk worden de methoden beschreven die gebruikt worden voor het pipetteren van oplossingen met volumina van 1 tot 100 pl (zogenaamde microdruppels). De 'droogresten' van deze microdruppels worden gebruikt als standaard in de kwantitatieve röntgenmicroanalyse. In dit onderzoek zijn microdruppels vervaardigd met een constrictiecapillair waarvan de pipetteernauwkeurigheid beter is dan 2%. Microdruppels moeten na het opbrengen op een drager gedroogd worden. Een vergelijking van twee methoden hiervoor (vriesdrogen en 'flash' verdampen) leert dat daarbij aan flash verdampen de voorkeur moet worden gegeven.

6.1. Inleiding

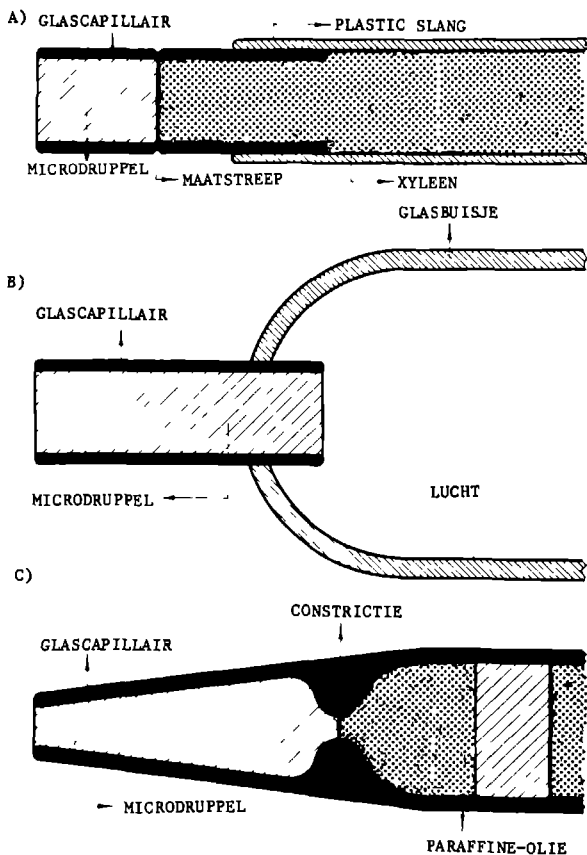
Bij de ontwikkeling van methoden voor de toepassing van de röntgenmicroanalyse in medisch-biologisch onderzoek is reeds vroeg aandacht besteed aan de mogelijkheid om kleine hoeveelheden 'fysiologische' vloeistoffen, zoals secretievloeistoffen en dergelijke te analyseren (Ingram en Hogben, 1967; Morel en Roinel, 1969; Lechene, 1974; Quinton, 1978). De methoden die door de verschillende onderzoekers zijn ontwikkeld, hoewel verschillend op detailpunten, hebben het volgende gemeen: Druppels met volumina in de orde van grootte van 1-100 pl van een standaardoplossing en druppels van de fysiologische vloeistof (met onbekende samenstelling) worden met hetzelfde capillair naast elkaar gepipetteerd op een drager. De druppels worden vervolgens gedroogd, waarbij het belangrijk is dat zich vormende zoutkristallen wat betreft de massadikte dunner dan 1 μm blijven (Morel en Roinel, 1969). Bij de kwantificering kunnen ingewikkelde matrixcorrecties dan achterwege blijven en de intensiteit van de karakteristieke röntgenstraling van een element is recht evenredig met de concentratie van dat element in de druppel. Door vergelijking met een standaard kan aldus de concentratie van een bepaald element in bijvoorbeeld een fysiologische vloeistof bepaald worden.

Voor de te gebruiken drager geldt dat (a) het atoomnummer van het materiaal laag moet zijn, zodat de achtergrondstralingsintensiteit laag blijft, (b) het materiaal goed de warmte moet kunnen geleiden, (c) deze dusdanige eigenschappen moet bezitten dat oplading zoveel mogelijk wordt voorkomen, (d) deze zo vlak moet zijn dat de locale kantelhoek en röntgenafnamehoek goed gedefinieerd zijn en dat de microdruppel goed 'zichtbaar' is, (e) de bijdrage

aan het röntgenspectrum niet zal interfereren met de analyse.

Voor massieve dragers is gebruik gemaakt van aluminium (Garland et al., 1973), van beryllium (Morel en Roinel, 1969; Bonventre en Lechene, 1974; Lechene en Warner, 1977), van pyrolytisch grafiet (Lechene en Warner, 1977) en van kwarts (Ingram en Hogben, 1967). Als materiaal voor dunne dragers is gebruik gemaakt van met kool versterkt collodion (Rick et al, 1977) en parlodion (Quinton, 1978; Van Eekelen, et al., 1980).

Voor het pipetteren van de microdruppels zijn drie methoden gehanteerd (zie Figuur 1). De eerste (Fig. 1a) is door Ingram (1967) ontwikkeld. Hierbij wordt een vloeistof opgezogen in een met xyleen gevuld microcapillair tot een aangegeven maatstreep. Het volume van de druppels ligt in de orde van nanoliters en de pipetteernauwkeurigheid is 4-5%. De tweede methode (Quinton, 1976) maakt gebruik van de capillaire opstijging in een geijkt microcapillair (Fig. 1b). Dit microcapillair is aangebracht in een ruimer buisje met behulp waarvan de



Figuur 1. Schematische weergave van de verschillende soorten capillairen, in gebruik voor het vervaardigen van microdruppels.

druppels uit het microcapillair kunnen worden geperst. Het volume van de druppels ligt in de orde van 0,1 nl en de pipetteernauwkeurigheid is ca 2% (Quinton, 1978). De in de laatste tijd vooral toegepaste methode (Roinel, 1975; Lechene, 1974; Rick et al., 1977; Van Eekelen et al., 1980) maakt gebruik van een zogenaamd constrictiecapillair (Fig. 1c). Het betreft hier een dun uitlopend capillair waarbij dicht bij de punt een vernauwing (constrictie) in de inwendige diameter is aangebracht. Op deze manier wordt een gegeven volume nauwkeurig gedefinieerd. Zeer kleine druppels met een volume > 1 pl kunnen met dergelijke capillairen onder lichtmicroscopische controle worden gepipetteerd. De pipetteerfout kan ondanks het kleine volume kleiner zijn dan 2%. De in de Hoofdstukken 6, 7, 8 en 9 onderzochte microdruppels zijn met een dergelijk constrictiecapillair gemaakt.

Teneinde te voorkomen dat tijdens het pipetteren verdamping van het water en vroegtijdige kristalvorming optreedt, worden microdruppels op de drager gedeponereerd onder een laagje met water verzadigde paraffineolie. Door afwisselend microdruppels en paraffineolie op te zuigen kan een pipet meerdere druppels bevatten, hetgeen de efficiency van de methode aanzienlijk verhoogt. De paraffineolie kan vóór de analyse worden verwijderd met een apolair oplosmiddel zoals hexaan of isopentaaan. Daarna dienen de druppels te worden gedroogd. Dit kan geschieden door de druppels eerst snel in te vriezen in bijvoorbeeld smeltende isopentaaan (Lechene, 1974), of in smeltende propaan (Rick, 1977), waarna deze bij een temperatuur van 190 K en een druk van ca. $1,3 \cdot 10^{-3}$ Pa kunnen worden gevriesdroogd. Een alternatief voor deze bewerkelijke methode is het 'flash' verdampen (Quinton, 1978). Hierbij worden de microdruppels na verwijderen van de paraffineolie abrupt aan een hoogvacuum blootgesteld.

6.2. Het vervaardigen van constrictiecapillairen

De constrictiecapillairen worden gemaakt uit glazen capillairen met een uitwendige diameter van 1,0 mm en een inwendige diameter van 0,6 mm. Deze capillairen worden uitgetrokken tot zeer dunne capillairen met behulp van een 'microelectrode puller' (Narishigi, Japan). Van het uitgetrokken capillair wordt eerst de punt afgebroken, hetgeen lichtmicroscopisch gecontroleerd wordt, zodat een open uiteinde ontstaat met een diameter van slechts enkele μm . Daarna wordt een nauwe constrictie aangebracht vlak bij het open uiteinde en wel door het capillair met een elektrisch verhitte platina draad (0,1 mm) lokaal te smelten (Lechene, 1974; Roinel, 1975).

De capillairen worden behandeld met een siliconen oplossing door een 1,5%

siliconen oplossing (Siliclad, Clay Adams, USA) in aqua bidest enige malen op te zuigen en weer uit te persen. Vervolgens wordt het capillair gedroogd bij 420 K. Hierna worden de capillairen geijkt met getritieerd water (specifieke activiteit 100 mCi/ml). Deze hoge specifieke activiteit is noodzakelijk wegens de zeer kleine volumina (1-100 pl) die moeten worden geijkt. Deze radioactieve oplossing wordt gehanteerd onder een paraffineolie en bij lage temperatuur.

Voor het ijken van het capillair wordt met een 'microcap' capillair (Drummond, USA; absolute nauwkeurigheid 1%) 1 µl van de stam-oplossing getritieerd water (100 mCi/ml) gepipetteerd in 100 ml aqua bidest. Met deze verdunde 1 µCi/ml oplossing wordt vervolgens een ijkreeks gemaakt die gemeten wordt in een vloeistof scintillatie teller (LKB 81000, Bromma, Zweden). Voor het bepalen van het pipetteervolume en de pipetteerfout van een constrictiecapillair wordt een aantal microdruppels radioactieve vloeistof gepipetteerd in telkens 100 µl aqua bidest. Op grond van de gemiddelde tritiumactiviteit kunnen het gemiddelde volume van het constrictie capillair en de pipetteerfout als volgt worden berekend:

$$\text{pipetteerfout}^2 = \text{S.D.}_x^2 - T^2 \quad (1)$$

waarbij, S.D._x = standaarddeviatie van de metingen

T = de bijdrage van de telstatistiek in de pipetteerfout.

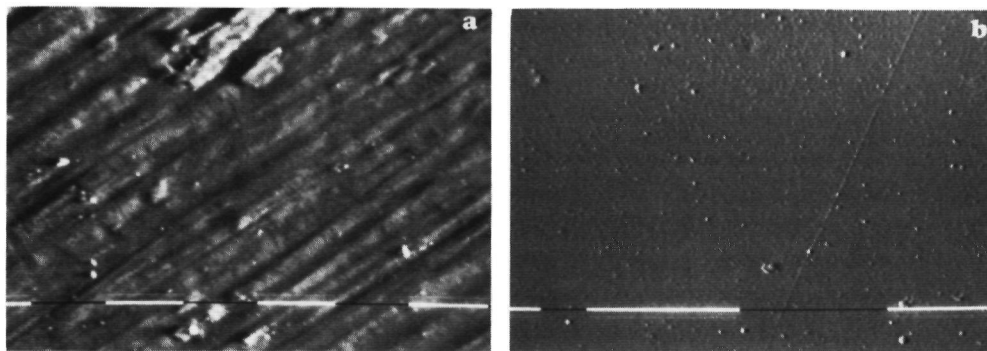
De grootte van de pipetteerfout zal onder andere samen hangen met de grootte van het pipetteervolume, met de vorm en grootte van de uitstroomopening, met de vorm en grootte van de constrictie en met de kwaliteit van de siliconenlaag. Daarom zullen alle constrictiecapillairen verschillend zijn en dienen preparaat en standaard bij voorkeur met hetzelfde capillair gepipetteerd te worden. In Tabel 1 zijn de ijkgegevens weergegeven van een serie van 7 pipetten. Voor het onderzoek is alleen gebruik gemaakt van capillairen met een fout kleiner dan 2%.

pipet	volume (pl)	pipetteerfout (%)
1	1,4	3,9
2	3,1	0,1
3	14,0	1,6
4	18,7	1,0
5	22,3	2,3
6	29,0	1,3
7	76,7	0,7

Tabel 1. Volumina en pipetteerfout van een aantal in het onderzoek gebruikte constrictiecapillairen.

6.3. Dragers

Als massieve drager is in deze studie gebruik gemaakt van een beryllium plaatje 7 mm x 4 mm x 0,5 mm gebruikt. Het oppervlak van het plaatje is gepolijst met behulp van diamantpasta's met korrelgrootte van resp. 2,5 μm en 1,25 μm (Scandia, West-Duitsland). Na het polijsten zijn de beryllium plaatjes steeds ultrasoon gereinigd in trichloorethyleen, ethanol en aceton. Figuur 2 toont het effect van het polijsten op het oppervlak van een beryllium plaatje.



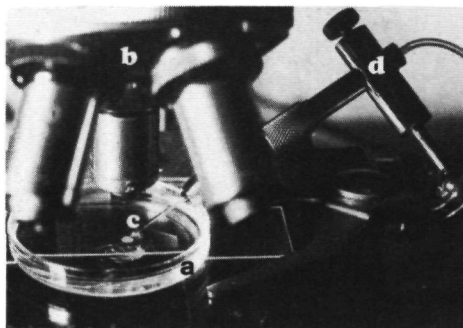
Figuur 2. SEM-opname (PSEM500) van het oppervlak van een beryllium plaatje: (a) ongepolijst; (b) gepolijst met diamantpasta (maatstreef = 10 μm)

Als dunne dragers voor de microdruppels is gebruik gemaakt van parlodion-films (Malinckrodt, St.Louis, U.S.A.) (dikte ca. 40 nm), verkregen uit een 1% oplossing van parlodion in amylocetaat. Het is noodzakelijk gebleken om deze films te verstevigen door opdampen van een ca. 10 nm dikke koollaag, waarna de vliezen voldoende stabiel zijn in de elektronenbundel. Dergelijke met kool² verstevigde vliezen kunnen een preparaatstroom van 1 $\mu\text{A}/1000 \mu\text{m}^2$ verdragen. Omdat dragerfilms moeten worden aangebracht op grids kunnen ook hiervan storende pieken in het spectrum verschijnen. Daarom kiest men bij voorkeur een materiaal dat een laag atoomnummer heeft. Hiervoor kan worden gekozen uit de nogal kostbare beryllium grids, nylon grids die echter problemen geven met de elektrische geleiding en aluminium grids die mechanisch nogal zwak zijn en bovendien een storende piek in het spectrum veroorzaken. Daarom is de voorkeur gegeven aan grids van koper, nikkel of titanium. De karakteristieke pieken hiervan interfereren niet met die van fysiologisch belangrijke elementen als Mg, P, K en Ca in de microdruppels. In de tweede plaats is het van belang om de mazen in het grid zo groot mogelijk te kiezen. De preparaatvreemde achtergrondstralingsintensiteit (zie Hoofdstuk 1) wordt namelijk onder andere bepaald door ongecollimeerde bundelelektronen (Goldstein en Williams, 1978). Gebleken is dat bij gebruik van 50 mesh grids er per maas een voldoende groot

gebied aanwezig is voor de analyse, waarin de achtergrondintensiteit niet afhangt van de afstand van het meetpunt tot de gridbalk (zie Hoofdstuk 8).

6.4. Opbrengen van microdruppels

Grids met dragerfilms of beryllium plaatjes worden gelegd op de bodem van een petrischaaltje dat is gevuld met paraffineolie (Fig. 3). Ook druppels van ca. 5 μ l van de standaardoplossingen en de te onderzoeken vloeistoffen worden op de bodem gedeponeerd. Het constrictiecapillair is bevestigd in een micromanipulator en kan in elke gewenste richting bewogen worden. Het opbrengen van microdruppels geschiedt verder onder lichtmicroscopische controle (Figuur 3).



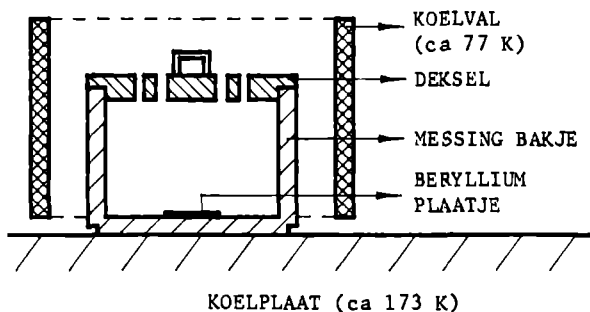
Figuur 3. Het opbrengen van microdruppels op grids onder lichtmicroscopische controle: (a) petrischaal met paraffineolie, te onderzoeken oplossingen en grids, (b) lichtmicroscop, (c) constrictie capillair, (d) micromanipulator.

In het constrictiecapillair worden de te onderzoeken vloeistoffen en de paraffineolie alternerend opgezogen, gebruik makend van een via een slang aan het capillair gekoppelde injectiespuit. Bij het opbrengen van een druppel wordt deze, zodra de druppel aan de punt van het capillair hangt, op de drager gebracht en wel door de drager met behulp van de objecttafel van het microscoop omhoog te brengen. Zodra de druppel de drager raakt, spreidt hij hierop in zijn geheel uit. Het wegwassen van de paraffineolie geschiedt door de drager minstens 3 maal 20 seconden te dompelen in hexaan of isopentaan.

Als standaarden zijn oplossingen gebruikt van zouten in water die goed oplosbaar zijn en die bij mengen geen neerslag geven. Op deze manier is het relatief eenvoudig mogelijk één standaard te bereiden voor meerdere elementen. Verder is het mogelijk om op één drager een groot aantal microdruppels te deponeren, zodat voor een reeks analyses geen preparaatwissel behoeft plaats te vinden in het elektronenmicroscop.

6.5. Drogen van microdruppels

De microdruppels kunnen worden gedroogd door vriesdrogen of door 'flash' verdampen. In dit laatste geval is in de microdruppels een eindconcentratie van 25% glycerol aanwezig om de vorming van te grote zoutkristallen tegen te gaan. In het algemeen is het van belang de afmetingen van de zich vormende kristallen kleiner dan ca. 1 μm te houden (Morel et Roinel, 1969). Hierdoor kunnen de anders noodzakelijke ingewikkelde correcties voor matrix effecten, zoals absorptie van röntgenstraling, achterwege blijven (zie Hoofdstuk 1). Voor het vriesdrogen wordt gebruik gemaakt van een speciaal vriesdroogbakje (zie Fig. 4). Dit wordt met vloeibare stikstof gekoeld alvorens de grids respectievelijk het beryllium plaatje worden ingebracht. Het bakje wordt vervolgens geplaatst in een vriesdroger, bestaande uit een aangepast opdampparaat met koelval en in temperatuur regelbare koelplaat (EPA 100, Leybold-Hereaus, Keulen, West-Duitsland). Hierna wordt het uit messing vervaardigde bakje gedurende 16 uur bij een druk van ca. $1,3 \cdot 10^{-3}$ Pa en een preparaattemperatuur van 170 K gevriesdroogd. Gebleken is dat bij het vriesdrogen de dragerfilms vaak beschadigd werden.



Figuur 4. Schematische voorstelling van het vriesdroogbakje voor microdruppels op beryllium plaatjes of dragerfilms.

Het flash verdampen bestaat uit het abrupt in hoogvacuum brengen van de microdruppels. De microdruppel wordt tijdens het verdampen van het water in een groot aantal kleinere druppeltjes gesplitst. De aanwezige glycerol verdampt of sublimeert langzamer en het zout blijft verdeeld in kleine kristalletjes achter (Quinton, 1978). In het algemeen is de morfologie van de droogresten afhankelijk van de concentratie en van de aard van het zout of zoutmengsel. Na het drogen worden de preparaten met koolstof bedampt om oplading te voorkomen. Figuur 5 en 6 tonen SEM opnamen van gevriesdroogde microdruppels van 100 en 10 mM KCl, zowel op beryllium plaatjes als op dragerfilms. In Figuur 7 zijn door flash verdamping verkregen droogresten van een microdruppel getoond.

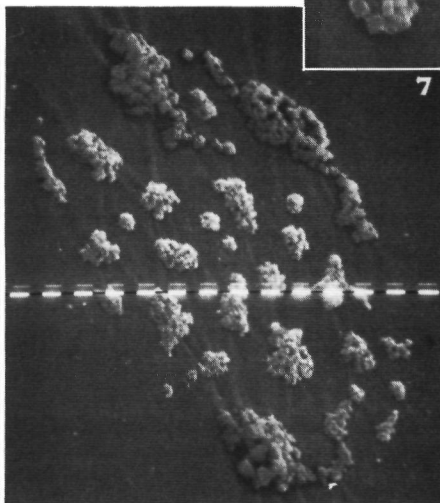
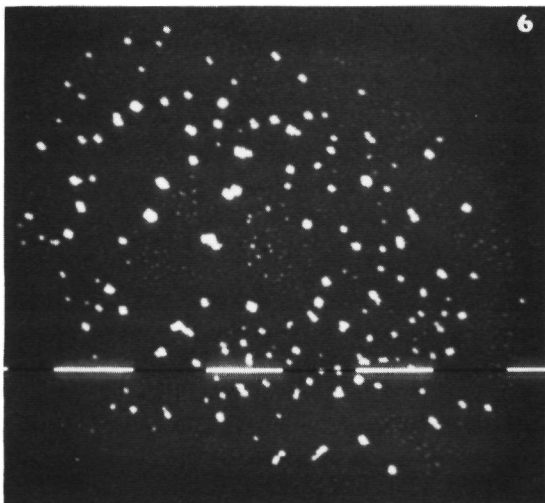
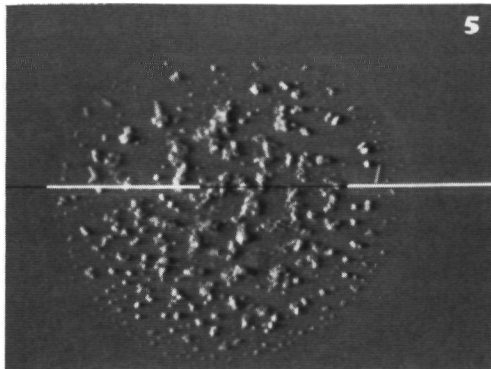
6.6. Discussie

Van de drie beschreven soorten microcapillairen blijken constrictiecapillairen het best te voldoen bij het vervaardigen van zeer kleine druppel-

Figuur 5. SEM-opname (PSEM500) van een beryllium plaatje met een gevriesdroogde microdruppel (76,7 pl, 100 mM KCl, kantelhoek = 45°) (maatstreef = 10 μm).

Figuur 6. SEM-opname (PSEM500) van een parlodion vlies met een gevriesdroogde microdruppel (76,7 pl, 10 mM KCl, kantelhoek = 45°) (maatstreef = 10 μm).

Figuur 7. SEM-opname (PSEM500) van een parlodion vlies met een 'flash'-verdampte microdruppel (18,7 pl, 200 mM NaCl + 5mM KCl, kantelhoek = 45°). Inzet: detail van microdruppel. Maatstreef = 1 μm .



tjes vloeistof (1 tot 100 pl). De capillairen zijn eenvoudig te maken en te gebruiken en vertonen ondanks het kleine pipetteervolume een goede pipetteernauwkeurigheid ($< 2\%$). Door het opzuigen van een serie druppeltjes in hetzelfde capillair, waarbij de druppeltjes onderling gescheiden zijn door kleine hoeveelheden paraffine olie, kan de efficiëntie van het werk sterk

worden verhoogd. Een moeilijkheid van het gebruik van deze capillairen is dat voor nauwkeurige ijking van het pipetteervolume een radioactiviteitsmeting moet worden uitgevoerd. In veel gevallen is echter bij kwantitatieve röntgenmicroanalyse bekendheid met het exacte volume niet noodzakelijk.

Massieve dragers blijken in de praktijk belangrijke nadelen te hebben ten opzichte van dragerfilms. Het oppervlak van de massieve dragers moet goed gepolijst worden. Bovendien neemt omdat er relatief veel massa van de drager wordt aangestraald, de intensiteit van de achtergrondstraling verhoudingsgewijs sterk toe. Met uitzondering van beryllium en koolstof veroorzaken de diverse soorten dragermaterialen storende pieken in het röntgenspectrum. Deze bezwaren gelden niet of in aanzienlijk mindere mate bij gebruik van dunne dragers (films). Daarom wordt in toenemende mate de voorkeur gegeven aan dunne films als drager voor microdruppels.

Bij het drogen van de microdruppels blijken dragerfilms wel een nadeel te hebben namelijk dat bij het vriesdrogen de films vaak beschadigd worden. Zogenaamd 'flash verdampen' blijkt echter in de praktijk een bruikbaar alternatief te zijn voor vriesdrogen.

Samenvattend kan gesteld worden dat de bereiding van microdruppels in technisch opzicht geen problemen behoeft op te leveren. Het belang voor de kwantitatieve röntgenmicroanalyse is dat microdruppels met zeer uiteenlopende samenstellingen te bereiden zijn en dat daarmee voor een groot aantal analyseproblemen standaardpreparaten voorhanden zijn.

Referenties

- Bonventre, J.V. and Lechene, C. (1974). A method for electron probe microanalysis of organic components in picoliter samples. In: Proc. 9th Annl. Conf. (Microbeam Analysis Society) 8A-8D.
- Garland, H.O., Hopkins, T.C., Henderson, I.W., Haworth, C.W. and Chester-Jones, I. (1973). The application of quantitative electron probe microanalysis to renal micropuncture studies in amphibians. *Micron* 4, 164-176.
- Goldstein, J.I. and Williams, D.B. (1978). Spurious X-rays produced in the scanning transmission electron microscope. *Scanning Electron Microscopy I*, 427-434.
- Ingram, M.J. and Hogben, C.A.M. (1967). Electrolyte analysis of biological fluids with the electron microprobe. *Analyt. Biochem.* 18, 54-57.
- Lechene, C. (1974). Electron probe microanalysis of picoliter liquid samples.

- In: Microprobe Analysis as Applied to Cells and Tissues (Hall, T. et al. (eds), Academic Press, New York) 351-367.
- Lechene, C. and Warner, R.R. (1977). Ultramicroanalysis. *Ann. Rev. Biophys. Bioengn.* 6, 57-85.
- Morel, F. and Roinel, N. (1969). Application de la sonde électronique a l'analyse élémentaire quantitative d'échantillons liquides d'un volume inférieur à 10^{-9} l. *J. Chim. Phys.* 66, 1084-1091.
- Quinton, P.M. (1976). Construction of pico-nanoliter selffitting volumetric pipettes. *J. Appl. Physiol.* 40, 260-262.
- Quinton, P.M. (1978). Ultramicroanalysis of biological fluids with energy dispersive X-ray spectrometry. *Micron* 9, 57-69.
- Rick, R., Horster, M., Dörge, A. and Thurau, K. (1977). Determination of electrolytes in small biological fluids samples using energy dispersive X-ray microanalysis. *Pflüg. Arch.* 369, 95-98.
- Roinel, N. (1975). Electron microprobe quantitative analysis of lyophilized 10^{-10} l. volume samples. *J. Microsc. Biol. Cell.* 22, 261-267.
- Van Eekelen, C., Boekestein, A., Stols, A.L.H. and Stadhouders, A.M. (1980). X-ray microanalysis of picoliter microdroplets: improvement of the method for quantitative X-ray microanalysis of samples of biological fluids. *Micron* 11, 137-145.

X-RAY MICROANALYSIS OF PICOLITER MICRODROPLETS. IMPROVEMENT OF THE METHOD FOR QUANTITATIVE X-RAY MICROANALYSIS OF SAMPLES OF BIOLOGICAL FLUIDS

C. A. G. VAN ELKILIN,* A. BOLKSTEIN, A. L. H. STOLS and A. M. STADHOUDERS

Department of Submicroscopic Morphology, University of Nijmegen, Nijmegen, The Netherlands

(Received 21 May 1979; in revised form 20 August 1979; accepted for publication 9 October 1979)

Abstract—A new practical approach to quantitative X-ray microanalysis of very small volumes of biological fluids, combining wavelength dispersive analysis and the use of thin films as supports is presented. The results from this technique are compared with those obtained using earlier methods and were found as predicted from theoretical considerations to be very accurate. Because of the favourable ratios between the detected characteristic radiation and the background radiation coupled with the resultant shorter periods of analysis, the use of this new technique of X-ray microanalysis for liquid samples not only saves time, but also smaller elemental concentrations can be detected. Suitable procedures to subtract background radiation are presented and discussed.

INTRODUCTION

Methods of quantitative X-ray microanalysis have been developed for the examination of biological tissues. In addition, several groups have utilized the X-ray microanalyser for the analyses of very small volumes of biological fluids (Ingram and Hogben, 1967; Morel and Roinel, 1969; Garland *et al.*, 1973; Quinton, 1978a,b; Bonventre and Lechene, 1974; Lechene, 1974; Rick *et al.*, 1977; Roinel, 1977, 1978). Briefly the following method is used. Droplets of reproducible size (10^{-9} – 10^{-10} l) of a number of standard solutions and of biological fluids, of unknown composition, are placed on a support, dried and analysed.

A prerequisite of the technique is the reproducibility of the droplet volume. Microdroplets were reported to be made using three different techniques employing glass capillary pipettes. Ingram and Hogben (1967) drew the samples into a capillary pipette to a consistent level using a fluid-filled syringe which was connected to the pipette by a tube. The reproducibility of their nanoliter micropipette was measured to be about 2% (S.D.).

Quinton (1976, 1978b) described the use of tiny self-filling capillaries which were attached to the end of a wider capillary in order to prepare microdroplets within a volume range from 50 picoliter to 25 nanoliter. The reproducibility of his pipettes was reported to be about 1% of their volume.

In the third method, microcapillary pipettes were used and provided with a constriction just behind their tip (Morel and Roinel, 1969; Lechene, 1974; Roinel, 1975, 1978; Rick *et al.*, 1977). With an air-filled syringe it is possible to draw small volumes of fluid very reproducibly into this kind of pipette. By alternating samples of water and paraffin oil, one constriction micropipette may contain up to 30 samples. No mixing of the samples occurs in a well silicized pipette. The reproducibility of this kind of pipette system is very high, even a very small volume (20 pl) micropipette has a reproducibility of 2% (S.D.) (Lechene, 1974).

The supports on which the microdroplets are placed can be separated into two major classes: bulk materials or thin films. Use has been made of aluminium (Garland *et al.*, 1973, 1978), beryllium (Morel and Roinel, 1969; Lechene, 1974; Lechene and Warner, 1977; Roinel, 1975, 1977, 1978), carbon (Lechene and Warner, 1977) and quartz (Ingram and Hogben, 1967) in the former

* Present address: Department of Biochemistry, University of Nijmegen, The Netherlands

class of supports. In the latter class Parlodion and Collodion films are used (Quinton, 1978a,b; Rick *et al.*, 1977). Of the bulk supports, beryllium is to be preferred because of the low atomic number and therefore low background radiation developed during analysis. For practical reasons other materials than Be, which is highly toxic and difficult to clean, are used. The film supports contribute even less to the continuum radiation during analysis and these supports are to be preferred to bulk supports, especially when an energy dispersive detector is used (this paper).

Two drying methods were employed in preparing the microdroplets for X-ray analysis: Freeze-drying and flash evaporation (Morel and Roinel, 1969; Lechene, 1974; Rick *et al.*, 1977; Quinton, 1978a,b). Both methods resulted in a rather uniform spread of the microdroplet contents on the support surface. Electron probe X-ray analysis was achieved by irradiation of an area of constant size enclosing the entire microcrystalline deposits from one microdroplet. The generated X-rays were counted by an energy dispersive (ED) or a wavelength dispersive (WD) analysing system. For the analyses the microdroplet volume and other measuring conditions (sample current, magnification, high tension, electron beam-sample-detector geometry) were kept constant. Calibration curves, constructed with the aid of standard solutions, made it possible to determine elemental concentrations in microdroplets of unknown composition. The calibration curves obtained showed characteristic X-ray counts per unit of time as a function of the elemental concentration in the microdroplet. They were linear when the absorption in the deposits of both accelerated electrons and generated X-rays was negligible. It is important to note that the droplets were small, the concentration in the droplets was not too high, also that the crystals in the dried droplets were very small ($< 1\text{nl}$ and $< 1\mu\text{m}$, respectively, according to Morel and Roinel, 1969; see also Lechene, 1974). When using too high a sample current, deviation from linearity of the calibration curves could occur because of volatilization of certain elements. Characteristic counts were calculated from detected count rates by subtraction of continuum radiation.

Previously the technique of X-ray microanalysis of picoliter microdroplets has been applied to droplets placed on thin films in combination with an ED analysing system and to droplets on Be supports in combination with a WD analysing system. Thin films were found preferable to Be

supports because of lower background radiation. WD analysis has the advantage over ED analysis of better peak-to-background ratios and of higher resolution. Consequently we tested the obvious combination of WD measurements from droplets on thin films and compared the results obtained with this method to those obtained using other methods. Subtraction of background radiation from measured count rates was performed using specially designed correction procedures described and discussed below under Materials and Methods.

MATERIALS AND METHODS

Supports

The high purity beryllium sheets were a gift of the Electron Optics Application laboratory of Philips, Eindhoven, the Netherlands. The surface of the Be was polished with diamond paste (Scandia, Copenhagen, grain sizes 2.5 and 1 μm) on an automatic polishing table. Before use the beryllium supports were cleaned ultrasonically in three solvents; trichloroethylene, ethylalcohol and acetone.

Parlodion films were prepared as described by Pease (1964), from 1% Parlodion solutions in amylacetate and mounted on 50-mesh copper grids. The films were strengthened and made conductive by indirect evaporation of a carbon layer.

Micropipettes

Capillary pipettes were drawn from glass tubes (internal diameter 0.6mm, external 1.1mm) with the aid of a Microelectrode Puller (model PN-3W, Narishige, Tokyo). Constrictions in the micropipettes were made using a microforge of the De Fonbrune type equipped with a 0.1mm platinum filament. The micropipettes were then silicone-coated with a commercially available water soluble silicone concentrate (Siliclad, Clay Adams). Calibration of the micropipettes was performed by pipetting samples of a solution of $^3\text{H}_2\text{O}$ (100mCi/ml) and counting these in a liquid scintillation counter. Volumes were calculated by comparing these figures with those obtained from samples of larger volumes of a diluted $^3\text{H}_2\text{O}$ solution (1 $\mu\text{Ci/ml}$).

Sample preparation

Microdroplets were prepared as described by Morel and Roinel (1969), Lechene (1974) using similar apparatus. Freeze-drying was performed overnight with the aid of a Leybold EPA 100

evaporator After washing the sample-carrying supports for 60sec in isopentane they were then quickly frozen at -160 C The supports were placed in a copper sample holder and transferred to the freeze dryer using a lid to prevent condensation on the sample When dry, the samples were warmed to 50 C before removal from the apparatus to avoid the condensation of water and resulting recrystallization of the small crystals

Flash evaporation was carried out essentially as described by Quinton (1978a b) Paraffin oil was removed from the grids by two serial washings of 30sec in hexane The grids were then mounted on a carbon grid holder of special design (Smits *et al.*, 1979) and flash evaporated at about 10^{-4} Torr

X-ray analysis

Energy dispersive X-ray analyses were performed using a Philips PSEM 500 equipped with an EDAX detector and a 707B multichannel analyser A carbon collimator was affixed to the detector (Smits *et al.*, 1979) The distance between the detector window and the analysed spot was 19mm The resolution of the detection system was 170eV The detector had an angle of 11° with the horizontal plane The carbon tube grid holder had a height of 30mm, an internal diameter of 2.5mm and an external diameter of 13mm Grids were mounted on the upper surface of the holder to an angle of 45° with the incident electron beam and fixed by a conductive glue

Wavelength dispersive analyses were performed using a Camebax microprobe (Camebax type MBS 70, kindly made available by Cameca S A Paris) The instrument was equipped with three wavelength dispersive detectors, with a resolution of about 12eV As a 'transmission sample holder' in this instrument we used a 13mm high carbon tube, external diameter 5mm, provided with a hole 5mm deep and diameter of 2.5mm

Background subtraction

ED analysis with beryllium support Due to the non-linearity of the background spectra in the region from 2 to 8keV, when Be is used as support (see Fig 4), a non-linear background subtraction procedure was developed Our method (see below) is only usable in those instances where one or a few non-overlapping peaks are present in the ED X-ray spectrum The microdroplet preparations used in this study fulfil this requirement

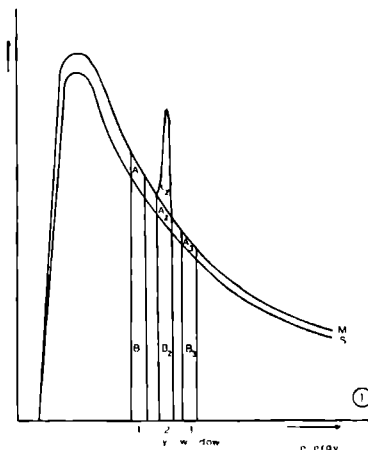


Fig 1 Schematic image of an X-ray spectrum obtained from a microdroplet placed on a Be support (M) and a spectrum measured during an equally long period of analysis when made under the same analysis conditions of the clean support (S)

Other background subtraction procedures which were not dependent on interpolation of off-peak count rates have been discussed (Fiore *et al.*, 1976, Statham, 1977) Figure 1 shows schematically the spectra measured on the clean Be support and on a microdroplet The last spectrum has a higher background because more continuum radiation is caused by the elements present in the microdroplets, due to their possessing a higher average atomic number than Be The count rates measured in the energy windows indicated in the figure can be represented as follows.

Window no	Spectrum M	Spectrum S
1	(A ₁ + B ₁)	(B ₁)
2	(A ₂ + B ₂ + C ₂)	(B ₂)
3	(A ₃ + B ₃)	(B ₃)

The value that is to be calculated is C₂, a value that approaches accurately the net characteristic counts (neglecting absorption edges) The six values mentioned above (A₁ + B₁ etc) can be measured C₂ is calculated as follows

$$B_2 = xB_1 + (1 - x)B_3 \quad \text{equation a}$$

$$(A_2 + B_2) = x(A_1 + B_1) + (1 - x)(A_3 + B_3) \quad \text{equation b}$$

$$(A_2 + B_2 + C_2) = (A_2 + B_2) + C_2 \quad \text{equation c}$$

Equation b holds when the background spectrum of the spectrum measured on the microdroplets is of the same form as the spectrum measured on the clean beryllium support. Using this method for measurements on microdroplets containing a constant amount (5mM) of KCl and a varying amount of NaCl (0–200mM), the net characteristic count rates were proportional to their concentrations (within statistical error) (data not shown).

ED analysis with thin film supports Because the background spectra obtained from ED analysis on microdroplets using thin films as supports were quite linear in the area of our studies, linear interpolation of background values (measured in energy windows adjacent to the peaks) was used. Moreover, the higher peak-to-background ratios obtained in this way indicated that the accuracy of the background subtraction had a less pronounced effect on the results than when use was made of Be as support.

WD analysis with be or thin film supports When only one pure compound is present in the microdroplet (i.e. when producing a calibration curve) no background subtraction is necessary. However, when other elements are present in varying amounts in the microdroplets background, subtraction is necessary due to the varying contribution made by the background radiation from these other elements. In these instances the most frequent method of determining the background radiation by measuring it on the clean support can result in errors. Background count rates can be determined more accurately when measurements are performed on the microdroplet as well as on the clean support while the WD detector is adjusted to a position off the characteristic peak. Referring to Fig 1 as a schematic spectrum obtained from a microdroplet, we found the values for $(A_1 + B_1)/B_1$ and $(A_3 + B_3)/B_3$ to be equal and considered them to be equal to $(A_2 + B_2)/B_2$. Thereafter C_2 was calculated. This procedure of background subtraction was applied to WD analyses from microdroplets containing a constant amount of KCl (5mM) and a varying amount of NaCl (0–200mM). The values calculated for C_2 (in this case $K K_{\alpha}$ radiation) were considered here as being closely correlated within the statistical error. Moreover they were independent of the NaCl concentration (data not shown).

When neglecting the extra contribution to the

background radiation caused by NaCl in a microdroplet containing 200mM NaCl and 5mM KCl, an error of about 10^0 , is inherent in the net characteristic $K K_{\alpha}$ count rates.

Another possible way of determining background radiation correctly is by interpolation of two off peak count rates measured on the microdroplet.

RESULTS

Supports

As we have mentioned above (see Introduction) thin films were preferred to beryllium as supporting material in quantitative X-ray microanalysis of picoliter microdroplets. One problem encountered when using thin films was their fragility during sample preparation and X ray analysis. In fact the carbon-coated Parlodion films used routinely were not able to withstand freeze-drying, but no problems were encountered when using flash evaporation. Furthermore, the films were resistant to a high sample current approaching $1\mu A/1000\mu m^2$, a value at which volatilization of many elements present in microdroplets takes place. It was concluded that film stability need not present a real problem.

Pipettes

The results of the calibration from four micropipettes are shown in Table 1. These results are at least comparable to the best published results.

Table 1. Mean volume and standard deviation (S.D.) of the four constriction pipettes used in this study.

Pipette no	Mean volume (pl.)	% S.D.
1	76.7	0.6
2	29.0	1.1
3	14.0	1.3
4	18.7	0.6

Drying procedures

Figures 2, 3 and 4 show scanning electron microscope images of dried microdroplets mounted on different kinds of supports using freeze-drying and flash evaporation.

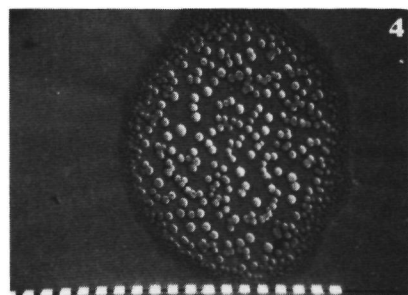
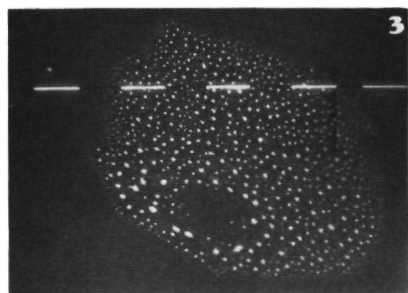
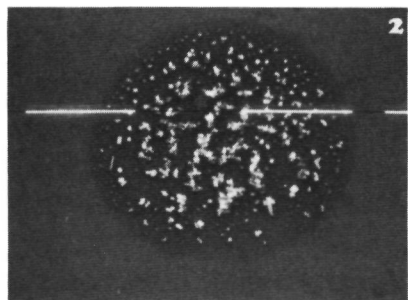
Energy dispersive analyses

(A) *Beryllium support* Figure 5 is representative of energy dispersive spectra when measured on dried microdroplets placed on Be. It can be

seen that the peak-to-background ratio (i.e. the ratio of the net characteristic radiation measured in an energy window and the continuum radiation measured simultaneously in the same win-

dow) is very low. Therefore, long periods of analysis are necessary to determine the net characteristic radiation accurately. The peak-to-background ratio under the analysing conditions mentioned in the legend of Fig. 5 for a KCl containing microdroplet is 1 for both K and Cl when the KCl concentration is 75mM.

Due to the very high contribution of the background radiation to the total detected counts in the energy window where the characteristic peak lies, accurate background subtraction is of importance. To this end a special interpolation procedure (non-linear, because of the non-linearity of the slope of the background spectrum in the

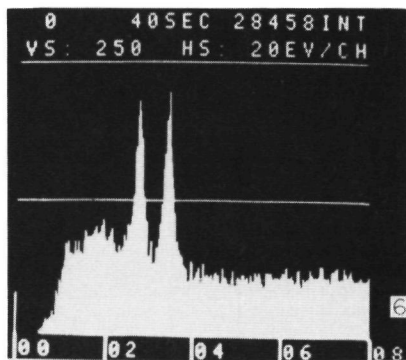
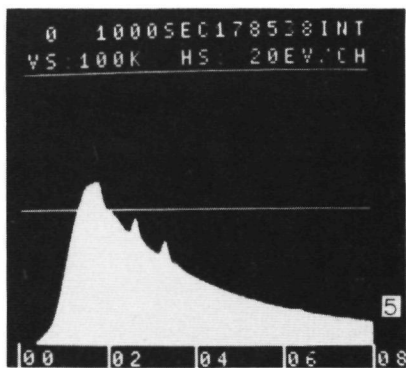


Figs. 2, 3 and 4. Scanning electron micrograph (secondary electron image) of dried microdroplets prepared for X-ray analysis.

Fig. 2. A freeze-dried 76.7 picoliter droplet containing 100mM KCl and placed on a polished Be surface.

Fig. 3. A freeze-dried 76.7 picoliter microdroplet containing 5mM KCl lying on a carbon-coated Parlodion film.

Fig. 4. A flash evaporated 18.7pl. microdroplet containing 200mM NaCl and 5mM KCl on a Parlodion film. The bars indicate 10 μ m (Figs. 2 and 3) and 1 μ m (Fig 4).



Figs. 5 and 6. Typical X-ray spectra obtained with energy dispersive microanalysis of microdroplets.

Fig. 5. A 76.7pl. microdroplet of a 10mM KCl solution lying on Be analysed during 1000sec, H.T. 25kV.

Fig. 6. A 18.7pl. microdroplet from a 2.5mM KCl solution analysed for 40sec, H.T. 25kV. Size of the scanned areas: 45 \times 30 μ m.

area in question), making use of count rates measured in energy windows adjacent to the peak, was developed (see Materials and Methods) From the count rates measured on a series of microdroplets containing increasing amounts of KCl and lying on a Be support, and using this procedure, the calibration lines shown in Fig 7 could be constructed

(B) *Thin film supports* Figure 6 shows a representative ED spectrum from a microdroplet lying on a Parlodion film Comparing Figs 5 and 6 it is evident that the peak-to-background ratios are much higher when using thin films as support The peak/background ratio for K as well as for Cl is about 1 for a droplet of 4.5mM KCl concentration analysed under the conditions men-

tioned in the legend to Fig 6 The contribution of the continuum radiation is much smaller here Background subtraction by linear interpolation of the count rates measured in two energy windows adjacent to the peak provides a sufficiently accurate subtraction method in this case

It should be mentioned that as a consequence of the lower continuum radiation respective to when Be is used as support, X-ray analysis is less time-consuming and shorter analyses are possible giving the same accuracy in the results

Figures 8 and 9 show calibration lines measured on microdroplets lying on Parlodion films for the elements K, Cl and Ca in different concentration ranges The correlation coefficients indicated in the figures bear witness to the good linearity of the calibration lines

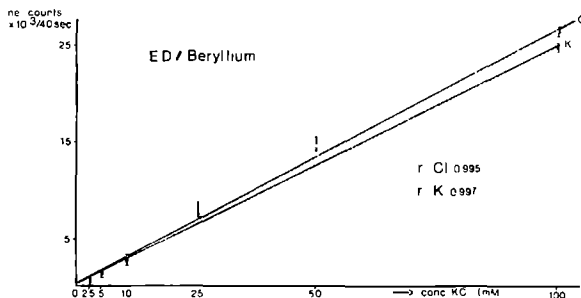


Fig 7, 8 and 9 Calibration curves calculated from energy dispersive analyses on dried microdroplets

Fig 7 Calibration curve measured on freeze dried microdroplets lying on Be support containing an increasing amount of KCl Each point represents the net calculated characteristic peak intensity for K or Cl measured on one microdroplet Time of analysis varied from 20 to 200sec H T 25kV Droplet volume 76 μ l Size of scanned area 45 \times 30 μ m

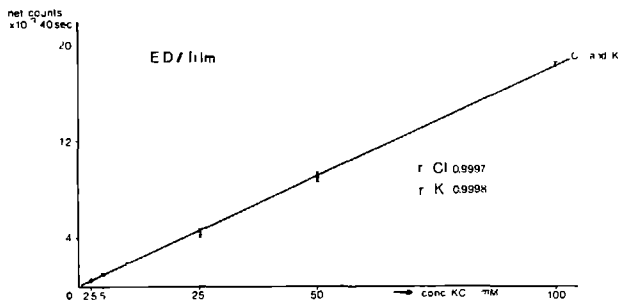


Fig 8 KCl calibration curve 18 μ l flash evaporated microdroplets on a Parlodion film Each point represents the calculated characteristic X ray counts from a 40sec analysis H T 25kV Scanned area 45 \times 30 μ m

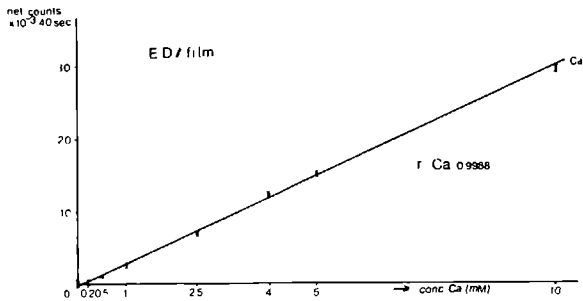
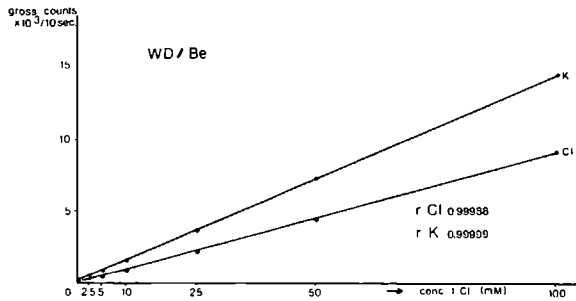


Fig 9 Ca calibration curve 18 7pl flash evaporated microdroplets on a Parlodion film Each point represents a 40sec ED analysis on one droplet H T 25kV Scanned area $22 \times 15 \mu\text{m}$



Figs 10, 11 and 12 Calibration curves calculated from wavelength dispersive analyses on dried microdroplets, using PET diffracting crystals

Fig 10 KCl calibration curve 76 7pl freeze-dried microdroplets on Be Each point represents the average value measured on five different droplets Analysis time 10sec H T 15kV Sample current 48 nanoampere

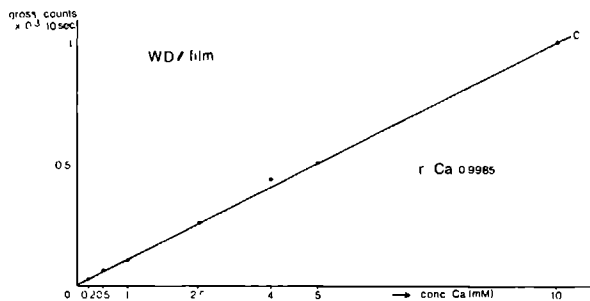


Fig 11 Ca calibration curve 18 7pl flash evaporated microdroplets on Parlodion film Each point represents the average of four 10-sec WD analyses on one droplet H T 15kV Sample current 42 nanoampere

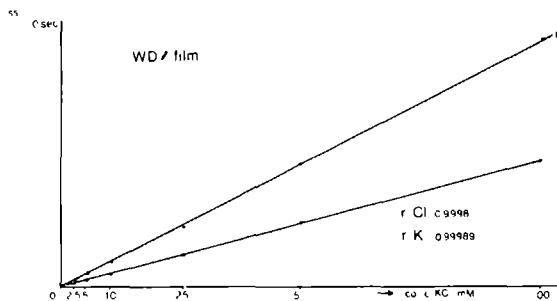


Fig 12 KCl calibration curve 18.7 pl flash evaporated microdroplets on Parlodion film. Each point represents the average value from four 10 sec analyses on one droplet. H.T. 15kV. Sample current 56 nanoampere.

Wavelength dispersive analysis

(A) *Beryllium support* The calibration lines measured on microdroplets placed on Be supports, using WD detection for the elements K and Cl are shown in Fig. 10

(B) *Thin film supports* Using thin films as supports the calibration lines shown in Figs. 11 and 12 for the elements K, Cl and Ca were measured.

DISCUSSION

A very important condition associated with the technique for quantitative X-ray analysis of picoliter microdroplets is the reproducibility of the droplet volume. The results presented in this paper obtained with constriction micropipettes are at least comparable to the results published by other investigators (Lechene, 1974).

Two sample drying methods, freeze-drying and flash evaporation were used and produced comparable results. Flash evaporation is to be preferred to freeze-drying when thin film supports are used as the latter method often causes breakage of the film.

Until recently the microdroplet technique has been carried out most successfully using two procedures. WD measurements on microdroplets on a Be surface and ED measurements on microdroplets placed on thin films. In this paper we report an approach that on a theoretical basis will provide the most accurate results. WD measurements on microdroplets placed on thin films. We compared our results from this method with those obtained from the other techniques.

The calibration lines for the various elements possessed good correlation coefficients (>0.998),

except when ED detection was used for the analysis of droplets on beryllium (Figs. 7, 12). The best results of the technique for X-ray microanalysis of microdroplets were obtained when using WD detection and films as supports. When applying these analytical methods it was possible to measure very small concentrations of elements due to the favourable high peak-to-background ratios obtained. The time needed to obtain a measurement with a given statistical reliability is inversely proportional to P^2/B (P is the net characteristic count rate, B the background count rate). Two factors were found important when comparing ED and WD analysis and are summarized below: (1) The more favourable peak-to-background ratios obtained when WD analysis was used and (2) the relative large counts obtainable with an ED detector. Table 2 shows the P^2/B ratios for K, Cl and Ca in 5mM concentration microdroplets using Parlodion films or Be as supports and ED or WD detection. The same preparations were used for ED as well as for WD analysis. The

Table 2. P^2/B ratios for K, Cl and Ca in 18.7 pl microdroplets of 5mM concentration measured on droplets lying on thin films or beryllium using WD or ED detection.

Detection support	P^2/B for K	P^2/B for Cl	P^2/B for Ca	Accel Voltage (kV)
ED Be	50	54		12
WD Be	6200	3700		15
ED film	1500	1500		12 and 15
WD film	12,500	5100		15
ED film			50,000	25
WD film			300,000	15

values of $P^2 B$ for Ca were much higher than for Cl and K in this case, because of the accidental poor spreading of the Ca containing droplets on the film. Therefore a smaller scanned area during analysis was used.

Under the conditions of analysis used in this study no volatilization of material from the microdroplets could be detected. This was tested by 10 successive measurements on microdroplets under the same experimental conditions established for the determination of the calibration curves. From our experiments we have concluded that X-ray microanalysis of very small volumes of biological fluids using the microdroplet technique can be achieved with a high degree of accuracy when using a wavelength dispersive detection system together with thin supporting films.

Acknowledgements We would like to thank Mr. H. Smits for excellent technical assistance, Mr. A. Desportes for instruction on the Camebax microprobe and Dr. F. D. Ingram and Mrs. M. J. Ingram for reading the manuscript.

REFERENCES

- Boventre, J. V. and Lechene, C., 1974. A method for electron probe microanalysis of organic components in picoliter samples. In *Proc. 9th Annl Conf., Microbeam Analysis Society*, 8A-8D.
- Fiort, C. E., Myklebust, R. L., Heinrich, K. J. and Yakowitz, H., 1976. Prediction of continuum intensity in energy-dispersive X-ray microanalysis. *Analyst Chem*, **48**: 172-176.
- Garland, H. O., Brown, J. A. and Henderson, I. W., 1978. X-ray analysis applied to the study of renal tubular fluid samples. In *Electron Probe Microanalysis in Biology*, Erasmus, D. A. (ed.) John Wiley and Sons, New York, 212-241.
- Garland, H. O., Hopkins, I. C., Henderson, I. W., Haworth, C. W. and Chester-Jones, I., 1973. The application of quantitative electron probe microanalysis to renal micropuncture studies in amphibians. *Micron*, **4**: 164-176.
- Ingram, M. J. and Hogben, C. A. M., 1967. Electrolyte analysis of biological fluids with the electron microprobe. *Analyst Biochem*, **18**: 54-57.
- Lechene, C., 1974. Electron probe microanalysis of picoliter liquid samples. In *Microprobe Analysis as Applied to Cells and Tissues*, Hall, T. et al. (eds) Academic Press, New York, 351-367.
- Lechene, C. and Warner, R. R., 1977. Ultramicroanalysis. *Ann. Rev. Biophys. Bioengn*, **6**: 57-85.
- Morel, F. and Roinel, N., 1969. Application de la sonde électronique à l'analyse élémentaire quantitative d'échantillons liquides d'un volume inférieur à 10^{-11} l. *J. Chim. Phys.* **66**: 1084-1091.
- Pease, D. C., 1964. *Histological Techniques for E.M.*, Academic Press, New York, 192-198.
- Prager, D. J., Bowman, R. L. and Vurek, G. G., 1965. Constant volume, self-filling nanoliter pipette construction and calibration. *Science*, **147**: 606-608.
- Quinton, P. M., 1978a. Techniques for microdrop analysis of fluids (sweat, saliva, urine) with an energy dispersive X-ray spectrometer on a scanning electron microscope. *Am. J. Physiol.* **234**: f255-f259.
- Quinton, P. M., 1976. Construction of pico-nanoliter self-fitting volumetric pipettes. *J. appl. Physiol.* **40**: 260-262.
- Quinton, P. M., 1978b. Ultramicroanalysis of biological fluids with energy dispersive X-ray spectrometry. *Micron*, **9**: 57-69.
- Rick, R., Horster, M., Dorge, A. and Thurau, K., 1977. Determination of electrolytes in small biological fluids samples using energy dispersive X-ray microanalysis. *Pflüg. Arch.*, **369**: 95-98.
- Roinel, N., 1977. Elementary quantitative analysis of lyophilized 10^{-10} l volume solutions. *35th Ann. Proc. Electron Microscop. Soc. Amer.*, Boston, 362-365.
- Roinel, N., 1975. Electron microprobe quantitative analysis of lyophilized 10^{-10} l volume samples. *J. Microsc. Biol. Cell*, **22**: 261-267.
- Roinel, N., Champigny, M., Meny, I. and Henoc, J., 1978. Quantitative analysis of lyophilized solutions. Experimental and theoretical evaluation of the limits of linearity of the calibration curves. *Microbeam Analysis Soc. Proc. 13th Annl Conf.*, 1978, 62A-62D.
- Smits, H., Stols, A. and Stadhouders, A., 1979. Some low background accessories for X-ray microanalysis with a scanning electron microscope. *Ultramicroscopy*, **4**: 143.
- Statham, P. J., 1977. Deconvolution of background subtraction by least-squares fitting with prefiltering of spectra. *Analyst Chem*, **49**: 2149-2154.

Samenvatting

In dit hoofdstuk wordt ingegaan op de analysecondities en de kwantificering in de röntgenmicroanalyse van microdruppels. De belangrijkste conclusies zijn:

-Uit een vergelijking van verschillende correctiemethoden voor aftrek van de achtergrondstraling is gebleken dat lineaire en niet-lineaire interpolatiemethoden aanvaardbare uitkomsten geven.

-Voor de preparaatkantelhoek is een optimale waarde gevonden tussen 22° en 30° in de Philips PSEM500 en van 30° in de Philips EM400G STEM.

-Preparaatvreemde achtergrondstraling blijkt geen significant effect te hebben op de meetresultaten als de microdruppels zich op een dunne dragerfilm op minstens 100 μm afstand van het massieve gridmateriaal bevinden.

-Toevoeging van een organische component aan een microdruppel met overigens anorganische bestanddelen heeft geen significant effect op de piekintensiteiten van de te bepalen elementen.

-Wat betreft de kwantificering zijn met microdruppels de uitgangsformules van een directe kwantificeringsmethode getest en valide gebleken. Een foutenanalyse leert dat met deze kwantificeringsmethode een nauwkeurigheid van ca. 10% haalbaar is.

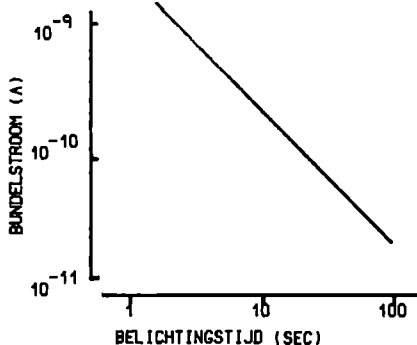
8.1. Inleiding

Microdruppels (Van Eekelen, et al., 1980) blijken ideale standaards te zijn voor de analyse van opgeloste bestanddelen in verschillende fysiologische vloeistoffen (Roinel en De Rouffignac, 1982; Lechene and Warner, 1980). De standaarden zijn over een groot gebied van concentraties en element-samenstellingen te bereiden; immers aan de belangrijkste voorwaarde, namelijk het oplosbaar zijn in water, is eenvoudig te voldoen. Het ligt daarom voor de hand te pogen het toepassingsterrein voor de microdruppel-standaard uit te breiden. Een terrein in de biologische röntgenmicroanalyse waar behoefte is aan goed gedefinieerde standaardpreparaten, is de analyse van compartimenten in biologische systemen. Hierbij moet worden gedacht aan hele cellen, kernen, granula voor opslag en transport van diverse substanties en dergelijke (zie bijv. Boekestein, et al., 1982). De hierboven genoemde microdruppels komen in aanmerking als standaards voor dergelijke analyseproblemen. De conventionele benadering dat een standaard 'ideaal' moet zijn gaat echter in eerste instantie niet op. Een ideale standaard moet namelijk in fysisch en chemisch

opzicht zeer goed gelijken op het preparaat (Roomans, 1979). Microdruppel preparaten spreiden echter uit over een ongeveer cirkelvormig oppervlak met een diameter van enkele tientallen micrometers, terwijl de meeste biologische compartimenten slechts een fractie van een micrometer zijn. Verder worden microdruppel preparaten bij voorkeur bereid uit anorganische componenten, terwijl daarentegen de samenstelling van biologische compartimenten vooral biologisch van aard is. In deze studie is daarom een aantal analysecondities onderzocht voor de röntgenmicroanalyse van microdruppels in een scanning transmissie elektronenmicroscop en een scanning elektronenmicroscop. Voorts is aandacht besteed aan de spectrumverwerking en de kwantificering en de te verwachten nauwkeurigheid van de analyse.

8.2. Het analytisch elektronenmicroscop

Voor de analyse van microdruppels is gebruik gemaakt van een Philips EM400G scanning transmissie elektronen microscop en een Philips PSEM500 scanning elektronen microscop. De EM400G is voorzien van een goniometer preparaattafel en een energie-dispersief röntgenmicroanalyse-systeem (EDAX 707B). De röntgen-detector is hierbij horizontaal opgesteld, zodanig dat de preparaatkantelas een hoek van 90° maakt met de lengteas van de detector. De energie-resolutie van deze röntgendetector, met een actief oppervlak van 10 mm^2 is ca 165 eV ($\text{Mn K}\alpha$). De afstand van het preparaat tot de detector bedraagt 20 mm . Er is voorts gebruik gemaakt van een preparaathouder met beryllium onderdelen om de intensiteit van de achtergrondstraling zo laag mogelijk te houden. De bundelstroom wordt indirect gemeten door de benodigde belichtingstijd voor fotografische opnamen te meten. In Figuur 1 is deze belichtingstijd uitgezet als functie van de bundelstroom. De belichtingstijd blijkt omgekeerd evenredig te zijn met de bundelstroom (Smits et al., 1982). De versnelspanning is instelbaar op 20, 40,

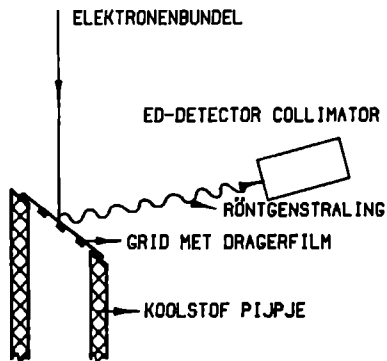


Figuur 1. Het verband tussen de benodigde belichtingstijd voor fotografische opnamen en de elektronenbundelstroom. De bundelstroom is gemeten met een speciaal voor de Philips EM400G vervaardigde preparaathouder, voorzien van een faradaykooi (Smits et al., 1982).

60, 80, 100 en 120 kV. Tenslotte zijn de STEM-beeld vergrotingen gecalibreerd met een replica van 2160 lijnen per mm. De verhouding van de gemeten afstand

en de door de fabrikant opgegeven afstand tussen twee lijnen, berekend voor verschillende vergrotingen, is gemiddeld 1,09 (S.D. 0,08).

De PSEM500 is gebruikt voor metingen van microdruppels zowel op beryllium plaatjes als op dunne dragerfilms. Om grids met dragerfilms te kunnen analyseren is een speciale preparaathouder van koolstof gemaakt, waarin de grids onder een bepaalde vaste kantelhoek zijn gemonteerd. In Figuur 2 is de situatie in de PSEM500 met betrekking tot de plaatsing van de energie-dispersieve detector en het preparaat weergegeven. De PSEM500 is voorzien van een energie-dispersief röntgenmicroanalyse systeem (EDAX 707B), waarbij de energieresolutie van de detector 165 eV is ($Mn K_{\alpha}$) (actief oppervlak 30 mm²). De collimator van deze detector is vervaardigd van grafiet om de bijdrage van het collimator materiaal aan het röntgenspectrum zo klein mogelijk te houden. De versnelspanning van de PSEM500 is instelbaar op 3, 6, 12, 25 en 50 kV.



Figuur 2. De elektronenbundel-preparaat-detector geometrie (schematisch) bij röntgenmicroanalyse van microdruppels op een dunne dragerfilm in de PSEM500.

8.3. Correctie voor de achtergrondstraling in de röntgenspectra

In het microdruppel onderzoek zijn verschillende correctiemethoden voor de achtergrondstraling gebruikt, namelijk de frequentiefilter methode (standaardprogramma van het EDAX systeem), lineaire en niet-lineaire interpolatie methoden en de 'multiple least squares fitting' methode (standaardprogramma van het TRACOR röntgenmicroanalyse-systeem). In eerste instantie is voor de verwerking van de spectra de software van EDAX gebruikt. Later is de mogelijkheid ontstaan, spectra tevens te verwerken met software van een TRACOR TN2000 systeem.

8.3.1. Een energie-dispersief röntgenspectrum kan worden beschouwd als te zijn opgebouwd uit een laagfrequent achtergrondsignaal, een middelfrequent elementkarakteristieke pieksignaal en een hoogfrequent ruissignaal. Bij de frequentie-filter methode wordt door 'digital filtering' van lage en hoge frequenties op deze manier de achtergrond en de ruis uit het spectrum 'verwijderd'. Voordelen van deze methode zijn dat hij niet gevoelig is voor

miscalibratie van het energie-dispersief systeem en dat de achtergrondaf trek methode eenvoudig te gebruiken en snel is. Een nadeel van deze methode is dat bij piekoverlapsituaties systematische kunnen fouten optreden.

8.3.2. Bij lineaire interpolatie worden energievensters in het spectrum gekozen ter plaatse van en naast de piek. In Tabel 1 zijn de resultaten vergeleken van de frequentiefilter methode en lineaire interpolatie bij analyse van microdruppels op dunne dragerfilms. Uit deze resultaten volgt dat lineaire interpolatie in dit geval te gebruiken is naast de frequentiefilter methode. Bij röntgenmicroanalyse van microdruppels op beryllium plaatjes is de intensiteit van de achtergrondstraling echter aanzienlijk hoger dan bij microdruppels op dunne dragerfilms. Hierdoor gaat het niet-lineaire karakter van het verloop van de achtergrondstralingsintensiteit bij lagere energie (<4 keV) een belangrijker rol spelen. Daarom is een niet-lineaire interpolatie methode ontwikkeld, waarbij onder dezelfde analysecondities spectra worden opgenomen van de microdruppel en van de drager naast de microdruppel. Hierbij is gebleken dat de achtergrond van beide spectra nagenoeg gelijkvormig is. Bij analyse van de microdruppel zijn de stralingsintensiteiten, gemeten in energievensters naast en op de piek (zie Figuur 3a), opgebouwd uit achtergrondstraling afkomstig van de drager, achtergrondstraling afkomstig van de microdruppel en element-karakteristieke straling afkomstig van de microdruppel. Bij analyse van de drager naast de microdruppel worden alleen de intensiteiten B1, B2 en B3 gemeten (Fig. 3b). Door lineaire interpolatie tussen venster 1 en 3 worden in venster 2 schattingen verkregen van

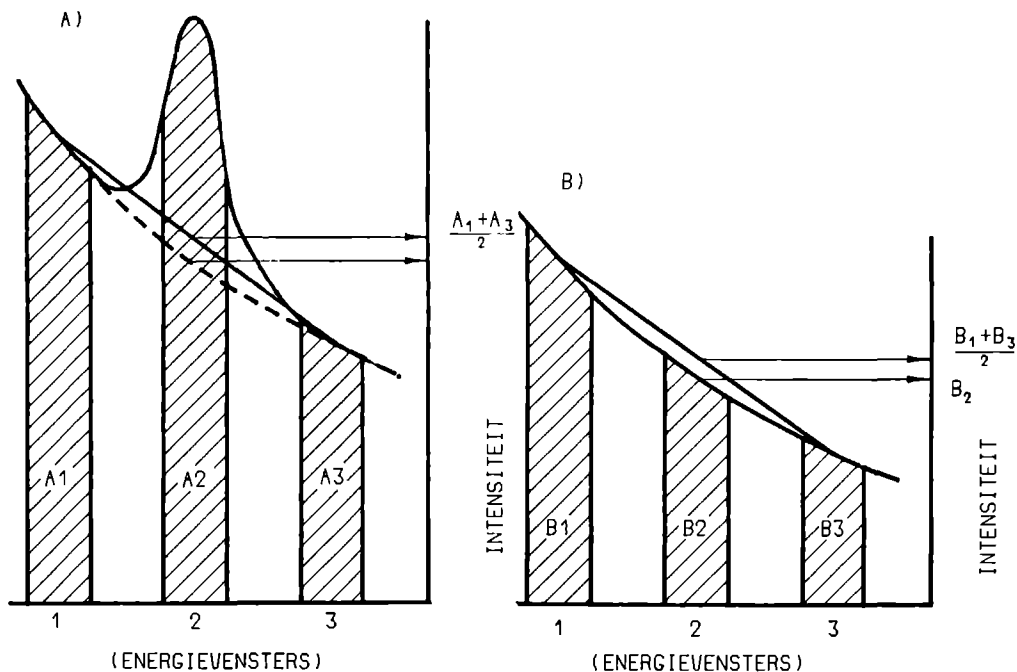
Tabel 1. Een vergelijking van lineaire interpolatie en frequentie-filter-methode. De röntgenspectra zijn afkomstig van een microdruppels met verschillende hoeveelheden calcium. Er is gemeten in de EM400G STEM bij 80 kV versnelspanning en 30° kantelhoek. De resultaten zijn gemiddelden van 8 metingen van 100 'live' seconden elk. De getallen tussen haakjes geven de standaardfouten in % aan. De correlatiecoëfficiënt van de lineaire regressie is steeds 0,998.

calcium concentratie (mM)	lineaire interpolatie piekintensiteit (counts)	frequentie filter methode piekintensiteit (counts)
1,56	177 (5,0)	87 (8,0)
3,13	342 (3,5)	320 (5,0)
6,25	1059 (2,3)	1038 (2,0)
25,0	3873 (2,6)	4047 (2,8)

respectievelijk de achtergrond van de drager, $(B_1+B_3)/2$ en van de drager plus microdruppel, $(A_1+A_3)/2$. Deze schattingen zullen afwijken van de werkelijke waarden, omdat de achtergrondvorm meestal niet lineair is. Onder de voorwaarde dat bovengenoemde aanname over de gelijkvormigheid geldt, kan worden afgeleid dat de correctiefactor gelijk is aan $2B_2/(B_1+B_3)$. De achtergrond onder de piek wordt hiermee:

$$\frac{B_2 (A_1 + A_3)}{(B_1 + B_3)} \quad (1)$$

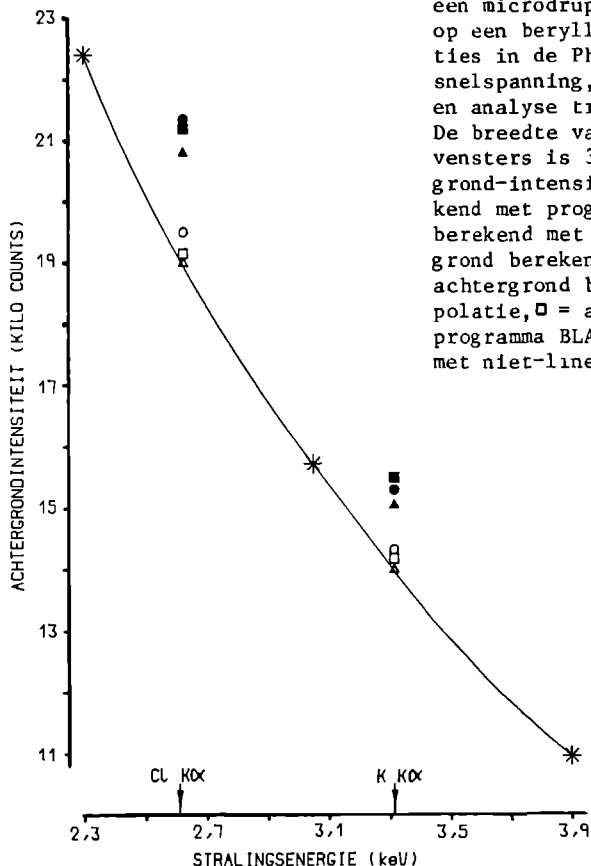
zodat de netto piekintensiteit kan worden uitgerekend. Bij wijze van controle van de hierboven beschreven methode is van een 100 mM KCl microdruppel op een beryllium plaatje de achtergrondintensiteit onder Cl K en de K K_{α} bepaald met behulp van niet-lineaire interpolatie, lineaire interpolatie en de programma's BLANK, INT, STRIP, BGSUB van de EDIT 7EM software van EDAX. Alleen in het geval van niet-lineaire interpolatie blijkt dat een correcte, vloeiende curve te trekken is door alle achtergrondpunten (zie Figuur 4). Het enige pro-



Figuur 3. Schematische weergave van de niet-lineaire interpolatiemethode voor het bepalen van de achtergrond intensiteit in een energie-dispersief röntgenspectrum.

gramma van EDAX dat de juiste waarde goed benadert, is het programma BLANK dat ook gebaseerd is op de gelijkvormige achtergrond van drager en microdruppel spectrum.

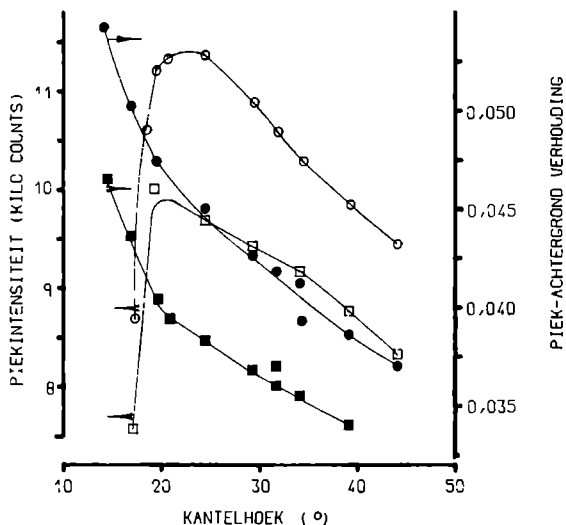
8.3.3. De achtergrondaf trek van het TRACOR systeem bestaat uit het fitten van een deel van standaardspectra van alle aanwezige elementen op het te verwerken spectrum ('multiple least squares fitting'). Hierbij wordt eerst door toepassing van een digitaal filter de achtergrond 'verminderd'. De mate waarin een bepaalde fit 'goed' is, wordt uitgedrukt in een zogenaamde 'reduced' χ^2 waarde. Van belang bij deze methode is dat de calibratie van de energieschaal van standaardspectra en te verwerken spectrum dezelfde is.



Figuur 4. De achtergrondintensiteiten onder de K en Cl pieken berekend met lineaire en niet-lineaire interpolatie en een aantal EDAX programma's. De röntgenmicroanalyse meting is uitgevoerd aan een microdruppel van 100 mM KCl gebracht op een beryllium plaatje. Analyse condities in de Philips PSEM500: 12 kV versnelling, 30° preparaat kantelhoek en analyse tijd 200 'live' seconden. De breedte van de gebruikte energievensters is 300 eV. * = de gemeten achtergrond-intensiteit, ● = achtergrond berekend met programma INT, ■ = achtergrond berekend met programma STRIP, ▲ = achtergrond berekend met programma BGSUB, ○ = achtergrond berekend met lineaire interpolatie, □ = achtergrond berekend met programma BLANK, △ = achtergrond berekend met niet-lineaire interpolatie.

8.4. Analysecondities

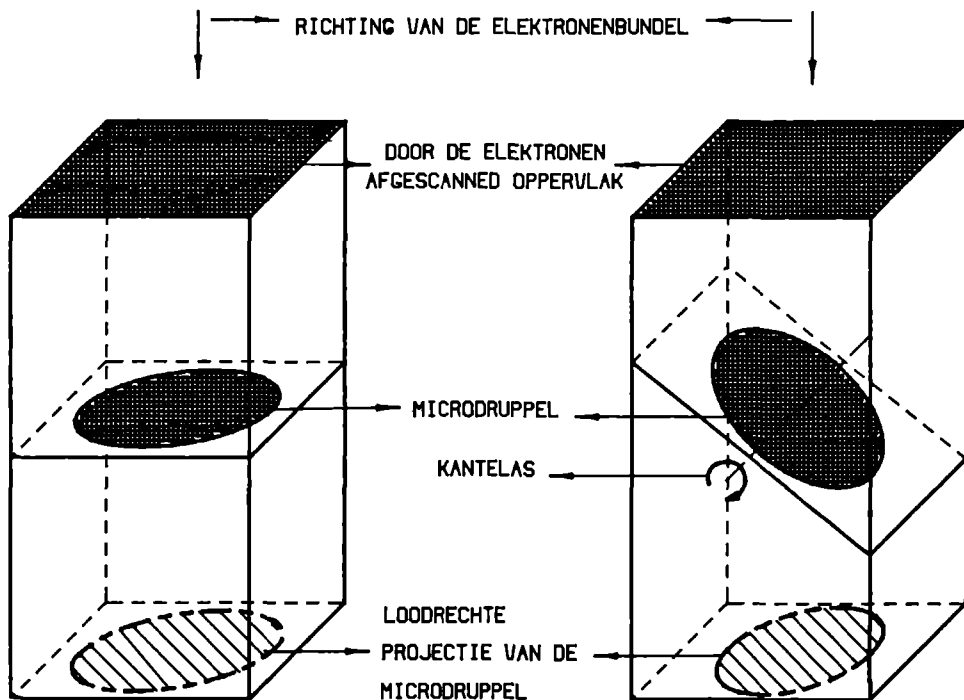
De invloed van de preparaatkantelhoek en de versnelspanning op de meetresultaten van het microdruppel onderzoek is nader onderzocht. Hierbij is getracht optimale waarden voor deze analysecondities te vinden voor de EM400G STEM en de PSEM500. Het effect van de kantelhoek op de piekintensiteiten en piek-achtergrond verhoudingen in de PSEM500 voor microdruppels op een beryllium plaatje is weergegeven in Figuur 5. Bij stijgende kantelhoek blijkt een daling plaats te vinden van de piek-achtergrond verhouding voor K en Cl, doordat er relatief minder massa van de microdruppel wordt aangestraald (zie Figuur 6). Voor de netto piekintensiteit wordt een optimum waargenomen tussen 22° en 30° . De verklaring voor het optreden van een maximum in de geregistreeerde piekintensiteit bij toenemende kantelhoek ligt waarschijnlijk in twee tegengesteld werkende effecten. Bij kanteling wordt voor een - bij kantelhoek 0° geheel bestraalde microdruppel - enerzijds de effectieve stroomdichtheid kleiner waardoor de piekintensiteit zal afnemen (zie Figuur 6). Anderzijds neemt de absorptieweg door het preparaat voor de opgewekte straling af zodat de piekintensiteit juist kan toenemen bij kanteling. De instelling van de kantelhoek blijkt boven het maximum zeer kritisch te zijn: 1% afwijking in de piekintensiteiten en dus uiteindelijk ook in de te berekenen massahoeveelheden wordt boven 25° kantelhoek reeds veroorzaakt door 1° afwijking. Dit gegeven komt overeen met het effect op de ZAF-gecorrigeerde concentraties van een fout in de kantelhoek van 1° (zie hoofdstuk 4). De



Figuur 5. De invloed van de preparaat kantelhoek in de Philips PSEM500. Analysecondities: 12 kV versnelspanning en analysetijd 40 'live' seconden. De meting is uitgevoerd aan een microdruppel van 100 mM KCl gebracht op een beryllium plaatje. ● = Cl piek-achtergrond verhouding, ■ = K piek-achtergrond verhouding, ○ = netto Cl piekintensiteit, □ = netto K piekintensiteit, ▲ = totale geregistreeerde röntgenintensiteit tot 8 keV.

piek-achtergrond verhoudingen dalen steeds bij toenemende kantelhoek doordat bij grotere kantelhoeken relatief meer massa van de beryllium preparaatdrager wordt aangestraald waardoor de bijdrage daarvan aan de achtergrondintensiteit toeneemt.

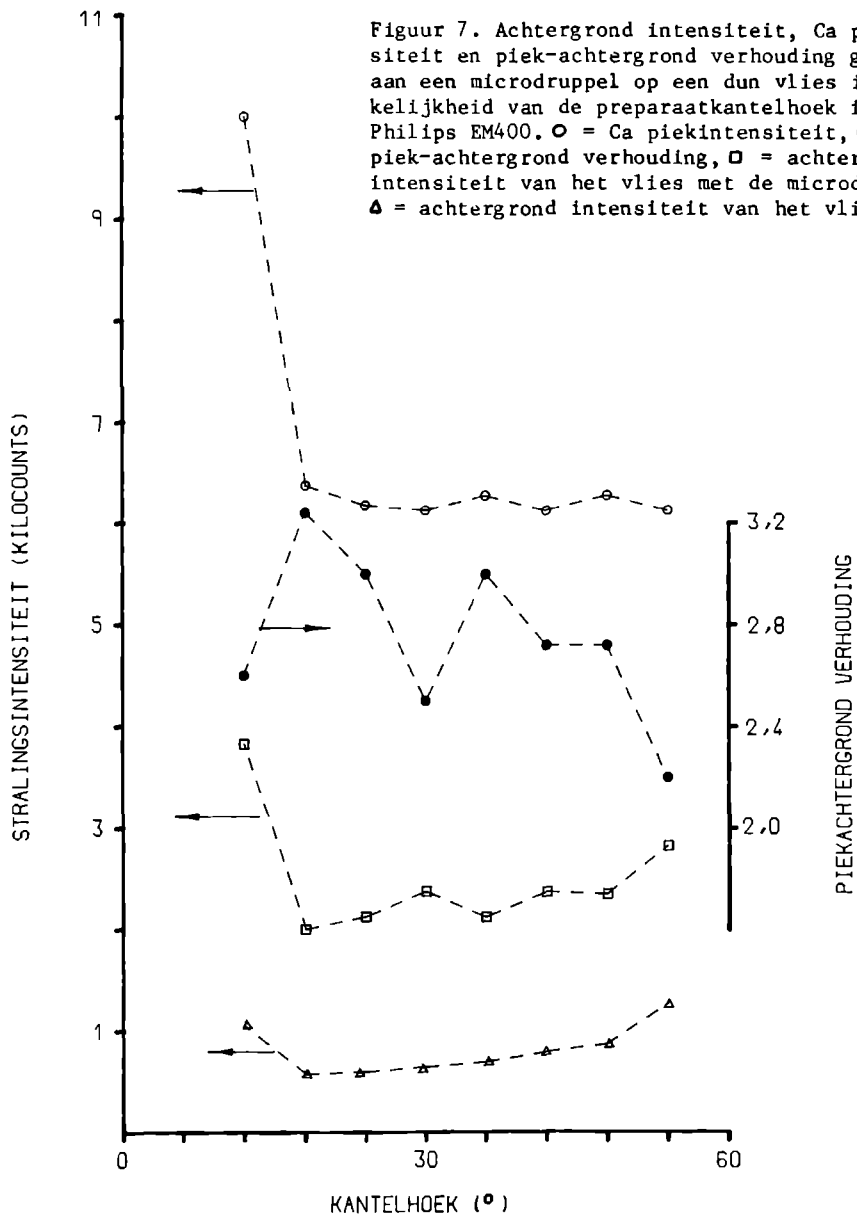
Het effect van de kantelhoek op piekintensiteiten en piek-achtergrond verhoudingen voor microdruppels op een dragerfilm in de EM400G STEM, is weergegeven in Figuur 7. Bij stijgende kantelhoek is tot ca 24° een daling van de piekintensiteit waargenomen, terwijl deze daarna constant blijft. Bij de achtergrondintensiteit wordt na een aanvankelijke daling een lichte toename geconstateerd. Het is dan ook voor de hand liggend dat de piek-achtergrond verhouding zal afnemen met toenemende kantelhoek. Dat hier niet het optimum wordt waargenomen zoals in Figuur 5 vindt waarschijnlijk zijn oorzaak in het feit dat de metingen zich niet tot de zeer lage kantelhoeken hebben uitgestrekt. De waarnemingen kunnen verder weer verklaard worden met behulp van Figuur 6. Er is voorts een stijging waargenomen van de relatieve hoeveelheid



Figuur 6. Schematische weergave van de invloed van preparaatkanteling op de preparaatstroomdichtheid.

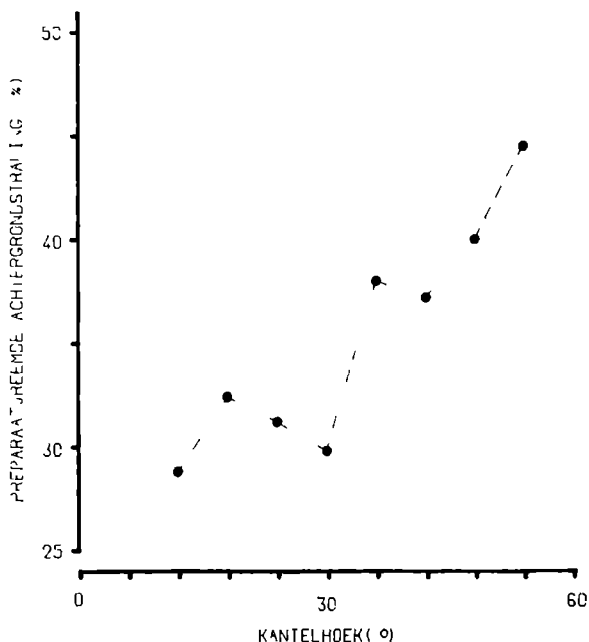
preparaatvreemde achtergrondstraling bij grotere kantelhoeken (zie Figuur 8). Op grond hiervan is besloten de verdere metingen te verrichten bij 30° kantelhoek.

In een verdere studie is nagegaan op welke afstand van het gridmateriaal de microdruppels gedeponerd moeten worden zodat de meetresultaten niet afhangen

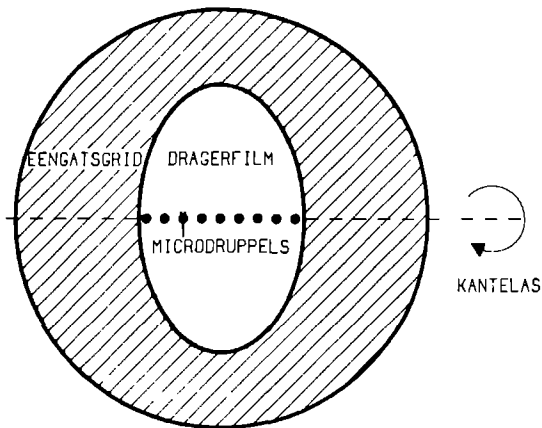


van de afstand tot het gridmateriaal. Een koperen 'one hole' grid (grootste afmeting van het gat ca. 2 mm), voorzien van een dragerfilm met microdruppels (zie Figuur 9) is hiertoe geanalyseerd in de EM400G STEM bij 80 kV versnelspanning en 30° kantelhoek. De piekintensiteit en piek-achtergrond verhouding als functie van de afstand tot het gridmateriaal is weergegeven in Figuur 10. In Tabel 2 zijn deze resultaten nog eens samengevat waarbij bleek dat de standaard deviatie in de gemeten piekintensiteiten voornamelijk een gevolg is van telstatistiek en de pipetteerfout van het capillair. Tot in elk geval $100 \mu\text{m}$ van het gridmateriaal is de piekintensiteit onafhankelijk van de positie van de druppel op het vlies. Anders is dit voor de piek-achtergrond verhouding die tot ca $200 \mu\text{m}$ beïnvloed blijkt te worden door het gridmateriaal. Dit verschijnsel wordt waarschijnlijk veroorzaakt door preparaatvreemde achtergrondstraling. Metingen aan microdruppels, gedeponeerd in het midden van een maas van een 50 mesh grid zullen op grond van het bovenstaande geen invloed ondervinden van het gridmateriaal.

De versnelspanning heeft invloed op de piek- en de achtergrond intensiteiten. Enerzijds neemt bij hogere versnelspanningen de kinetische energie en de

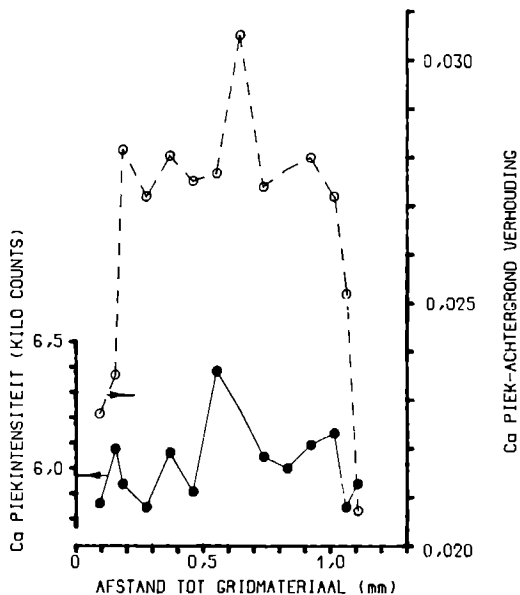


Figuur 8. Het percentage preparaatvreemde achtergrond intensiteit veroorzaakt door de microdruppel als functie van de preparaatkantelhoek.



Figuur 9. Schematische weergave van de meetopstelling met een 'one-hole' grid waarbij een aantal microdruppels van dezelfde oplossing in transversale richting op een dun dragervlies werd gebracht, ter plaatse van de kantelas.

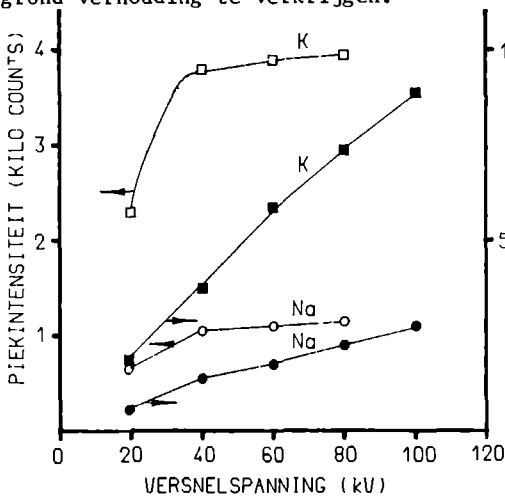
Figuur 10. Het effect van de afstand microdruppel-gridmateriaal in de meetopstelling van figuur 9 op de calcium piekintensiteit en piek-achtergrond verhouding.
 ● = calcium piekintensiteit,
 ○ = calcium piek-achtergrond verhouding.



Tabel 2. De nauwkeurigheid van de Ca K_{α} en Cl K piekintensiteiten. De microdruppels zijn gelegen op verschillende afstanden van het gridmateriaal van een 'one hole' grid.

	Ca	Cl
gemiddelde intensiteit ('counts')	6055	10961
standaard deviatie ('counts')	168	255
variatiecoëfficiënt (%)	2,77	2,32
fout door telstatistiek (%)	1,6	1,2
pipetteerfout capillair (%)	1,1	1,1

reikwijdte van de elektronen toe waardoor bij eenzelfde bundelstroom meer röntgenstraling wordt opgewekt. Anderzijds zal bij analyse van microdruppels op een massieve beryllium drager, een hogere versnelspanning een lagere piek-achtergrond verhouding te zien geven omdat zich dan relatief veel beryllium in het excitatievolume bevindt. Optimale waarden voor de versnelspanning blijken 12 en 25 kV te zijn in de PSEM500, gegeven de instelmogelijkheden. Het effect van de versnelspanning bij metingen aan microdruppels op een dragerfilm in de EM400G is weergegeven in Figuur 11. Hierbij blijken zowel de piekintensiteiten als de piek-achtergrond verhoudingen te stijgen met toenemende versnelspanning. De toename in de piek-achtergrond verhouding kan verklaard worden omdat de drager in dit geval slechts bestaat uit een dunne dragerfilm zodat bij toenemende versnelspanning er niet meer dragermateriaal wordt aangestraald. De waarneming dat vanaf ca. 40 kV de piek-achtergrond verhouding voor Na en K niet meer verandert terwijl de netto piekintensiteit nog wel stijgt kan verklaard worden door een toename van de preparaatvreemde achtergrondstraling bij hogere versnelspanning. Bij de EM400G is als optimale waarde voor de versnelspanning een waarde van 80 kV gekozen in verband met de stabiliteit van de dragerfilm en om een maximale piek-achtergrond verhouding te verkrijgen.



Figuur 11. Het effect van de versnelspanning op de piekintensiteiten en de piek-achtergrond verhoudingen van Na en K, aanwezig in microdruppels en gemeten in de Philips EM 400. Analysecondities: 30° preparaatkantelhoek, analyse tijd 100 'live' seconden. Punten zijn gemiddelden van twee analyses. ● = piek-achtergrond verhouding Na, ■ = piek-achtergrond verhouding K, ○ = piekintensiteit Na, □ = piekintensiteit K.

	helling	intercept op y-as	correlatie coëfficiënt
Mg	-1,063	14,56	-0,999
P	-1,005	15,60	-0,999
Cl	-1,054	15,41	-0,999
K	-1,018	15,83	-0,999

Tabel 3. Het effect van de vergroting op de piekintensiteiten bij analyse van een microdruppel. Analysecondities: Versnelspanning 80 kV, preparaat kantelhoek 30°. Analyse uitgevoerd in Philips EM400G STEM. Scanning raster is groter of gelijk aan de omvang van de microdruppel. Aantal metingen = aantal verschillende vergrotingen = 10.

8.5. Kwantificering

Om na te gaan of de microdruppel standaard ook gebruikt kan worden voor kwantitatieve elementbepaling in cellen of celorganellen, zijn de meetresultaten aan microdruppels met elkaar vergeleken waarbij naast de te bepalen elementen al of niet een organische component aanwezig was. In Figuur 12 zijn ijkreeksen van KNa tartraat en KCl-oplossingen getoond. Er zijn hierbij geen significante verschillen gevonden tussen beide reeksen. In Figuur 13 zijn ijkreeksen getoond van calciumnitraat oplossingen met resp. 0%, 1% en 10% ascorbinezuur. De toevoeging van een organische component blijkt ook hier geen significante invloed te hebben. Hieruit volgt dat microdruppels bestaande uit anorganische componenten als standaard kunnen worden gebruikt in de kwantificering indien deeltjes worden onderzocht met een organisch-chemische samenstelling. Bij de feitelijke kwantificering worden de piekintensiteiten van een bepaald element in standaard en preparaat met elkaar vergeleken. Preparaat en standaard moeten hierbij beide van het zogenaamde scherp begrensde deeltjes-type zijn, dat wil zeggen dat de te bepalen elementen zich in een duidelijk begrensd compartiment bevinden en daarbuiten niet.

De basisformule waarvan dan uitgegaan wordt, is:

$$P_x \sim \frac{W_x}{O} \quad (2)$$

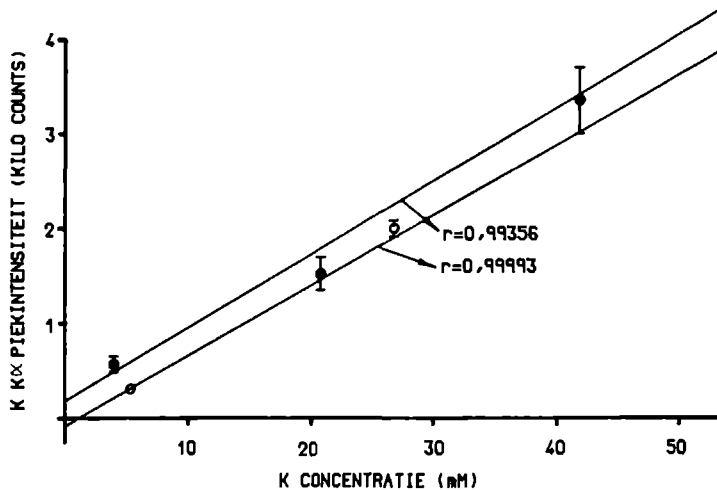
hierin is, x het te analyseren element

W_x de massa van element x in het excitatievolume
 O het geanalyseerde oppervlak

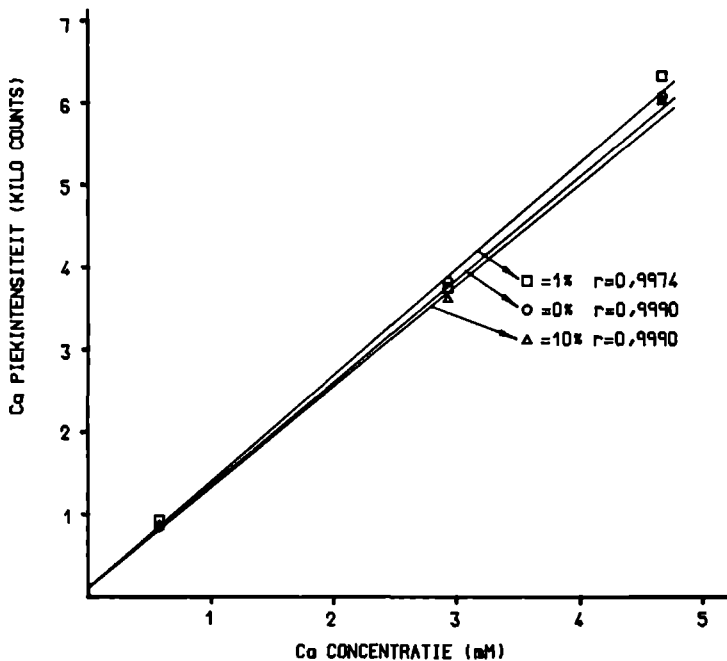
Vergelijking (2) kan worden geschreven in de vorm:

$$\ln \left(\frac{P_x}{O} \right) = \text{constante} - \ln(O) \quad (3)$$

indien de preparaatstroom en de massa van het element x constant blijven, terwijl de vergroting verandert. Vergelijking (3) is getest door een microdruppel met daarin de elementen H, O, Mg, P, Cl en K te analyseren bij verschillende vergrotingen. De resultaten hiervan zijn getoond in Tabel 3. Gezien de goede correlatiecoëfficiënten en de grote overeenkomst in de waarden voor de constante en de helling van de lijn voor de verschillende elementen mag worden aangenomen dat vergelijking (2) geldig is. Uit vergelijking (2) volgt met $O \sim 1/M^2$:



Figuur 12. IJklijnen van K bevattende microdruppels (3,1 pl) gemeten bij 80 kv versnelling in de Philips EM400G. ○ = NaK tartraat, ● = KCl.



Figuur 13. IJklijnen voor calcium van microdruppels met verschillende ascorbinezuur toevoegingen gemeten in de Philips EM400G STEM bij 80 kv. Meetpunten zijn gemiddelden van minstens 4 metingen. ○ = 0% ascorbinezuur, □ = 1% ascorbinezuur, Δ = 10% ascorbinezuur. De variatiecoëfficiënt van de metingen bij de drie onderzochte Ca concentraties zijn respectievelijk 20%, 6,8% en 10,8%. r = correlatie coëfficiënt.

$$W_{sp} = \frac{P_{sp} I_{st} M_{st}^2}{P_{st} I_{sp} M_{sp}^2} W_{st} \quad (4)$$

hierbij is M de vergroting waarbij geanalyseerd is.

De relatieve fout die gemaakt wordt in het berekenen van W_{sp} met vergelijking (4) is:

$$\delta W_{sp}^2 = \delta P_{sp}^2 + \delta P_{st}^2 + \delta W_{st}^2 + 2\delta M_{sp}^2 + 2\delta M_{st}^2 + \delta I_{sp}^2 + \delta I_{st}^2 \quad (5)$$

δP is de fout in de piekintensiteit op grond van de telstatistiek tezamen met een eventuele systematische fout tijdens de achtergrondaf trek. De statistische fout neemt sterk af bij grotere intensiteiten (zie Tabel 4). De systematische fout is moeilijker te schatten doch als dit steeds dezelfde relatieve afwijking is van de nominale waarde dan valt het effect hiervan weg in vergelijking (4). δM is de fout in de vergrotingsijking. De vergroting is meestal nauwkeurig genoeg bekend. Eventuele fouten hierin zijn meestal klein en te voorkomen door goede ijking. δW is de fout in de gewichtshoeveelheid van een bepaald element in de microdruppel standaard. De samenstelling van de standaardoplossing kan zeer nauwkeurig bekend zijn hetgeen inhoudt dat de fout in W voornamelijk wordt bepaald door de pipetteerfout van het capillair die maximaal 2% is (Hoofdstuk 6). Met δI is de fout in de preparaatstroom bedoeld. Als er relatief langzame veranderingen in de preparaatstroom met de tijd optreden, dan kan er door middel van interpolatie gecorrigeerd worden. Het verdient echter aanbeveling om de metingen zoveel mogelijk bij constante preparaatstroom uit te voeren. Indien de preparaatstroom stabiel wordt verondersteld dan wordt de fout in W_{sp} grotendeels bepaald door de pipetteerfout van het capillair en de fout in de meting van de piekintensiteit van het element in het onbekende preparaat (zie Tabel 4). In de standaard kan men namelijk meestal de piekintensiteit nauwkeurig genoeg bepalen. De 'overall' analysefout van deze kwantificerings methode kan aldus worden beperkt tot ca. 10%.

8.6. Discussie

De eerste stap bij de kwantificering in de röntgenmicroanalyse is het verkrijgen van netto piekintensiteiten of piek-achtergrondverhoudingen. Voor de daarvoor noodzakelijke berekening van de hoogte van de achtergrondstraling

onder de betreffende piek bestaan verschillende methoden. Aan welke methode men de voorkeur geeft hangt af van analyseapparatuur en van de gewenste nauwkeurigheid. Meestal zullen de met de apparatuur meegeleverde computerprogramma's geschikt zijn voor het berekenen van de netto piekintensiteit. Echter, in het geval van microdruppels aanwezig op een massieve drager, blijken de standaard-computerprogramma's van EDAX, die berusten op de frequentie-filter methode, minder goed te voldoen (zie Figuur 4). Met een niet-lineaire interpolatie methode kunnen voor deze analysesituatie nauwkeuriger uitkomsten worden verkregen.

Van de analysecondities hebben vooral de preparaat-kantelhoek en de versnelspanning invloed op de uiteindelijk uitkomsten. Voor de kantelhoek zijn optimale waarden gevonden tussen 22° en 30° (zie Fig. 5 en 7). Dit is verklaarbaar als men de effectieve bundelstroombichtheid in beschouwing neemt (zie Figuur 6). Mede gelet op de toename van de relatieve hoeveelheid preparaatvreemde achtergrondstraling bij stijgende kantelhoek (zie Figuur 8), verdient het aanbeveling de kantelhoek te beperken tot waarden tussen 22° en 30° . Binnen de mazen van een 50 mesh grid blijkt een voldoende groot gebied aanwezig waar microdruppels gedeponeerd kunnen worden zonder dat ongecollimeerde bundelelektronen of preparaatvreemde straling een verstorende invloed hebben op de piekintensiteiten of piek-achtergrond verhoudingen. De druppels dienen dan te liggen op een afstand groter dan $100 \mu\text{m}$ van het gridmateriaal.

De kwantificeringsmethode die in dit hoofdstuk wordt voorgesteld berust op de algemeen aanvaarde aanname dat er een evenredigheid bestaat tussen de piekintensiteit en de aangestraalde massa van een element. In de uitwerking van deze relatie dient echter rekening te worden gehouden met het analyseren van

Tabel 4. De procentuele relatieve fout ($100 \frac{\delta P}{P}$) in de netto piekintensiteit P op grond van de telstatistiek. B is de achtergrondintensiteit.

B	20	200	2000
P			
50	19,0	42,4	127,3
500	4,7	6,0	13,4
5000	1,4	1,5	1,9

preparaat en standaard bij verschillende vergrotingen in de scanning transmissie elektronenmicroscop. Variabele vergroting impliceert immers een variabele stroombichtheid op het geanalyseerde oppervlak. De uitgangformule

is getest door eenzelfde druppel te analyseren bij verschillende vergrotingen. Uit de waarneming dat hierbij voor alle onderzochte elementen een identieke relatie werd gevonden volgt dat de uitgang formule geldig is. Toevoeging van een organisch-chemische component aan een anorganische microdruppel blijkt geen significant effect te hebben op de ligging van de ijklijnen. De bevindingen voeren tot de conclusie dat de uit anorganische bestanddelen bestaande microdruppels geschikt zijn voor het gebruik als standaard in de kwantitatieve röntgenmicroanalyse van individuele aanzienlijk kleinere cellen of celorganellen.

Referenties

- Boekestein, A., Kuijpers, G.A.J., Peters, E. en Stadhouders, A.M. (1982). Quantitative X-ray microanalysis of Mg, P and Ca in rat blood platelets. Proc. 10th Int. Congr. Electron Microscopy, 3, 369-370.
- Lechene, C.P. en Warner, R.R. (1980). An overview of the applications of microdroplet analysis: past, present and future. In: Microbeam Analysis (Wittry, D. (ed.), San Francisco Press, San Francisco) 108-111.
- Roomans, G.M. (1979). Standards for X-ray microanalysis of biological specimens. Scanning Electron Microscopy, 2, 649-658.
- Roinel, N. en De Rouffignac, Ch. (1982). X-ray analysis of biological fluids: contribution of microdroplet technique to biology. Scanning Electron Microscopy 3, 1155-1171.
- Smits, H.T.J., Linders, P.W.J., Stols, A.L.H. en Stadhouders, A.M. (1982). Modification of a TEM specimen holder to permit beam current measurements for use in quantitative X-ray microanalysis. Proc. 10th Int. Congr. Electron Microscopy, 1, 679-680.
- Van Eekelen, C.A.G., Boekestein, A., Stols, A.L.H. en Stadhouders, A.M. (1980). X-ray microanalysis of picoliter microdroplets: improvement of the method for quantitative X-ray microanalysis of samples of biological fluids. Micron, 11, 137-145.

ELEMENTAL ANALYSIS OF INDIVIDUAL RAT BLOOD PLATELETS BY ELECTRON PROBE X-RAY
MICRO ANALYSIS USING A DIRECT QUANTIFICATION METHOD

Abraham Boekestein, Gemma A.J. Kuypers, Alexander L.H. Stols and Ad M.
Stadhouders

Institute for Submicroscopic Morphology, University of Nijmegen Medical School,
Nijmegen, The Netherlands

Histochemistry,
submitted for publication

Summary

The elemental content of individual rat blood platelets and their dense granules was determined by electron probe X-ray microanalysis using a direct quantification method with microdroplets as standards. The quantification procedure was a modification of the 'direct mass' method involving a correction for differences in electron beam intensity in the analyses of standards and specimens. Whole air-dried platelets had a mean magnesium content of $12 \cdot 10^{-8}$ nmol (SE = $1 \cdot 10^{-8}$, n = 68) and a mean calcium content of $3.2 \cdot 10^{-8}$ nmol (SE = $0.3 \cdot 10^{-8}$, n = 68). A good correlation was found between the magnesium content and the phosphorus content of the dense granules of the platelets (r = 0.95).

There was also a good correlation (correlation coefficient 0.77) between the number of dense granules per platelet and the magnesium content of the platelets.

Introduction

In human platelet stimulation studies it has been shown that calcium is mobilized, presumably from Ca-accumulating structures with the consequence that the free Ca concentration rises in the cytoplasm (Massini, 1977). This causes a localized contractile activity followed by the tendency of the platelets to aggregate. Increase in the cytoplasmic Ca concentration also leads to the so-called release reaction and to an increase in cell membrane permeability for Ca (Massini, 1977).

Although relatively large amounts of Mg have been reported to be present in blood platelets of some species (e.g. pig and cat, Imandt et al., 1980), little is known about the function of Mg in blood platelets. In order to study this role it is important to know the Ca and Mg contents of blood platelets preferably per individual platelet. Furthermore it is of importance to know the localization of Ca and Mg pools in the platelet.

Several techniques have been applied to determine the elemental content of blood platelets. Most procedures involve the destruction of a large but known number of platelets and the subsequent analysis of Ca and Mg content by atomic absorption spectrophotometry (Kinlough-Rathbone et al., 1973, Heptinstall, 1976; Imandt et al., 1980). The restriction of this approach is that no measurement of individual platelets can be performed and that no information is obtained about the subcellular distribution of the elements.

Electron probe X-ray microanalysis (EPXMA) appears to be a suitable non-destructive method to study the elemental content of individual blood platelets (for a review, see Yarom, 1983). With EPXMA Ca and Mg can be localized at the subcellular level and can be analysed quantitatively. In human platelets the so-called dense granules have been shown to contain relatively large amounts of Ca and P (Costa et al., 1977; Skaer et al., 1976). The major part (ca. 80%) of the total Ca content of human blood platelets is found to be present in the dense granules (Murer and Holme, 1970). Until now, however, X-ray microanalysis studies of blood platelets have only yielded semi-quantitative results, based on comparison of net peak intensities or peak to background ratios (Costa et al., 1977, 1979, Skaer et al., 1974) without an attempt to directly quantify the elemental content.

In this study we present a relatively quick and simple method to quantify the Ca, Mg and P contents of both individual blood platelet and their dense granules (see also Boekestein et al., 1982).

Materials and methods

Preparation of whole mounts of blood platelets

Blood was obtained from adult Wistar rats with a mass of approximately 300 g, by direct heart puncture using 3.8% w/w tri sodiumcitrate as anticoagulant. Platelet rich plasma (PRP) was prepared by centrifugation of the blood at 2000 N/kg for 10 minutes (Imandt et al., 1977). One ml of PRP was subsequently centrifuged for 10 minutes at 4500 N/kg. The platelet containing pellet was resuspended in 2.5 ml of a $\text{HCO}_3^-/\text{CO}_2$ -buffered medium containing NaCl (116.5 mM), KCl (4.2 mM), NaHCO_3 (32.3 mM), EDTA (0.5 mM) and albumin (6%). The platelets were centrifuged once more at 4500 N/kg for 10 minutes. The pellet was resuspended in 1 ml of the latter medium and 10 μl of this suspension was deposited on copper grids (75-mesh) covered with a parlodion film. After 30 seconds the fluid adhering to the film was removed by blotting with filter paper (according to Costa et al. (1977) with minor modifications). Finally the platelets were briefly rinsed with 20 μl of the buffer medium, blotted dry again and stored under vacuum.

The Mg and Ca content of rat blood platelets has also been determined by a wet-chemical method according to the procedure described by Imandt et al. (1980), using atomic absorption spectrometry (AAS).

Preparation of microdroplet standards

Constriction pipettes were prepared and calibrated as described by Van Eekelen et al. (1980). Drops of standard salt solutions (5 μ l) containing KH_2PO_4 , CaCl_2 , MgCl_2 and 25% glycerin as well as parlodion-coated copper grids were placed on the bottom of a petri-dish filled with H_2O -saturated paraffin oil. Several picoliter samples of the standard solutions separated by equally small volumes of paraffin oil were drawn into the constriction pipette (Lechene et al., 1974). The samples were put on parlodion coated grids, using a micromanipulator. They were deposited in the central part of the grid meshes in order to obtain a minimum of background radiation intensity. The paraffin oil adhering to the film was dissolved in isopentane, and the water and glycerol in the droplets were flash evaporated according to the method described by Quinton (1978). Before analysis a carbon layer was evaporated onto the specimens and the standards in order to prevent charging during electron bombardment.

Because in quantitative X-ray microanalysis one often uses so called 'ideal' standards, which resemble the unknown specimen both chemically and physically as closely as possible (Roomans, 1980), we have compared microdroplets containing mineral salts only with microdroplets containing mineral salts and an organic component.

In particular we have used ascorbic acid as the organic component because this compound has a good solubility in water and there were no indications that this compound was unstable in the electron microscope. The mass thickness in microdroplets with 10% ascorbic acid, added as the organic component, was approximately $6 \cdot 10^{-13} \text{ g}/\mu\text{m}^2$. The mass thickness of air-dried blood platelets is orders of magnitude smaller ($10^{-16} \text{ g}/\mu\text{m}^2$) (calculated from data of Linders et al., 1984).

Addition of ascorbic acid caused no significant changes in the net calcium Ka peak intensity. This indicated that an organic component present in a mass thickness which is orders of magnitude larger than in blood platelets, caused no significant change in the absorption of X-rays in the standard. Therefore it is justified to use inorganic microdroplet standards for the X-ray microanalysis of whole mounts of blood platelets.

Electron probe X-ray microanalysis (EPXMA)

EPXMA was carried out using a Philips EM400G transmission electron microscope with a scanning attachment, equipped with an energy dispersive X-ray

microanalysis system (EDAX 707B, EDAX international, Inc.). The resolution of the X-ray detector was 165 eV, while the detector elevation and azimuth were both 0°. In order to minimize the background radiation intensity, a beryllium specimen holder was used. During analysis individual microdroplets, blood platelets or dense granules were scanned which required varying magnification settings.

Analyses were carried out at 80 kV accelerating voltage, 18° specimen tilt angle and with live time settings of 100 seconds. The total beam current was measured indirectly using the exposure time measurement circuitry of the microscope after suitable calibration.

Quantification procedure

Net peak intensities in the X-ray spectrum were calculated for P-K, K-K_α and the sum peak of Ca-K_α and K-K_β using the INT routine of the EDAX software (EDIT 7 EM). In order to calculate the net Ca-K_α intensity, K-K_β had to be subtracted from the sum peak. Therefore the K_β/K_α peak intensity ratio for potassium was determined experimentally (see Sumner (1983) for a discussion on the K - Ca interference).

The net Mg-K intensity was found by linear extrapolation from the high energy side of the peak, after removing the sum peak of Na-K and Cu-L by the STRIP routine of the EDAX software. Calibration lines are shown in Figure 1. Net element-characteristic X-ray peak intensities (P_x) can be related to the amount of material present (W_x) and the surface area (O) scanned during analysis

$$P_x \sim W_x I / O \quad (1)$$

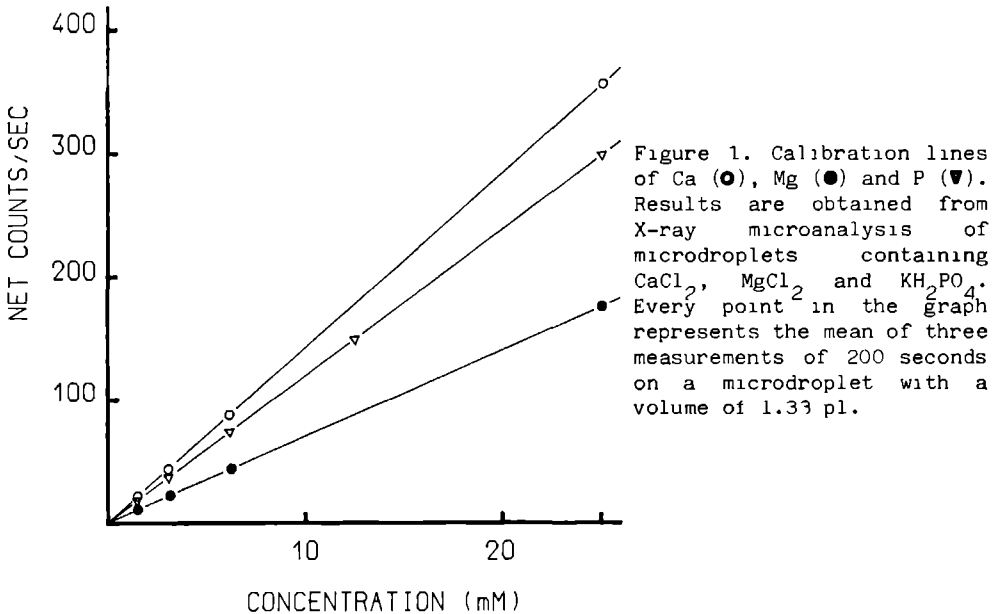
Since $O \sim 1/M^2$ (M is the actual magnification) the following formula can be derived for quantitative X-ray microanalysis in STEM with different magnification settings for specimen and standard:

$$W_{sp} = \frac{P_{sp} I_{st} M_{st}^2}{P_{st} I_{sp} M_{sp}^2} W_{st} \quad (2)$$

where, W = elemental mass
P = net peak intensity
I = total beam current
M = actual magnification

index sp = specimen
 index st = standard
 index 1 = element

Net peak intensities of platelets or dense granules were compared with those of microdroplet standards and the Ca, Mg and P contents were calculated with (2). See Russ (1978) and Sumner (1983) for a discussion on quantification procedures.



Results

The platelets to be analyzed were selected on the basis of their overall morphological appearance. Platelets, showing 'spike' formation, abnormal sizes and other characteristics of platelets which are not in the resting state, were disregarded. Notwithstanding, each grid contained sufficient numbers of platelets suited for analysis (see Fig. 2).

The dimensions of rat platelets varied from 2.4 μm to 5.2 μm with a mean value of 3.4 μm (standard deviation: 0.6 μm). The dimensions of dense granules varied from 160 nm to 400 nm with a mean value of 240 nm (standard deviation: 60 nm). The number of dense granules per platelet varied from 0 to 15 with 4 dense granules as mean number (standard deviation: 3).

Figure 3 shows an energy-dispersive X-ray spectrum obtained from a dense granule. The Si-K peak in the spectrum most likely originates at least in part from contamination of the specimen by the electron bombardment. The Na, S, Cl and K peaks in the spectrum will be generated mainly by elements present in the platelet, but it should be noted that these elements were also present in the washing medium. The peak around 1 keV in fact will be a sum peak of Cu-L and Na-K because copper grids were used. In view of the thorough washing of the platelets to remove adhering plasma and because the washing medium does not contain these elements it seems justified to assume that the Ca, Mg and P peaks present are platelet-characteristic. It appeared that the Mg and P peak to background ratio's in spectra from cytoplasmic areas are considerably lower than in spectra from dense granules, indicating that these elements are not homogeneously distributed over the content of the platelet.

In Table 1 the results of the measurements of the Ca, Mg and P content of the platelets and their dense granules are summarized. It is evident from this

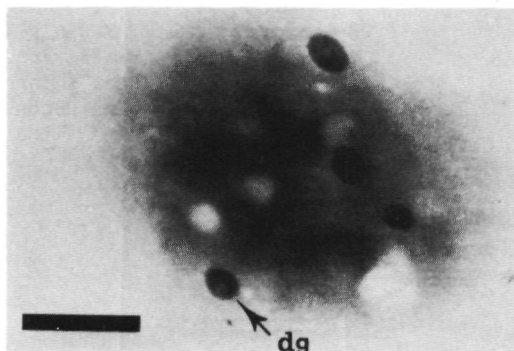


Figure 2. Whole mount of a rat blood platelet. Bar is 1 μ m, dg= dense granule.

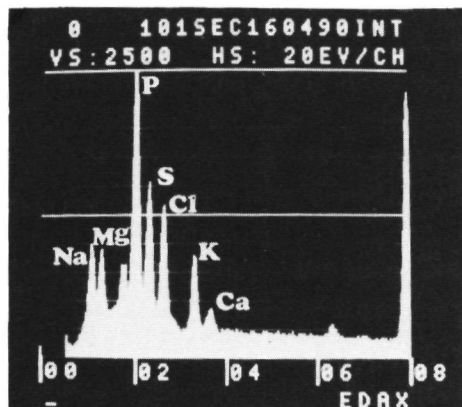


Figure 3. Energy-dispersive X-ray spectrum of a dense granule in a whole mounted rat blood platelet.

	platelets (n=68)		granules (n=50)		platelets (n=68)		granules (n=50)	
	10^{-8} nmol	C.V.(%)	10^{-8} nmol	C.V.(%)	ratio	C.V.(%)	ratio	C.V.(%)
Ca	3.2	76	0.24	82	Ca/P 0.049	75	0.047	45
Mg	12	67	8.0	87	Mg/P 0.16	46	0.29	27
P	81	63	5.6	82				

Table 1. Mean calcium, magnesium and phosphorus content of rat blood platelets and their dense granules as measured by X-ray microanalysis.

Table 2. Mean molar ratios between calcium and phosphorus, and between magnesium and phosphorus in rat blood platelets and their dense granules as measured by X-ray microanalysis. n= number of measurements, C.V.= coefficient of variation.

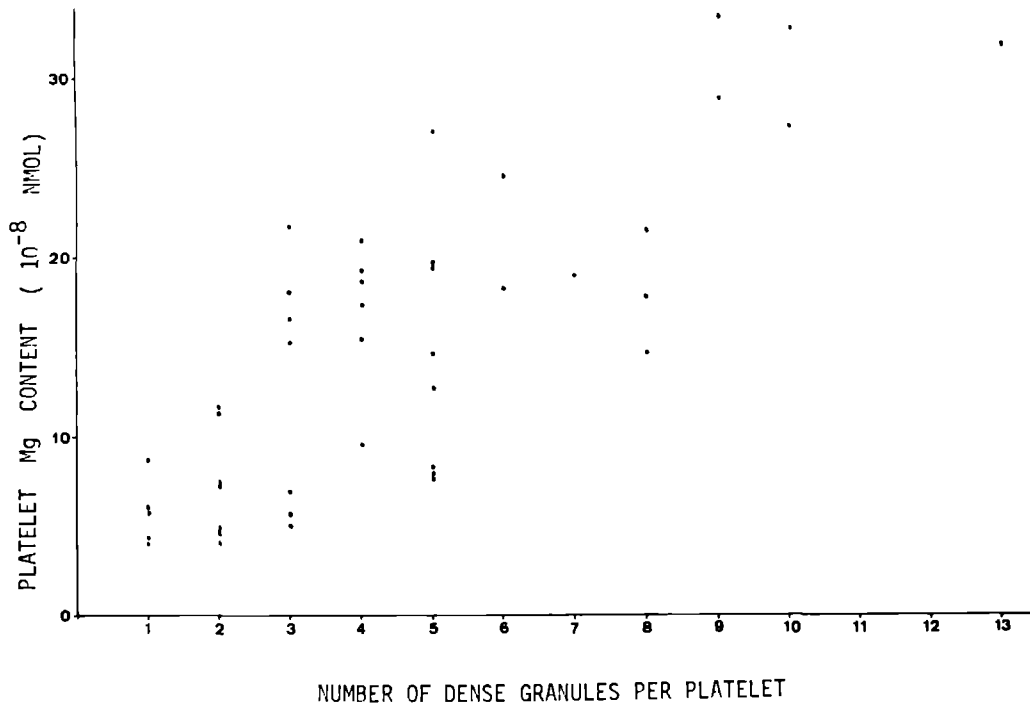


Figure 4. The correlation between the number of dense granules per platelet and the Mg content of a platelet.

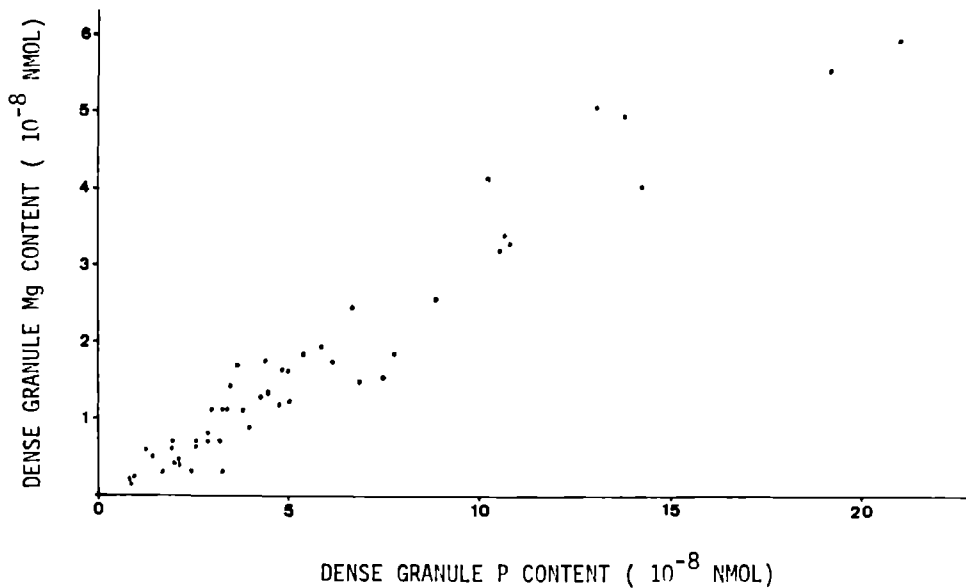


Figure 5. The correlation between the Mg content and the P content in dense granules.

table that the mean Mg content of the platelets is considerably larger than is the mean Ca content.

In Table 2 the molar ratios of Ca/P and Mg/P in individual platelets and dense granules are shown. It can be note worthy that the Mg/P ratio in dense granules is relatively constant.

In Figure 4 the Mg content of 44 platelets is plotted against the total number of dense granules in these platelets. Linear regression analysis shows a correlation coefficient of 0.77. Linear regression analysis of the number of dense granules per platelet and the Ca or P content of the platelets, yielded smaller correlation coefficients ($r = 0.37$, resp. $r = 0.55$). In Figure 5 the magnesium and the phosphorus content of 50 dense granules from different platelets randomly chosen are plotted against each other. Here linear regression analysis revealed a correlation coefficient of 0.95. Regression analysis of the Mg and Ca contents and of the Ca and P contents in dense granules yielded also small correlation coefficients ($r = 0.50$, resp. $r = 0.49$). All the correlation coefficients mentioned were found to be significant.

The Mg and Ca content of the platelets, as determined by atomic absorption spectrometry according to Imandt et al. (1980), has been found to be $9.8 \cdot 10^{-8}$ nmol Mg per platelet (standard deviation $0.2 \cdot 10^{-8}$ nmol) and $5.2 \cdot 10^{-8}$ nmol Ca per platelet (standard deviation $0.2 \cdot 10^{-8}$ nmol).

Discussion

The main advantage of X-ray microanalysis is that useful information on the elemental content of individual cells or cell organelles can be obtained. In this study a direct quantification method was used with microdroplets as standards for the determination of the Ca, Mg and P content of individual rat blood platelets.

The reliability of the method used for preparation of the platelet specimens was already assessed by Costa et al. (1977).

The major part of the platelets on the grids showed a normal ultrastructural morphology (Fig. 2). No leakage was observed of dense granules from the platelets and the whole appearance of these air-dried specimens showed no disturbances of the known normal character of a blood platelet in the resting state (Costa et al., 1977).

As mentioned in the introduction, until now only few quantitative results have been published on the elemental content of individual blood platelets and their dense granules (Costa et al., 1977; Yarom, 1983). Skaer et al. (1976) calculated the amount of Ca in the dense granules of human blood platelets, by calibration of the P/Ca peak intensity ratio with known P-Ca compounds. The values found for the Mg and Ca content of the rat platelets, using EPXMA, lie remarkably close to the values found with a wet-chemical analysis using AAS. With EPXMA the Mg content is somewhat higher and the Ca content is lower: the sums of the Mg and Ca contents are surprisingly equal. The differences in the Mg and Ca contents can be explained partly by the enormous difference in sampling size, i.e. about 50 platelets measured with EPXMA and about $2 \cdot 10^9$ platelets used for the AAS. Recently Linders et al. (1984) quantified the Mg and Ca content of individual rat blood platelets using the electron scattering signal for the dry mass determination and the X-ray signal for the elemental mass determination. Our results for the Mg content ($12 \cdot 10^{-8}$ nmol, C.V. = 67%) were in good agreement with the Mg content found by Linders et al. (1984) ($14.8 \cdot 10^{-8}$ nmol, C.V. = 47%).

From Table 1 we conclude that in rat blood platelets approximately four times as much Mg is present than is Ca, and the Mg content of the dense granules was an order of magnitude higher than is the Ca content. In blood platelets of many other species Ca is present in larger amounts than is Mg (Imandt et al., 1980). Heptinstall (1976) found in human platelets $18.6 \cdot 10^{-8}$ nmol Ca and $9.3 \cdot 10^{-8}$ nmol Mg. In pig platelets, however, Kinlough-Rathbone et al. (1973) found $11.8 \cdot 10^{-8}$ nmol Ca and $25.2 \cdot 10^{-8}$ nmol Mg. In platelets of rabbit and guinea pig Pletscher and Da Prada (1975) also found more magnesium than calcium in dense granules.

Regarding the absolute amounts of Mg and Ca found in our study, we can conclude that they are within the published range of values for other species obtained with different analysis methods (Heptinstall, 1976; Kinlough-Rathbone et al., 1973; Imandt et al., 1980).

Few investigators have determined the elemental composition of individual dense granules. In a study of human platelets, Skaer et al. (1976) found a value of $0.6 \cdot 10^{-11}$ mg Ca per platelet. Given an average of 11 dense granules per platelet. This results in $1.4 \cdot 10^{-8}$ nmol Ca present in one dense granule. Our value ($1.7 \cdot 10^{-8}$ nmol Mg per dense granule) is surprisingly close to that value.

From Table 1 and 2 we can conclude that ratio's between Ca and P concentration

and between Mg and P concentration vary less than do the absolute Ca, Mg and P amounts. This is particularly the case in the dense granules. A possible explanation is that Ca and P as well as Mg and P show an interdependency in the accumulation in the dense granules, whereas Ca, Mg and P amounts vary in relation to the varying sizes of the granules.

The correlation coefficient found in the linear regression analysis of the number of dense granules per platelet and the Mg content of the platelets, underlines that a large fraction of the platelet Mg is concentrated in the dense granules ($r = 0.77$, Figure 4). The correlation coefficient found in the linear regression analysis of the Mg and P content of the dense granules ($r = 0.95$, Fig. 5) gives further evidence that Mg and P are not stored independently in the dense granules. This is also consistent with the relatively fixed ratio found between the Mg and P content in dense granules (Table 2).

This study shows that quantitative X-ray microanalysis, carried out on individual blood platelets and their dense granules, can be useful in the explanation of phenomena related in the storage of biologically important compounds in certain cell compartments.

References

- Boekestein, A, Kuypers, GAJ, Peters, E, Stadhouders, AM (1982) Quantitative X-ray microanalysis of Mg, P and Ca in rat blood platelets. In: Proc. 10th Int. Congr. Electron Microsc. 3: 369-370.
- Costa, JL, Tanaka, Y, Pettigrew, K, Cushing, RJ (1977) Evaluation of the utility of air-dried whole mounts for quantitative electron microprobe studies of platelet dense bodies. J. Histochem. Cytochem. 25: 1079-1086.
- Costa, JL, Pettigrew, KD, Murphy, DL (1979) Electron probe microanalysis of changes in dense-body phosphorus and calcium content following alterations in platelet serotonin levels. Biochem. Pharmacol. 28: 23-26.
- Eekelen, CAG van, Boekestein, A, Stols, A, Stadhouders, AM (1980) X-ray microanalysis of picoliter microdroplets: Improvement of the method for quantitative X-ray microanalysis of samples of biological fluids. Micron 11: 137-148.
- Heptinstall, S (1976) The use of a chelating ion-exchange resin to evaluate the effects of the extracellular calcium concentration on adenosine diphosphate induced aggregation of human blood platelets. Thrombos. Haemostas. (Stuttgart) 36: 208-220.

- Imandt, L, Genders, T, Wessels, H, Haanen, C (1977) An improved method for preparing platelet-rich plasma. *Thrombos. Res.* 11: 429-432.
- Imandt, I, Tjhuis, D, Wessels, M, Haanen, C (1980) Observation on ADP-aggregation of lithium-chloride incubated platelets in a variety of mammalian species. *Haemostasis* 9: 275-287.
- Kinlough-Rathbone, RL, Chahil, A, Mustard, JF (1973) Effect of external calcium and magnesium on thrombin-induced changes in calcium and magnesium of pig platelets. *Am. J. Physiol.* 224: 941-945.
- Lechene, C (1974) Electron probe microanalysis of picoliter liquid samples. In: *Microprobe analysis as applied to cells and tissues*. Eds: Hall, TA, et al., Acad. Press, New York, pp 351-367.
- Linders, PWJ, Van de Vorstenbosch, RA, Stadhouders, AM (1984) Elemental analysis of individual rat blood platelets by an improved method for quantitative electron probe X-ray microanalysis. *J. Histochem. Cytochem.* (in the press).
- Massini, P (1977) The role of calcium in the stimulation of platelets. In: *Platelets and thrombosis*. Serono Symposium vol. 10, Eds.: Mills, DBC, Paretì, FI, Acad. Press, London, pp 34-44.
- Murer, EH, Holme R (1970) A study of the release of calcium from human blood platelets and its inhibition by metabolic inhibitors, N-ethylmaleimide and aspirin. *Biochem. Biophys. Acta* 222: 197-205.
- Pletscher, A, Da Prada, M (1975) The organelles storing 5-hydroxy-tryptamine in blood platelets. In: *Biochemistry and pharmacology of platelets*. Ciba Foundation Symposium 35 (new series), Elsevier, Amsterdam, pp 261-286.
- Quinton, PM (1978) Ultramicroanalysis of biological fluids with energy dispersive X-ray spectrometry. *Micron* 9: 57-69.
- Russ, JC (1978) Electron probe X-ray microanalysis-principles. In: *Electron probe microanalysis in biology*. Ed: Erasmus, DA, John Wiley and Sons, New York, pp 5-36.
- Skaer, RJ, Peters, PD, Emmines, JP (1974) The localization of calcium and phosphorus in human platelets. *J. Cell Sci.* 15: 679-692.
- Skaer, RJ, Peters, PD, Emmines, JP (1976) Platelet dense bodies: a quantitative microprobe assay. *J. Cell Sci.* 20: 441-457.
- Sumner, AT (1983) X-ray microanalysis: a histochemical tool for elemental microanalysis. *Histochem. J.* 15: 501-541.
- Yarom, P (1983) X-ray microprobe analysis of platelets. *Haemostasis* 13: 17-24.

ELECTRONPROBE X-RAY MICROANALYSIS OF BIOLOGICAL SPECIMENS IMPROVEMENT OF A
NUMBER OF QUANTIFICATION PROCEDURES

Summary

In this thesis an investigation is described to establish which quantification procedures can be used in the X-ray microanalysis of biological specimens. Two classes of specimens have been distinguished from each other, i.e. thick specimens (opaque to the beam electrons) and thin specimens (transparent to the beam electrons). Since these two classes have their own specific possibilities and problems regarding quantification, they are dealt with separately.

For a better understanding of material presented in the thesis a description is given in chapter 1 of a number of physical principles underlying quantitative X-ray microanalysis. These are the interaction of beam electrons with matter, the emission of X-rays and the detection of X-rays with energy-dispersive and wavelength-dispersive spectrometers. Furthermore this chapter gives a survey of a number of quantification procedures used in X-ray microanalysis.

The first part of this thesis covers various aspects of quantitative X-ray microanalysis of biological bulk specimens (chapter 2). In order to test the performance of known ZAF-correction formulae in light element analysis, we compared the results obtained when experimental data from well-defined binary systems with atomic numbers below 31 were processed with these formulae (chapter 3). The formulae with the best performance were assumed to be also optimal for ZAF-correction in biological analysis problems and were included in a specially designed ZAF-correction computer program called BIOFLEX. With BIOFLEX the effect on the results was studied of two specific factors which can cause inaccuracies in biological X-ray microanalysis. From the studies it became evident that in ZAF-correction the organic matrix of the specimen should be specified in mass fractions of the elements present. Further it was noted that the poorly defined local specimen tilt angle can introduce errors in the mass fractions after ZAF-correction of 2% or more (chapter 4). A study on specimens with a rough surface in which variations of net peak intensity and variations of peak to background ratio were compared, indicates that use of the peak to background ratio in the quantification is to be preferred. Errors due to counting statistics amount to about 11% (chapter 5).

The second part of this thesis deals with the quantitative X-ray

microanalysis of thin biological specimens, with particular emphasis on the analysis of microdroplets (volume from 1 to 100 pl), used as standards. The so-called constriction capillaries, used for the preparation of microdroplets standards, had pipetting errors less than 2% (chapter 6). A comparison of X-ray detection methods and supporting materials for microdroplets resulted in the observation that thin supporting films combined with wavelength-dispersive X-ray detection, yielded maximum peak to background ratios, as could be expected from theory (chapter 7). If massive supports are used for the microdroplets, the background will be curved considerably especially in the low energy region (<4 keV). Therefore a special non-linear background subtraction procedure was developed. A number of analytical conditions was investigated and for the specimen tilt angle optimal values were found between 22° and 30° . The method for quantitative X-ray microanalysis with microdroplet standards is described and made applicable to the analysis of whole cells and distinct cell organelles. The estimated overall accuracy of the quantification procedure is 10% (chapter 8). The procedure is applied to the determination of the Mg and Ca content in rat blood platelets. It was found that the average content was $12 \cdot 10^{-8}$ nmol Mg and $3.2 \cdot 10^{-8}$ nmol Ca per platelet (chapter 9).

Samenvatting

In dit proefschrift wordt een onderzoek beschreven dat tot doel had na te gaan welke kwantificeringsprocedure moet of kan worden gevolgd in de rontgenmicroanalyse van biologische preparaten. Hierbij zijn twee klassen van preparaten onderscheiden, namelijk dikke - voor de bundelelektronen ondoor- dringbare - preparaten en dunne - voor de bundelelektronen transparante - preparaten. Omdat elk van deze twee klassen van preparaten zijn eigen specifieke mogelijkheden en problemen kent ten aanzien van de kwantificering worden deze apart behandeld. Voor beter begrip van de materie is in Hoofdstuk 1 een beschrijving gegeven van een aantal fysische achtergronden van de kwantitatieve rontgenmicroanalyse namelijk de interactie van elektronen met materie, de emissie van rontgenstraling en de detectie van rontgenstraling met energie- en golflengtedispersieve spectrometers. Voorts is in dit hoofdstuk een overzicht opgenomen van een aantal kwantificeringsprocedures in de rontgenmicroanalyse.

In het eerste deel van dit proefschrift worden verschillende aspecten van de kwantitatieve rontgenmicroanalyse van dikke biologische preparaten behandeld (Hoofdstuk 2). Om de score van bekende ZAF-correctie-formules voor de analyse van lichte elementen te kunnen nagaan, werden de resultaten vergeleken, die verkregen waren door experimentele gegevens van een aantal goed gedefinieerde binaire systemen met atoomnummers lager dan 31 met deze formules te verwerken (Hoofdstuk 3). Van de beste formules werd aangenomen dat deze ook optimaal zijn door de ZAF-correctie in biologische analyseproblemen. Deze formules werden opgenomen in een speciaal ontworpen computerprogramma voor ZAF-correctie, genaamd BIOFLEX. Met BIOFLEX is het effect op de resultaten bestudeerd van twee specifieke factoren die oorzaak kunnen zijn van onnauwkeurigheden in de biologische rontgenmicroanalyse. Uit deze studie werd duidelijk dat in de ZAF-correctie de organisch-chemische matrix van het preparaat gespecificeerd dient te worden in massafracties van de aanwezige elementen. Verder bleek dat een slecht gedefinieerde locale preparaat kantelhoek fouten in de massafracties kan introduceren na ZAF-correctie van 2% of meer (Hoofdstuk 4). Een studie aan preparaten met een ruw oppervlak waarin de variaties in de netto piekintensiteit en in de piek-achtergrondverhouding werden vergeleken, gaf aan dat gebruik van de piek-achtergrond verhouding in de kwantificering de

voorkeur verdient, waarbij de fout ten gevolge van de telstatistiek ca. 11% is (Hoofdstuk 5).

Het tweede deel van dit proefschrift handelt over de kwantitatieve rontgen-microanalyse van dunne biologische preparaten, waarbij de nadruk ligt op de analyse van microdruppels (volume van 1 tot 100 pl) als standaard. Voor de bereiding van microdruppel standaards werden zogenaamde constrictie-capillairen gebruikt met pipetteerfouten kleiner dan 2% (Hoofdstuk 6). Een vergelijking van rontgen-detectie methoden en dragermaterialen voor microdruppels leerde dat dunne dragerfilms gecombineerd met golflengte-dispersieve rontgen-detectie, maximale piek-achtergrond verhoudingen veroorzaken, zoals volgens de theorie verwacht kan worden (Hoofdstuk 7). Als massieve dragers worden gebruikt voor de microdruppels dan wijkt de achtergrond aanzienlijk af van de lineaire vorm vooral in het lage energie gebied (< 4 keV). Daarom werd een speciale niet-lineaire interpolatie-methode ontwikkeld om de achtergrond uit het spectrum op concrete wijze te verwijderen. Een aantal analysecondities is onderzocht en voor de preparaat kantelhoek werden optimale waarden gevonden tussen 22° en 30° . De methode voor kwantitatieve rontgen-microanalyse met microdruppels als standaard is beschreven en toepasbaar gemaakt op de analyse van hele cellen en goed te onderscheiden organellen in de cel. De geschatte 'overall' nauwkeurigheid van deze procedure is 10% (Hoofdstuk 8). De procedure is toegepast op de bepaling van het Mg en Ca gehalte van bloedplaatjes van de rat. De gevonden gemiddelde gehalten waren $12 \cdot 10^{-8}$ nmol Mg en $3,2 \cdot 10^{-8}$ nmol Ca per plaatjes (Hoofdstuk 9).

Curriculum vitae

A.Boekestein werd op 23 december 1951 geboren in Naaldwijk. Na de HBS-B aan het Stevin Lyceum in Den Haag te hebben voltooid, ging hij Scheikundige Technologie studeren aan de Technische Hogeschool in Delft. Na het kandidaatsexamen in 1974 koos hij als afstudeerrichting de Biologische Chemie/ Technische Microbiologie (Professor T.O. Wiken) met als afstudeeronderzoek 'Methaanassimilatie bij bacterien'. De afstudeerscriptie handelde over 'De biosynthese van lanosterol tot ergosterol bij schimmels'. In 1975 werd een aanvang gemaakt met het promotieonderzoek aan de Katholieke Universiteit in Nijmegen onder leiding van professor A.M. Stadhouders. Dit onderzoek vond plaats in het Insituut voor Submicroscopische Morphologie van de Medische Faculteit en betrof de kwantificeringsmethoden in de röntgenmicroanalyse van biologische preparaten. In 1980 werd hij medewerker van de afdeling Elektronenmicroscopie van de Technische en Fysische Dienst voor de Landbouw in Wageningen (Directeur: Drs. A.M.K. van Beek), waar hij tot taak kreeg de elektronensonde röntgenmicroanalyse techniek verder uit te bouwen voor het landbouwkundig onderzoek. In 1982 werd hij hoofd van deze afdeling die belast is met de gecentraliseerde dienstverlening op elektronenmicroscopisch terrein aan het landbouwkundig onderzoek.

